PLACE CELLS TO PATH PLANNING: A NEURAL STUDY OF COMPLEX LOCOMOTOR BEHAVIORS AS AN INSPIRATION FOR ROBOTICS

by

Shahin Gharakozlou Lashkari

A dissertation submitted to The Johns Hopkins University in conformity with the requirements for the degree of Doctor of Philosophy.

Baltimore, Maryland

October, 2023

Abstract

Even with the advancements of mobile robots in recent years, robots still lag behind animals such as squirrels in performing agile behaviors. Drawing inspiration from animal cognitive planning and navigational strategies has proven beneficial in enhancing robot functionality. Particularly, examining animals' spatial decision-making strategies can aid in advancing robots that can perform complex locomotor tasks.

This dissertation delves into how neuronal activity in the hippocampus, a brain region crucial for spatial cognition, is involved during complex locomotor behaviors. Previous studies have explored decision-making processes in the hippocampus, predominantly during animal navigation on the surfaces of the experiment rigs. This research builds on that by looking at voluntary animal navigation in 3D spaces. It investigates how hippocampal place cell activity encodes and predicts different 3D trajectories based on the routes taken (retrospective coding) or will be taken (prospective coding) by the animals.

The study explores Long-Evans rats navigating a linear track with an adjustable gap, where they must choose between 'jumping' (crossing over the gap with a single leap) or 'ditching' (jumping into and out of the gap) to cross the gap. Neuropixels 2.0 silicon probes recorded neural activity from the hippocampus in sessions with both jumping and ditching

behaviors. Recordings revealed place cell activity during the airborne phase of jumping. Moreover, in sessions involving both jumping and ditching behaviors, place cells exhibited 'splitter-like' behavior by encoding these trajectories differently. For example, some place cells showed strong selectivity for jumping, while others exhibited a strong preference for ditching. Place cells even discriminated between trajectories at locations beyond the gap, indicating retrospective coding. These findings provide evidence that place cells adjust their firing properties to reflect the complex behavioral choices made by animals [1].

This research also investigates the predictive nature of place cell activity. A Bayesian decoder was trained to predict the animal's behavior based on the average firing rates of place cells in the time interval preceding takeoff. The decoder achieved accuracies ranging from 60% to 85%, significantly surpassing the chance level. This finding demonstrated that place cells encode anticipatory information during the complex locomotor task, enabling the prediction of complex locomotor behaviors solely based on firing rates before takeoff [2].

In conclusion, this dissertation enhances the understanding of the role of place cells in spatial navigation. It highlights their ability to adapt their firing properties to reflect the structure of complex locomotor tasks. By gaining insights from animals, we can deepen our understanding of spatial cognition and, ultimately, use these findings to create bioinspired algorithms that enhance the functionality of robots in solving complex navigational challenges.

Thesis Committee

Noah J. Cowan (Primary Advisor)

Professor

Department of Mechanical Engineering

Johns Hopkins Whiting School of Engineering

James J. Knierim

Professor

Department of Neuroscience

Johns Hopkins School of Medicine

Chen Li

Assistant Professor

Department of Mechanical Engineering

Johns Hopkins Whiting School of Engineering

Acknowledgements

I would like to express my deepest gratitude and appreciation to all those who have supported me throughout the journey of completing my PhD. I would like to take this opportunity to acknowledge the invaluable contributions of various individuals who have helped me in ways big and small.

First and foremost, I would like to extend my genuine thanks to my advisor, Noah Cowan, for his guidance, insightful feedback, and continuous support. His expertise and encouragement have been instrumental in shaping the direction and quality of this research. Moreover, I would also like to express my gratitude to Jim Knierim, whose knowledge and teachings have enriched my academic experience and provided a solid foundation for this work, and also to Chen Li for his constructive feedback on this dissertation.

Additionally, I would like to acknowledge the assistance and collaboration of my peers and colleagues and engagement in meaningful discussions that have significantly contributed to the development of my research: Brian Woronowicz, who helped at all facets of this multifaceted work; Pel Ozel, who performed all the animal surgeries and helped with the neurophysiological recordings; Murtaza Hathiyari, Vyash Puliyadi, and Balázs Vágvölgyi for helping at crucial steps of the project; Manu Madhav, and Ravi Jayakumar, for their

mentorship at the early stages of my PhD and for teaching me a lot of technical skills.

I am immensely grateful to my friends, especially Yu Yang, Bharath Krishnan, and Brian Woronowicz, who created unforgettable experiences for me. I would like to thank all LIMBS lab members: Di Cao, Siming Deng, Debojyoti Biswas, Ismail Uyanik, Nicole Ortega, and specifically Gorkem Secer and Michael Wilkinson, who were at some point involved in the jumping project. Also, all Knierim lab members, especially Geeta Rao, Audrey Branch, Yueqing Zhou, Brian Li, Arjuna Tillekeratne, Will Hockeimer, and Francesco Savelli who have generously shared their expertise and provided valuable insights for this research.

Finally, I wish to express my gratitude to my other friends at Hopkins for their constant support and understanding have been a source of strength throughout this challenging endeavor: Ehsan Azimi, Gabe Baraban, Ali Ebrahimi, Mohit Singhala, Farshid Alambeigi, and Mahsan Bakhtiarinejad. Additionally, I would like to extend my thanks to faculty members at Hopkins who have shaped my vision and enriched my experience with their invaluable insights: Louis Whitcomb, Jin Seob Kim, and Donniell Fishkind. A special mention goes to Bob Full, Lucia Jacobs, and especially Dan Koditschek for their persistent encouragement and insightful feedback that greatly contributed to the multidisciplinary scope of this research.

Dedication

I dedicate this dissertation

to my beloved wife, whose unwavering support and encouragement have been my stronghold through the roller-coaster of my PhD journey,

to my dear mother, who always believed in my abilities and motivated me to strive for excellence,

to my late grandparents, who planted the seeds of curiosity and the joy of learning within me.

Contents

Abstract **ii**

Acknowledgements **v**

Dedication **vii**

List of Tables **xiv**

List of Figures **xv**

1 Introduction **1**

1.1 Background 2

1.2 Research Objectives 4

1.3 Significance of the Study 5

1.4 Scope and Limitations 6

1.5 Research Contribution 8

1.6 Organization of the Dissertation 9

1.7 Dissemination 10

2 Literature Review **11**

2.1 Bioinspired Robotics 11

2.2 Bioinspired Algorithms 13

2.3 Place Cells and the Cognitive Map 15

2.4 Hippocampus and Memory 18

2.5 Hippocampus as a Predictive Map 20

2.6 Splitter Cells 21

2.7 Vicarious Trial and Error 23

2.8 Hippocampal LFP and Behavior 24

2.9 Theta Phase 26

2.10 Behavioral Studies 27

2.10.1 Psychometrics 27

2.10.2 Head Bobbing 28

2.11 Recording Neural Activity 28

2.12 Decoding Neural Activity 29

2.13 Gaps in the Literature 31

2.14 Summary 34

3 Methods **36**

3.1 Experimental Procedures 37

3.1.1 Animal Subjects 37

3.1.2 Animal Surgery 39

3.1.3 Experimental Paradigm 40

3.2 Experimental Setup 43

3.2.1 Actuators 45
3.2.2 Rat Cap and Marker Crown 46
3.2.3 Cameras 47
3.2.4 Force Sensors 49
3.2.5 Data Acquisition and Control 50
3.2.6 Experiment Computers 50
3.3 Neurophysiological Recording Setup 51
3.3.1 Neuropixels 2.0 Probes 52
3.3.2 Neural Data Acquisition Hardware 52
3.3.3 Neural Data Acquisition Software 53
3.4 Data Analysis 54
3.4.1 Animal Tracking 54
3.4.2 Behavioral Data Analysis 55
3.4.2.1 Head Bobbing Analysis 56
3.4.2.2 Ground Reaction Force 57
3.4.2.3 Time of Flight 58
3.4.3 Neural Data Analysis 59
3.4.3.1 Spike Sorting 59
3.4.3.2 Measuring Firing Rates 60
3.4.3.3 Theta Analysis 61
3.4.3.4 Theta Phase Analysis 62
3.4.3.5 Theta Frequency Analysis 63
3.4.4 Development of the Bayesian Decoder 63

4 Behavioral and Neural Correlates of Jumping and Ditching 65

4.1 Behavioral Analysis 66

4.1.1 Psychometric Function 66

4.1.2 Hysteresis Effect 67

4.1.3 Head bobbing 69

4.2 Neural Correlates of Jumping 70

4.2.1 Theta Phase Precession 71

4.2.2 Theta Frequency Versus Speed 77

4.2.3 Correlation of Theta Phase with Action 79

4.2.4 Theta Frequency and Kinematic Phases 79

4.3 Discussion 82

5 Firing Properties of Place Cells During Complex Locomotor Behaviors 84

5.1 Anchoring Frames of Reference 85

5.2 Place Cell Activity During Jumping and Ditching 87

5.3 Analysis of Trajectory Selectivity 90

5.3.1 Selectivity for Jumping 90

5.3.2 Selectivity for Ditching 92

5.3.3 Special Cases 94

5.4 Retrospective Encoding by Place Cells 96

5.5 Statistical Analysis 98

5.6 Discussion 102

6 Predictive Nature of Place Cell Activity 107

6.1 Prospective Encoding of Place Cells 108

6.2 Differential Encoding in Similar Physical Location 108

6.3 Bayesian Decoder 112

6.3.1 Neural Bayesian Decoder 113

6.3.2 Behavioral Bayesian Decoder 113

6.4 Statistical Analysis of Bayesian Decoders 115

6.5 Discussion 118

7 Conclusion and Future Directions 120

7.1 Summary of Key Findings 121

7.2 Implications of the Findings 123

7.3 Potential Future Research Directions 125

7.4 Final Remarks 128

A Data Acquisition and Analysis 130

A.1 Comparison of Data Acquisition Devices 130

A.2 Extracting Phase and Amplitude of a signal using Hilbert Transform 132

B Bayesian Decoder 133

B.1 Performance Metrics 133

B.1.1 Accuracy 134

B.1.2 Precision 134

B.2 Pseudocode for the Bayesian Decoder 134

C Statistical Concepts 136

C.1 P-value 136

C.2 Z-test 137

C.3 T-test 138

C.3.1 One-Sample T-test 138

C.3.2 Two-Sample T-test 139

C.3.2.1 Student's T-test 139

C.3.2.2 Welch's T-test 139

C.4 F-test for Equality of Variances 140

C.5 The Mann-Whitney U-test 140

C.6 Cohen's d 141

C.7 The Rayleigh Test 142

Bibliography **143**

Curriculum Vitae **169**

List of Tables

3.1 Summary of selected experiments 41
3.2 Specification of PW6D single point load cell 49
3.3 Summary of cluster statistics 60

4.1 Significance of the hysteresis effect 69
4.2 Comparison of head bobbing frequency 71
4.3 Correlation of theta frequency and speed for different rats 77

6.1 Accuracy of the Bayesian decoders 116
6.2 Performance of the neural Bayesian decoders 117
6.3 Performance of the behavioral Bayesian decoders 118

A.1 Comparison of data acquisition devices 131

List of Figures

1.1 Experimental paradigm 4

2.1 Different stages of bioinspiration 13
2.2 3D place fields in rats 17
2.3 Splitter cell in a T-maze 22

3.1 A rat jumping and ditching 37
3.2 Gap length changes during a titration experiment 42
3.3 Gap length changes during a hysteresis experiment 42
3.4 Experiment rig 43
3.5 Experiment Setup Schematic 45
3.6 Rat cap and marker crown 47
3.7 Cameras and the tracking system 47
3.8 SpikeGLX in action 54
3.9 Cameras and the tracking system 55
3.10 Kinematics of a representative jump 56
3.11 Head bobbing detection 57
3.12 Theta rhythm during a jumping trial 61

4.1 Hysteresis plot 67
4.2 Head-bobbing frequency before jumping and ditching 70
4.3 Neural activity observable in the LFP prior to takeoff 72
4.4 Theta phase precession with the position on a runway 73
4.5 Theta phase precession with the position during jumping 75
4.6 Theta phase precession with the time during jumping 75
4.7 Statistics of theta phase correlation 76
4.8 Theta frequency versus speed 78
4.9 Correlation of theta phase and time of action 80
4.10 Different kinematic phases of jumping 81
4.11 Theta frequency during different kinematic phases of jumping 81

5.1 Place fields anchoring to different frames of reference 86
5.2 Place field aligned with the stationary platform 88
5.3 Place field aligned with the stationary platform 88

5.4 Alignment with different frames of reference for all the rats 89
5.5 Place cell firing during jumping 91
5.6 Place cell firing during ditching 91
5.7 Place cell selective for jumping 93
5.8 Comparison of firing rates for a cell that is selective for jumping 94
5.9 Place cell selective for ditching 95
5.10 Comparison of firing rates for a cell that is selective for ditching 96
5.11 Cell selective for jumping out of the gap at both sides 97
5.12 Retrospective splitter cells 99
5.13 Place cell selective to jumping 100
5.14 Place cell selective to ditching 100
5.15 Significantly selective cells 101
5.16 Selectivity of splitter cells 103
5.17 Differential encoding of splitter cells 105

6.1 Cell firing at the decision point 109
6.2 Predictive firing of a cell that for jumping 110
6.3 Similar pose of the rat at decision point 111
6.4 3D firing rate 111
6.5 Accuracy of the neural Bayesian decoder for a rat 114
6.6 Accuracy of the behavioral Bayesian decoder for a rat 115

Chapter 1

Introduction

Throughout evolution, animals have developed remarkable abilities to navigate, adapt, and respond to diverse environmental challenges. Their adeptness in navigating complex terrains without the assistance of sophisticated technologies, their capability to make rapid decisions under high-stakes conditions, and their innate propensity to learn and apply knowledge to subsequent encounters are all hallmarks of nature's designs. At the heart of these incredible abilities, the brain serves as a repository for the various tactics and processes that govern these actions.

This dissertation aims to shed light on the intricacies of the hippocampus, a brain region crucial for spatial navigation, memory, learning, and decision making [3]. By studying rats as they undertake complex locomotor tasks, this work seeks to look closer at the intricate functionality of the brain during these tasks. The insights gained from this dissertation could potentially lead to the development of novel bioinspired algorithms for the navigation of mobile robots.

1.1 Background

Historically, the nervous system was hypothesized to be a static network that receives sensory information from the environment, processes it, and sends motor commands to interact with the environment [4]. This view, known as the 'sensorimotor hypothesis', sees behaviors as simple reactions to sensory triggers. However, this perspective has been refuted over the last century, with accumulating evidence suggesting that nervous systems actively change their connectivity and spontaneously generate behavior [5].

Such plastic neural dynamics assist organisms in achieving goals, including modulating their sensory feedback. While earlier scientific works favored the notion of nervous systems as passive systems reacting to stimuli, newer findings introduce the idea of central pattern generators and spontaneous neural activity, indicating the presence of an intrinsically dynamic and active nervous system [6]. Given this paradigm shift, it is crucial to perceive the nervous system as an entity that proactively produces behavior and is shaped by sensory feedback rather than merely reacting to the external world [5].

Many researchers have built upon the principle that states every behavioral action is associated with neural activity within the brain, thereby exploring the relationships between specific neuronal circuits and behavioral outcomes [7]. The renowned psychologist Donald Hebb proposed a neuropsychological theory of behavior based on the physiology of the nervous system and the concept of 'cell assemblies', which represent perceptual integration through repeated transmission across synapses[1]. Carla Shatz rephrased Hebb's principle as "cells that fire together wire together" [8]. This principle provided a framework to explain

[1] Junctions between neurons where neural signals are transmitted.

how repeated neural connections strengthen and shape behavior, leading to the formation of learned patterns and memories [9].

Another classic illustration of this principle is the 'operant conditioning' behavior observed by Skinner in the mid-20th century, where animals learn from past experiences, and the neural substrate of this behavior was discovered in the 1990s [10]. Building upon this foundation of understanding behavior through neural activity, this dissertation aims to delve deeper by focusing specifically on the neural representation of complex locomotor behaviors demonstrated by animals.

Squirrels are excellent models for investigating the complex locomotor behavior in animals [11]. They display exceptional agility, navigating complicated environments by striking a balance between distance and branch flexibility when jumping [12]. This impressive ability results from evolved biomechanical adaptations and learned behaviors. This thesis aims to identify the neural underpinnings of such extraordinary behaviors. To accomplish this, rats, close evolutionary relatives of squirrels [13], were studied as they undertake complex locomotor tasks.

Previous studies, such as those using virtual reality [14, 15] or honeycomb mazes [16], have relied on intricate and innovative engineering setups to explore hippocampus-dependent spatial navigation. In a similar approach, this dissertation presents a novel experimental rig designed and constructed to collect kinematic and neural data from rats.

This thesis presents the neural basis of complex locomotor behaviors and contributes to the field of behavioral neuroscience. It also provides insight into the neural encoding inside the hippocampus during behaviors mentioned above, and the underlying principles could potentially be applied in algorithms to facilitate robots in replicating such behaviors.

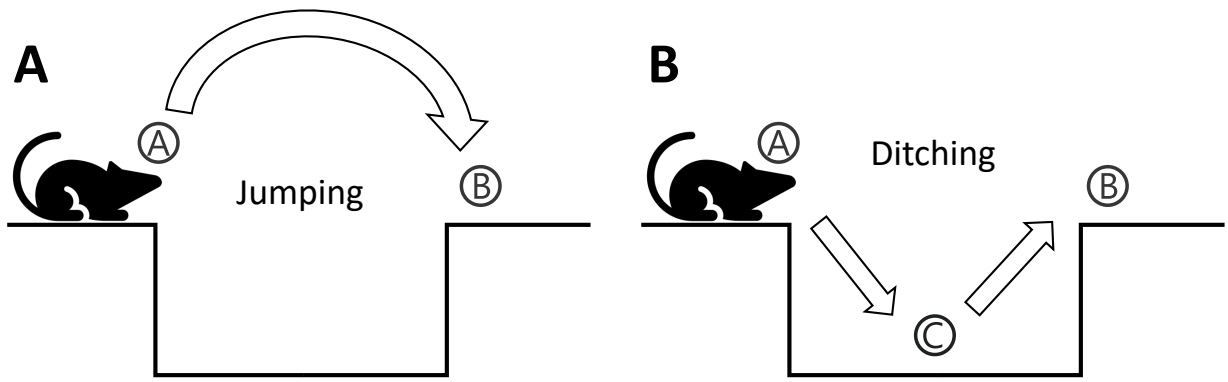

Figure 1.1: Schematic illustrating two actions of a rat: (A) Jumping over the gap and (B) 'Ditching' the gap, where the rat jumps into the gap and then jumps out.

1.2 Research Objectives

The primary objective of this dissertation is to unravel the role of the hippocampus in encoding 3D trajectories during complex locomotor tasks. The hippocampus, also known as 'inner GPS', is a brain region integral to spatial cognition [17]. This research provides insight into whether the neuronal activity in the hippocampus differentiates between distinct 3D trajectories resulting from an animal's navigational choices. As depicted in Figure 1.1, a rat faces a gap it must cross to receive a food reward. The animal has the option to jump over the gap or jump into and then out of the gap, a process called 'ditching' in this thesis.

The study investigates whether hippocampal cells exhibit selectivity in their firing patterns when an animal opts to traverse directly from point (A) to (B) by jumping (see Figure 1.1) or instead chooses to navigate from point (A) to an intermediary point (C) before reaching point (B). Even though these two distinct 3D trajectories would appear similar when projected onto the surface of the experiment rig, it remains an open question whether the hippocampal cells respond differently to them. Ultimately, this investigation probes whether the hippocampus encodes a rat's navigation across various real-world 3D trajecto-

ries in unique and identifiable ways.

Furthermore, this thesis also aims to inspect the retrospective coding aspect of hippocampal cell activity, wherein hippocampal cells discriminate between the aforementioned 3D trajectories at locations beyond the gap after the rat has crossed it. This aspect of encoding is closely related to memory and learning processes, and by differentiating between past experiences, rats may be able to use this information to make well-informed decisions in the future.

Additionally, the predictive aspect of hippocampal cell activity forms another significant pillar of this study. The research aims to investigate whether these cells contain anticipatory information, offering foresight into the animal's forthcoming actions based on the properties of their hippocampal cells, such as the average firing rates before the initiation of a locomotor task. This predictive information, if present, will be utilized to train a Bayesian decoder to predict the rats' future behaviors.

The broader objective of this thesis encompasses the potential applications of the obtained insights. It attempts to enhance our understanding of spatial cognition, complex locomotor actions in animals, and their influence on neuronal activity. It is hoped that these findings will inspire advanced engineering techniques and algorithms that can enhance the navigational abilities of robots in complex environments.

1.3 Significance of the Study

This dissertation advances our understanding of spatial cognition by analyzing the role of place cells in the hippocampus during complex locomotor behaviors. The hippocampus is

a crucial brain region involved in memory consolidation, cognition, and spatial navigation, and the hippocampal place cells encode the location of an animal (see Section 2.3 for more details). The hippocampus uses spatial and temporal markers as mainstays to structure experiences into specific contexts, thereby creating episodic memories [18]. Yet, the mechanism through which encoding occurs within the hippocampus remains to be fully understood. The findings of this research contribute to ongoing investigations aimed at unraveling the intricate functions of the hippocampus.

Moreover, the research underscores the potential implications for enhancing robotic functionality in addressing complex navigational tasks. Inspired by animal optimization strategies, scientists have sought to emulate these algorithms to advance artificial computing. This study provides novel insights into the decision-making and path-planning strategies evident in the complex locomotor behaviors of animals. Understanding how place cells in the hippocampus encode and predict various 3D trajectories provides insight into possible applications in an engineering context, enhancing the decision-making and navigational capabilities of mobile robots.

1.4 Scope and Limitations

For this dissertation, Long-Evans rats were chosen as the animal subjects due to their well-documented cognitive abilities [19]; however, since they were inherently terrestrial animals and raised in cages, they were not capable of performing complex locomotor tasks comparable with wild arboreal squirrels. Despite these limitations, and by using the training techniques developed for this thesis (see Section 3.1.1 for more details), laboratory rats jumped up to

three times their body length during the experiments.

Regarding the experiment paradigm, the focus was on specific behaviors such as jumping and ditching. These behaviors are the building blocks of more complex agile proto-parkour behaviors that animals are capable of, as their survival in nature depends on them. Although this thesis includes a kinematic analysis, a comprehensive biomechanical analysis of jumping and ditching is beyond its scope. Moreover, the focus of this research is on the neural basis of the short-distance and short-time navigation and planning of rats. Therefore, the neural mechanism of long-distance navigation of migratory birds [20], aquatic animals, and insects [21] is beyond the scope of this dissertation.

In terms of the neurophysiological scope, this dissertation is restricted to the hippocampus, a specific region of the brain involved in cognitive navigation, due to the intricacies of neurophysiological studies and the expertise and focus of the collaborative lab on hippocampal formation. The hippocampus has a crucial role in cognitive path planning. Still, it is not the only brain region involved in executing complex locomotor behaviors and the decision-making processes related to these behaviors. Other regions, including the primary motor cortex, premotor cortex, prefrontal cortex, and the posterior parietal cortex—a brain region that encodes head and body posture [22], are integral to these functions. Preliminary data were also gathered from the posterior parietal cortex during the hippocampal recordings. However, a comprehensive investigation of these regions fell outside the scope of this dissertation.

1.5 Research Contribution

Although the hippocampus has been extensively studied in the context of spatial navigation, its role during complex 3D locomotor behaviors such as jumping has not been thoroughly explored. Previous investigations of place cells in rats have typically involved encoding of 2D surfaces, as the physical limitations necessitated that rat navigation remains restricted to the surface of the experiment rig. However, when a rat jumps over a gap, it effectively bridges two topologically disconnected locations, thereby moving beyond the constraints of conventional navigation on the surface.

This research represents a departure from prior studies, as it is one of the few that focuses on the functioning of place cells during such complex locomotor behaviors. A key finding of this research is that place cells encode 3D trajectories differently when rats choose to perform different actions, even in the absence of reward contingency or any external cue.

Splitter cells are a type of place cells that exhibit different firing rates at a specific location depending on the animal's previous or upcoming path [23], essentially splitting the trajectories (see Section 2.6 for more information). One of the essential contributions of this dissertation is the identification of a splitter-like functionality in place cells. These cells exhibited different firing patterns for different behaviors, a trait reminiscent of the splitter cells identified in earlier studies [24]. This evidence implies that place cells can modify their firing properties to align with the structure of the task at hand.

This research shed light on the role of place cells in encoding predictive information before complex locomotor behaviors. Such predictive encoding might hint at a causal role in decision making or path planning, thereby enriching the perspective on these cells. This provides

fresh insights regarding the brain's methods of prediction or planning before traversing 3D environments.

1.6 Organization of the Dissertation

This dissertation is organized into seven chapters. After this introductory chapter, Chapter 2 presents a literature review on spatial encoding, the firing properties of place cells during different tasks, predictive coding, and the role of place cells in 3D navigation. Chapter 3 outlines the methodology employed in the study, detailing the subjects, experiment paradigm, data acquisition techniques, and data analysis approaches used. Chapter 4 explores the behavioral, kinematic, and neural correlates of jumping and ditching, with a particular emphasis on examining the properties of neural signals during the various kinematic phases of jumping. Chapter 5 examines the firing properties of place cells during these complex locomotor behaviors, with a particular focus on trajectory selectivity and retrospective coding. Chapter 6 delves into the predictive nature of place cell activity, exploring the differences in firing rates for jumping and ditching and evaluating the accuracy of a Bayesian decoder in predicting these behaviors. The final chapter, Chapter 7, recapitulates the main discoveries of the research, explores their significance in the context of spatial navigation, and suggests potential directions for future research.

1.7 Dissemination

Elements of the work completed in this dissertation have been shared with the wider academic community. Parts of the findings from Chapter 4 were shared at the Dynamic Walking Conference in 2020 [25]. Likewise, salient anecdotes from Chapter 5 were presented at the Society for Neuroscience Conference in 2022 [1]. Lastly, the integral components of Chapter 6 have been submitted for presentation at the upcoming Society for Neuroscience Conference in 2023 [2]. I have been extensively involved in all aspects of the research, including the design of the experiment rig, the development of both hardware and software, as well as data collection and extensive data analysis. However, tasks such as constructing the experimental rig, training the animals, conducting experiments, performing animal surgeries, and preprocessing the neural data were carried out with the invaluable assistance of the collaborators. The principal investigators provided consistent oversight and guidance across all research stages.

Chapter 2

Literature Review

This chapter reviews the existing literature on bioinspired robotics, hippocampal studies, and neural recording technologies, alongside exploring the decoding techniques and the current gaps in the field. This collection of knowledge serves as the foundation for understanding the research questions that drive this dissertation.

2.1 Bioinspired Robotics

Bioinspired robotics is an expanding field that involves designing and implementing principles, mechanisms, or algorithms derived from biological organisms, systems, and processes. This approach to robotics draws inspiration from the adaptive and versatile behaviors observed in nature to enhance robotic functionality and overcome various challenges with which traditional robotic methods struggle [26]. Specifically, studying animals' locomotor dynamics, sensory perception, and even social behaviors has inspired engineers and researchers to develop advanced algorithms and innovative robotic creations. Bioinspired roboticists create

and utilize models of animal locomotion that integrate biomechanics, neural control, sensing, planning, and learning [6]. The objective of bioinspired robotics is to draw inspiration from biological principles to design robots with at least some of the desirable properties, such as adaptivity, robustness, versatility, and agility comparable to animals [27–29].

An exemplary category of bioinspired robotics is jumping robotics. Many terrestrial and aquatic animals, including locusts, fleas, frogs, kangaroos, and dolphins, utilize jumping strategies [30]. Some of these strategies have been studied and subsequently inspired the design of state-of-the-art jumping robots. The studies take into account factors such as takeoff kinematics (e.g., angle, direction, velocity) and stability to understand the biomechanics of jumping [31]. These studies provide valuable insights for the future development of bioinspired jumping robots [32]. For instance, one study demonstrated that gliding geckos first hit vertical surfaces by head at high speed and then pitch back, relying on their tail to absorb the impact and stabilize the landing, a finding corroborated by experiments with bioinspired robotic models that also showed better landing success with an active tail reflex [33].

As illustrated in Figure 2.1, bioinspiration can happen at different levels: biomechanics, locomotion control, and high-level cognitive control [34]. Examples of biomechanical bioinspiration include mass-spring models of monopodes [35, 36], soft robots [37] and gecko-inspired surface climbing robots [38, 39]. Bioinspired locomotion control includes feedforward control[1] in hexapod robots such as RHex [35, 36], and also getting inspiration from central pattern generators (CPGs)[2] for the control of robot locomotion [6, 40, 41]. Reinforcement learning is an example of high-level cognitive bioinspiration, which is inspired by the learn-

[1]Preflex is a form of passive control.
[2]CPGs are neural circuits that produce coordinated rhythmic outputs from simple inputs.

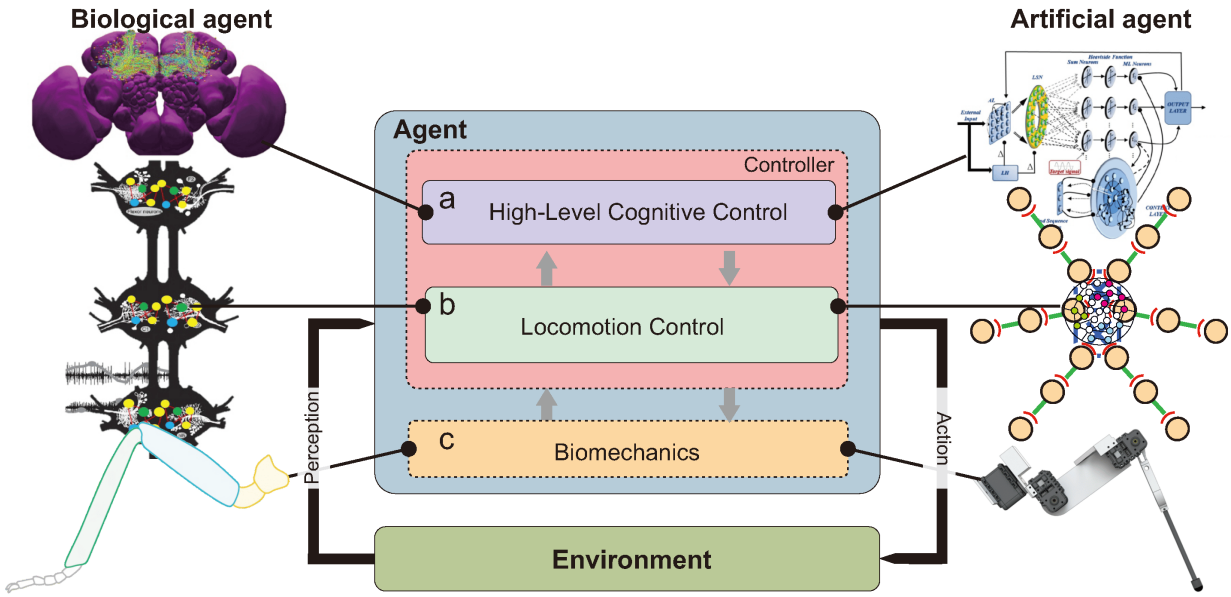

Figure 2.1: Illustration of the various levels of bioinspired robotics, comparing the biological components of an insect to their robotic counterparts: (a) High-level cognition control, (b) locomotion control, and (c) Biomechanics. Image reprinted from [34]. Copyright 2021, MDPI. Used under the terms of the Creative Commons CC BY license.

ing process animals undergo during operant conditioning [42]. Other examples of high-level cognition include bioinspired localization, mapping, and spatial planning (see Section 2.2).

The focus of this dissertation is to study the hippocampus of rats during complex locomotor tasks. This research aims to broaden our understanding of the intricate capabilities of the brain and potentially inspire high-level cognitive algorithms for future robots. In the next section, bioinspired algorithms are explained in detail.

2.2 Bioinspired Algorithms

Bioinspired algorithms (also known as bioinspired computing [43]) is a category of bioinspiration that focuses beyond animal locomotion to investigate optimization strategies uti-

lized by nature [44]. A prime example is the artificial neural network, inspired by the neural network in the brain, as described in McCulloch and Pitts' seminal paper [45]. Other examples of bioinspired algorithms include genetic algorithms [46], particle swarm optimization [47], and cuckoo search [48]. For instance, the cuckoo search algorithm, derived from the breeding behavior of certain cuckoo species, utilizes the natural behaviors of these birds to efficiently search for optimal solutions in computational contexts [48]. These examples highlight how animal behavior can inspire advanced computational methodologies.

One example of bioinspired algorithms used in robotics is a neuro-inspired spatial navigation model based on the model of the rodent hippocampus. It was first developed and tested on mobile robots in the early 1990s [49]. Subsequent studies extended this idea by incorporating other elements in the rat brain, such as head direction cells, to achieve comparable performance on robots as animals during similar behavioral tasks [50]. RatSLAM (Short for Rat Simultaneous Localization and Mapping) is another bioinspired algorithm inspired by computational models of the rat hippocampus. RatSLAM mimics the biological models related to animal navigation to create a computational model that enables a robot to build a map of the nearby environment while determining its location within that map [51]. The development of RatSLAM and similar algorithms highlights the importance of bioinspired approaches in robotics, demonstrating how studying natural processes can lead to significant technological innovations.

Therefore, a behavioral and neural study of animals is not only crucial for advancing our scientific knowledge but also important for broadening technological methodologies and algorithms. In the subsequent sections, the focus will transition to reviewing neuroscience literature to get familiar with the neural foundations underlying this research. The majority

of these studies are based on rodents, particularly rats. Any studies involving humans or other species will be explicitly highlighted.

2.3 Place Cells and the Cognitive Map

The idea of spatial representation inside the brain was conceptualized as a 'cognitive map' by Edward Tolman in 1948 when studying the behavior of lab rats in mazes. Tolman proposed that rats can learn and navigate their environment using mental spatial representations, suggesting that behavior is guided more by understanding the overall spatial layout rather than solely by individual sensory stimuli [52].

Later, O'Keefe and Dostrosky provided evidence that this cognitive map has a neural representation inside the hippocampus. They demonstrated that the firing rate of the pyramidal cells in the hippocampus of freely behaving rats increases substantially when the animal occupies a specific location within its environment. In other words, these neurons encode the spatial information. This showed the existence of a spatial map of the environment inside the hippocampus [53]. In subsequent studies, O'Keefe referred to these cells as 'place cells', with their corresponding locations known as the 'place field' [54]. Building on these findings, O'Keefe and Nadel proposed that the hippocampus integrates various stimuli into a coherent cognitive framework rather than separate stimulus traces or disconnected pairwise associations [55].

Many other researchers corroborated this theory. In one study, Morris devised a water navigation task to investigate spatial memory in rats. He demonstrated that rats can learn to locate an unseen, unheard, and unscented object in a fixed position relative to the room's

distal cues [56]. Other studies showed the importance of task structure and context in the information encoded by the hippocampus. For example, McNaughton et al. showed that the firing of place cells on linear tracks was not only associated with a rat's location but also with its direction of movement. Specifically, place cells exhibited a distinct firing pattern depending on whether the rat was moving one way or the other, revealing the cells' sensitivity to directionality [57]. However, such directionality was not generally observed in random foraging tasks where rats moved randomly on a horizontal plane, suggesting that the linear structure of the track might induce this directional firing property. There have been many studies to understand how the hippocampus forms the cognitive map [58, 59]; however, there is still no conclusive answer to this question.

Place cell research has predominantly focused on 2D and horizontal tasks, such as planar mazes, despite animals interacting with a 3D world [60, 61]. Kate Jeffery led a novel study observing rats navigating vertical pegboards and discovered the presence of 3D place fields [62]. The study found that the encoding of 3D space in the mammalian brain is anisotropic, meaning cognitive maps have less resolution for vertical spaces than horizontal ones. After studies in flying bats revealed isotropic spherical place fields [63], Jeffery and her team conducted a comprehensive study on place cells in 3D space in rats [64]. In their research, a tiltable 3D lattice was used, allowing for more natural locomotor behavior of the rats while moving in a 3D environment (see Figure 2.2). The study found that ease of movement in a certain direction, not the direction of gravity, impacts how accurately the rats' brains map out the environment. Therefore, even though rats are terrestrial animals, their place cells encode 3D space. As will be explained later in this dissertation, the feature is useful when rats perform complex locomotor actions such as jumping.

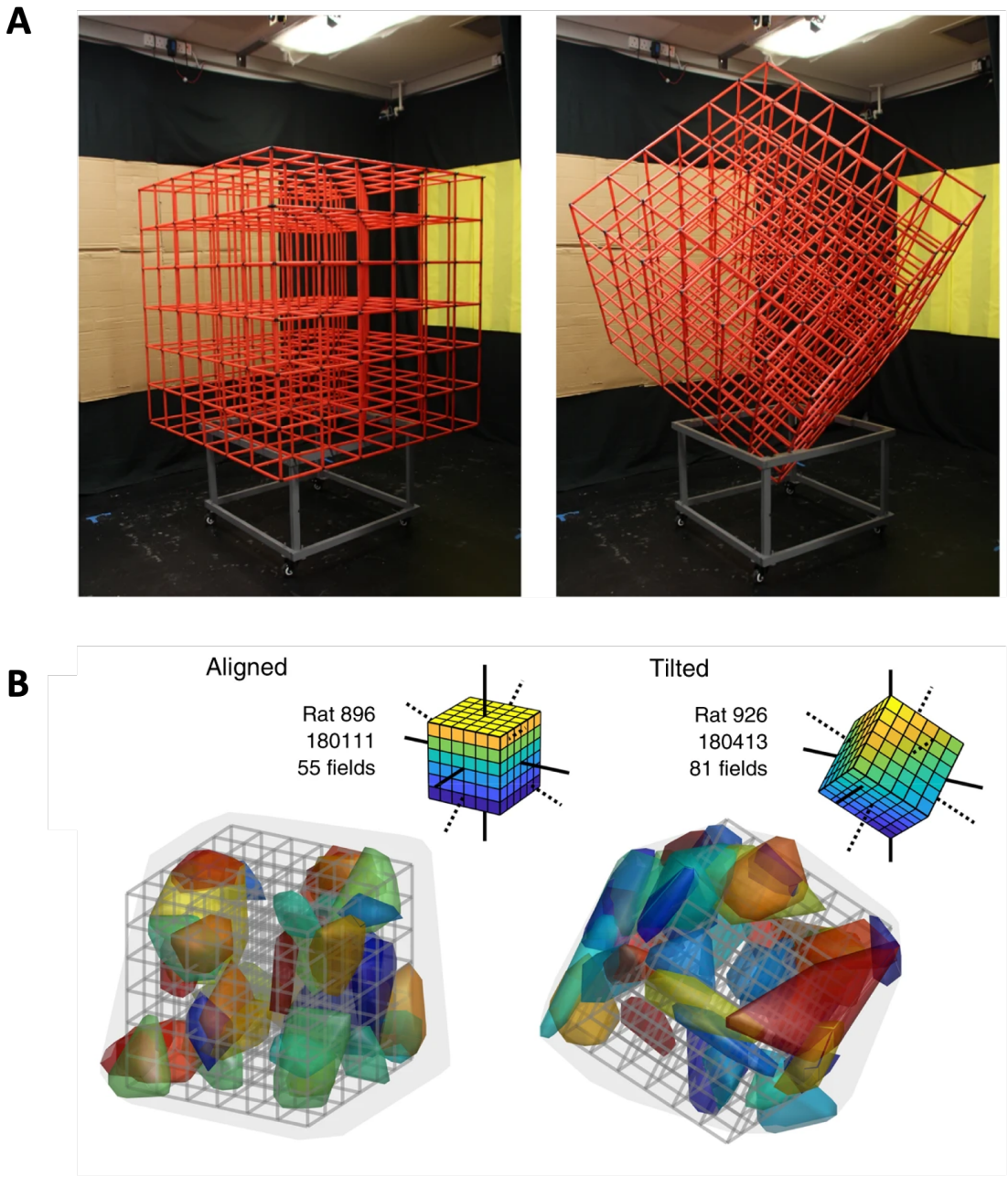

Figure 2.2: Illustration of 3D place fields in rats. (A) A 3D lattice both in its aligned (left) and tilted (right) configurations. (B) 3D place fields for the aligned (left) and tilted (right) orientations are depicted by different colors. Place fields appear elongated along the lattice's axis, indicating the ease of movement affects the shape of the place field. Image modified from [64]. Copyright 2020, Springer Nature. Used under the terms of the Creative Commons CC BY license.

Despite being named for their spatial encoding abilities, place cells can encode much more than just space [65]. For example, in time-based experiments, place cells fire at specific moments during the experiment, representing the progression of time in memories and providing an additional dimension to spatial mapping [66]. Consequently, these cells—despite being anatomically identical to place cells—are referred to as 'time cells' in these studies. Other nonspatial encoding examples by hippocampal place cells include auditory temporal and pitch information during auditory-discrimination tasks [67] and odor during odor-discrimination tasks [68].

This dissertation investigates rats engaged in natural yet complex locomotor behaviors, such as jumping, to enhance our understanding of both spatial and nonspatial encoding of the hippocampus. However, it is important to note that the hippocampus functionality is not limited to encoding current information alone. Research has revealed that hippocampal neurons are multifaceted in their encoding capabilities. These cells not only encode present experiences, but they also retain past events through retrospective encoding and anticipate near-future occurrences via prospective encoding [69]. Such capacities play a pivotal role in memory formation and decision making, especially within the context of spatial navigation tasks. An overview of these aspects is provided in the following sections.

2.4 Hippocampus and Memory

The association of memory with the hippocampus was originally an accidental discovery. In 1953, when Henry Molaison had his hippocampi removed bilaterally as a treatment for his epileptic seizures, it was observed that he was incapable of creating new episodic

memories[1] [70]. This critical finding was replicated by subsequent research on rats. In these studies, lesions to the hippocampus demonstrated its important function in memory consolidation and learning [71].

Neurophysiological studies on hippocampal place cells in rats displayed increased firing activity during sleep after exposure to their specific place fields, suggesting potential information processing regarding the previous tasks during sleep [72]. The following studies in rats revealed that place cells that were active during spatial tasks not only exhibited correlated firing during subsequent sleep but also the patterns during sleep reflected both the activity and temporal order of firing from earlier exploration. This ordered rather than scattered re-expression of the information from waking experiences suggests a role in memory consolidation [73, 74]. This phenomenon is called 'replay' as if it is replaying the firing pattern during an experience.

A later study by Foster and Wilson demonstrated that the rat hippocampus replays recent spatial experiences in a reversed sequence during awake periods [75]. This reverse replay of past movements is hypothesized to play a role in evaluating event sequences in reinforcement learning models and potentially represent a general mechanism of learning and memory. Moreover, disruption of the replay events in awake rats caused a deficit in learning spatial memory-related tasks, indicating the role of replays in memory consolidation [76].

As the research on the hippocampus and its role in memory expanded, it became apparent that this brain structure is instrumental in a complex form of memory known as 'episodic memory' or the more cautiously phrased 'episodic-like memory' in the context of

[1] As will be further elaborated later in this section, episodic memory refers to the ability to recollect specific events or episodes from one's life, including the 'what', 'where', and 'when' of the event.

nonhuman animals [77–79]. This type of memory is characterized by the ability of animals to integrate information about the objects (what), their location (where), and the time of the event (when) from past episodes, hence forming a comprehensive memory of specific experience [80].

It has been theorized that the hippocampus organizes information within a multidimensional cognitive map encompassing spatial, temporal, and associational contexts. It utilizes the cognitive map as a substrate for encoding experiences as episodic memories [17, 18].

2.5 Hippocampus as a Predictive Map

Similar to the reverse replay experiment mentioned in the previous section, Diba and Buzsaki demonstrated that, on a linear track, place cells of rats not only fire in a reverse replay at the end of the track but also fire in a forward sequence before the start of the run at the beginning of the track [81]. This firing sequence has been termed 'forward replay', suggesting that the cells might anticipate the impending run.

Studies have shown that the hippocampus has a significant role in planning and decision making, particularly in spatial navigation tasks [82]. For example, a study by Pfeiffer and Foster showed that the rat hippocampus generates brief sequences before goal-directed navigation in an open area. These sequences anticipate future behavior by encoding the trajectories from the rat's current location to a known goal location [83]. It indicates the potential of these forward replay sequences in supporting a goal-directed, trajectory-finding mechanism in navigation and exhibits prospective coding for planning future trajectories in the hippocampus. Moreover, damage to the hippocampus in humans has been shown to

impair the ability of patients to envision future events [84].

Research led by Loren Frank demonstrated that in a spatial decision-making task, place cells could predict the outcome of the trial. During the decision-making time, the hippocampal activity portrayed several paths that covered both the chosen and unchosen options. This indicates that the hippocampus is involved in evaluating potential choices during memory-driven decision making [85, 86]. A similar activity occurs in the hippocampus during vicarious trial and error and is involved in decision making and planning [87]. See Section 2.7 for more details about this phenomenon.

Hippocampal place cells encode both predictive and reward information; from a reinforcement learning view, they form a predictive representation [88]. For these reasons, the hippocampus is called not only the cognitive map but also the predictive map. The cognitive map is utilized in order to plan ahead and make informed decisions [89].

2.6 Splitter Cells

As discussed in the preceding sections, hippocampal place cells can encode retrospective trajectories, which represent the paths an individual has previously taken, and prospective trajectories, which represent potential future paths. In a study by Frank and Wilson, many neurons in the hippocampus exhibited different firing rates for the same position based on the rat's previous location or intended destination [90]. These hippocampal neurons are referred to as 'splitter cells' since they split trajectories. They differentiate and encode distinct memory tasks, even when the rat's physical behavior and location remain unchanged. This means that despite a lack of change in observable behavior or location, these cells are still

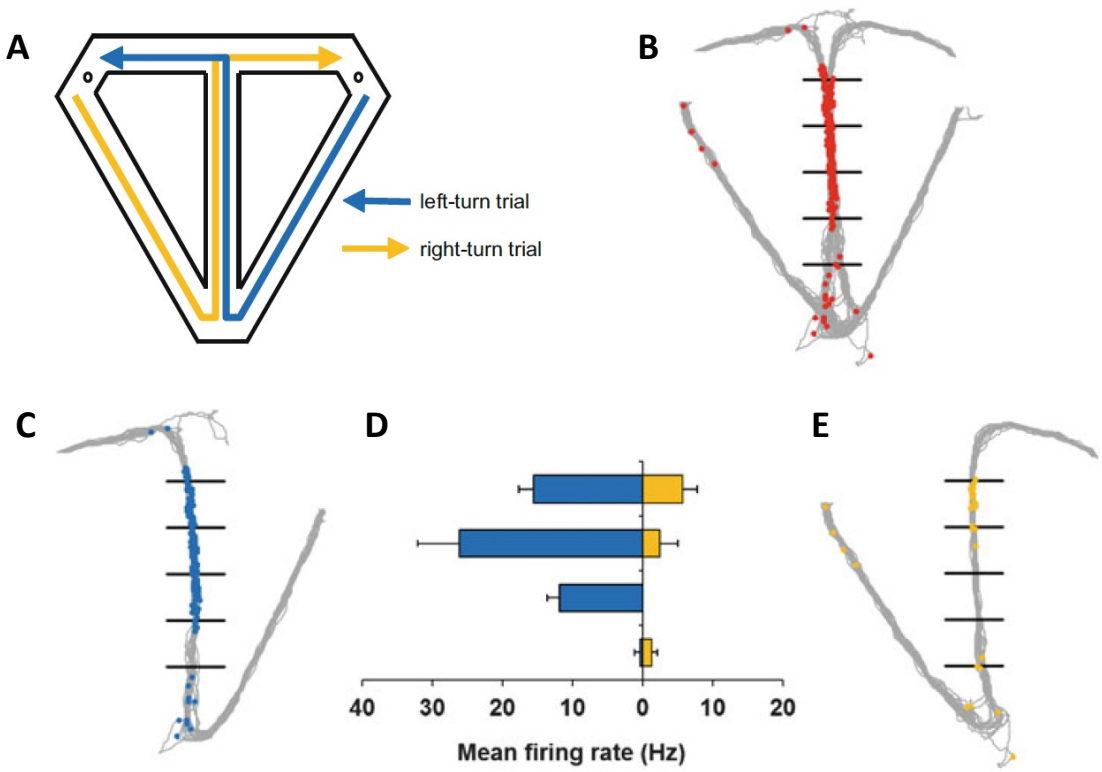

Figure 2.3: Illustration of activity of a splitter cell in the modified T-maze used in the Wood et al. study [92]. (A) Arrows demonstrate the trajectory of the rat during the alternation task. (B) The occupancy of the animal is shown as gray dots, and the place field is highlighted in red. (C) The place field in the left-turn trials is shown in blue. (D) Comparison of the firing rates of the cell in left-turn and right-turn trials in different segments of the middle arm. (E) The place field in the right-turn trials is shown in yellow. The splitter cell is active during left-turn trials but almost silent during right-turn trials. The place cell splits the trajectories based on the previous or future paths. Image modified from [23]. Copyright 2014, Springer Nature. Used with permission.

actively encoding different information based on the cognitive task at hand [23]. The activity of splitter cells is based on the chosen trajectory, irrespective of the external cues [91].

In a concurrent study by Emma Wood et al., rats were trained on a modified T-maze in which they alternated between turning right and left, creating a movement pattern resembling a figure-eight [92]. Figure 2.3 illustrates a splitter cell in the modified T-maze used in the study. The animal should alternate between left and right turns to get the food reward. The figure shows the occupancy of the animal, the place field of the cell in different trials,

and a comparison of the firing rates of the cell in left-turn and right-turn trials in various segments of the middle arm. The study demonstrated that most of the hippocampal place cells in the central stem showed different firing rates based on the rat's direction of journey, while the remaining exhibited consistent firing. This indicates that while some cells encode the present location of the animal, others may encode details about the task in the ongoing trial.

Splitter cells encoding information about the recent past, the present, and the imminent future can be interpreted as a neuronal mechanism for episodic memory for a specific experience [69]. There is also substantial evidence that within a trial, splitter cells are involved in decision making in spatial tasks [93].

2.7 Vicarious Trial and Error

Vicarious trial and error (VTE) refers to a specific behavior observed in rats when faced with a challenging decision [94]. When at a choice point, rats often pause and move their heads from one direction to another, seemingly attempting to choose between the options [95]. This behavior was first documented and named by Muenzinger et al. in the 1930s [96, 97].

Neurophysiological studies have shown the relationship between hippocampal function, VTE, and learning. Rats with hippocampal lesions and without (sham-lesioned) were trained on a nonspatial discrimination task. The number of times a rat moved its head between stimuli was counted as a VTE instance. Findings showed that rats with hippocampal lesions exhibited fewer VTEs and either learned much more slowly or did not learn the task at all. As rats became more proficient in the task, VTE frequency decreased [98].

A key study by Johnson and Redish indicated that neural ensembles in the hippocampus of rats transiently encode potential future paths when the animal is at a decision point [99]. Representing future trajectories rather than recently traveled trajectories is likely influenced by cognitive mechanisms and task demands rather than a passive computation; therefore, hippocampal spatial processing is an active process. Moreover, it suggests that VTE is a behavioral correlate of an underlying neural search process during deliberative decision making. This hippocampal activity of alternating between potential path options suggests a neural mechanism for contemplating future outcomes akin to human deliberative decision making and mental time travel [87].

2.8 Hippocampal LFP and Behavior

Local Field Potential (LFP) refers to the electrical activity recorded in the brain, representing the ensemble activity of a population of neurons. This collective activity exhibits variation across different brain areas and can be sorted into several distinct patterns based on signal frequency content.

Specifically in the hippocampus, LFP comprises both rhythmic (including theta at 6-12 Hz and ripples at 100-200 Hz) and non-rhythmic patterns, such as the Large (amplitude) Irregular Activity (LIA) [100]. LIA is identifiable by sharp waves, an intermittent burst of synchronized neural activity, and is observable as a large deflection in the LFP signal [101]. Sharp waves happen about a hundred milliseconds, but the LIA state can last seconds to minutes, depending on the behavior. LIA is observable at times when the animal is sitting quietly, predominantly during eating, grooming, drowsiness, and the slow wave sleep (SWS)

phase [100]. High-frequency ripples occur concurrently with sharp waves, making sharp waves and ripples (SWRs) a hallmark activity in the hippocampus [102]. Figure 3.8 depicts hippocampal sharp waves and ripples of a freely moving animal during a sleep session. The forward and backward replay phenomena discussed in earlier sections take place during SWR events.

Seminal research by Case Vanderwolf established robust correlations between LFP patterns and various behaviors, illustrating changes in the frequency and amplitude of theta rhythm across different actions [103]. The theta rhythm, a distinct oscillatory pattern, happens in animals during activities like walking, running, jumping, exploratory head movements, attentive pauses (like exploratory sniffing or fear-induced freezing), and the rapid eye movement (REM) phase of sleep [100]. Although pronounced theta rhythm is observed during the jumping behavior, studies have shown that disruption of theta does not change the jumping performance of rats, suggesting that theta might be an indicator but not an initiator for jumping behavior [104]. VTE (as explained in Section 2.7) is also another phenomenon during which theta rhythm is clearly visible in the neural recordings [87]. It is important to note that SWRs rarely occur during the theta rhythm [100].

The hippocampus is traditionally believed to mainly represent higher cognitive and locomotor variables like position, speed, and direction [57]. Meanwhile, limb movements are typically linked to subcortical circuits, spinal cord, brainstem, and cerebellum [105, 106]. However, many studies have shown the link between different motor behaviors and theta rhythm. For instance, head movements of running rats display oscillations in the same frequency range as the hippocampal theta rhythm [107].

Moreover, recent work by Joshi, Frank, et al. examined the correlation between hip-

pocampal spatial representations and the stepping rhythm during locomotion [108]. In their study, synchronization between the forelimb stepping cycle of the rats and the modulation of hippocampal activity was observed, both peaking at around 8 Hz during movement. When the forelimbs of the rats touched the ground, the hippocampal representation closely aligned with the actual position of the rat's nose (head). This coordination became especially pronounced when rats faced spatial decisions, highlighting a rapid interplay between cognitive and sensory-motor circuits.

2.9 Theta Phase

Hippocampal place cells use both temporal and rate coding to represent spatial aspects of an animal's environment. A key component in the temporal coding of hippocampal LFP is 'theta phase precession'. O'Keefe and Recce observed rats traversing through their place fields on a linear track. They noted that the place cells began firing at a specific phase of the theta cycle as the rats entered the respective fields. As the rat continued moving through the corresponding place field of these cells, the cells fired at steadily earlier phases of the theta cycle, a pattern referred to as theta phase precession [109]. Their findings illustrated a correlation between the phase of cell firing and the position of the rat within the relevant place field.

Studies showed that the theta phase correlates with both position and time, with a notably stronger correlation with position than time [110]. Phase precession is observed both on linear tracks and open environments. On linear tracks, most place cells show sequential activities within the theta cycles, following the same order as their fields on the track.

Temporal sequences from these cells are condensed within theta cycles, potentially facilitating sequential learning and enhancing the time dimension of hippocampal memories [111].

2.10 Behavioral Studies

2.10.1 Psychometrics

Psychometric analysis is employed in various fields, including psychology and neuroscience, to quantitatively assess the relationship between stimulus levels and a subject's responses [112]. The psychometric functions (curves), usually presented as sigmoid functions[1], describe how the perceptual processes relate to decision making in different tasks, such as detecting a faint stimulus or discriminating between two stimuli [113]. For example, in a study by Zhong et al., mice had to detect if an audio frequency was high or low to get a food reward. The plot of the ratios that the animals reported high versus the corresponding audio frequencies formed the psychometric curve for this discrimination task [114].

Non-perceptual decision-making tasks can also be described using psychometric functions, especially when they involve decision making based on accumulated evidence or information. For instance, psychometric functions can be applied to economic decision-making tasks, such as risk preference [115]. Specifically, in the jumping and ditching context, this dissertation presents psychometric functions as a means to show how the likelihood of choosing a risky option (e.g., jumping) versus a safe but more energy-costly option (e.g., ditching) changes as a function of the level of risk (see Section 4.1.1)

[1] S-shaped functions

2.10.2 Head Bobbing

Head bobbing, characterized by 'up and down' head motions, is a behavior observed in nocturnal species like rats. It is hypothesized that this behavior serves as an adaptive mechanism to function in low-light conditions. The rapid movement of the head and body provides them with motion parallax. Motion parallax allows depth estimation from the relative motion of objects as the observer changes their viewpoint, allowing them to perceive depth and distance [116]. This phenomenon appears to be particularly crucial for nocturnal species that might have evolved this behavior to compensate for their lesser reliance on high visual acuity mechanisms such as retinal imaging, which diurnal species like squirrels and Mongolian gerbils utilize [117, 118].

The findings from Parker et al. further reinforce the significance of motion parallax in rodents, demonstrating that when lab mice were deprived of stereo vision, they increased vertical head movements, essentially switching to rely on motion parallax [119]. Building on these insights, this dissertation touches upon a behavioral question: Is head bobbing at the decision point, before jumping or ditching, more indicative of the decision process (similar to VTE), depth estimation, or a combination of both?

2.11 Recording Neural Activity

Since this dissertation involves neural recording, a review of hippocampal studies would be incomplete without discussing the technologies developed for recording the extracellular activity of neurons in freely moving animals. As early as the 1940s, microelectrode recording has been used to capture the activity of individual neurons in living animals [120]. This

method was instrumental in providing insights into the fundamental properties and functions of neurons. The introduction of silicon probes [121] and tetrodes [122] into the field in the mid-1990s marked a significant advancement in the area of neural recording. It enabled the simultaneous recording of neural activity from a larger population of neurons, a feat that was not possible with single-electrode technologies [123].

In recent years, there has been a significant leap forward in the capabilities of neural recording technologies with the development of miniaturized silicon probes, such as Neuropixels 1.0 [124] and Neuropixels 2.0 [125]. These revolutionary devices simultaneously record the activity of hundreds of neurons at 384 distinct recording sites distributed across 10 mm shanks. In animals such as rats and mice, this feature enables recording from multiple brain regions [126]. These probes' small size and lightweight design are particularly noteworthy as they can be utilized in freely moving animals, offering a more accurate representation of neural activity during realistic animal behavior (see Table A.1 for comparison).

In summary, the field has seen a substantial evolution from the single-electrode recording to now being able to observe the intricate networks of activity across hundreds of neurons with tools like Neuropixels. These technological advances have broadened our understanding of neuronal interactions and functions, especially for population activity, paving the way for future discoveries in neuroscience.

2.12 Decoding Neural Activity

Physical variables, such as the animal's position or direction, or behavioral variables, including those related to the animal's decisions, are encoded as activity levels in populations

of neurons. Decoders have been utilized to address the 'inverse problem' by estimating these variables based on the observed neural activity [127]. This process helps measure the amount of information regarding the physical or behavioral variables encoded in the neuronal population.

Bayesian inference is a probabilistic approach neuroscientists use to analyze the neural encoding during perception and decision making [128]. It is also an effective method for decoding the activity of relatively small numbers of neurons [129]. There is also a theory called 'Bayesian brain theory' that claims the brain views sensory data as probability distributions and has a mental model of the environment to make predictions. This mental model is constantly updated based on the Bayesian inference given the error between the predictions and the sensory data [130].

A Bayesian decoder is a statistical tool that applies Bayes' rule to interpret the information content of the neural activity and estimate the probability of specific outcomes [131]. Bayes' rule is a principle in probability theory that formulates the probability of a hypothesis given the evidence [132]. The mathematical representation is:

$$P(H|E) = \frac{P(E|H)P(H)}{P(E)} \tag{2.1}$$

where $P(H|E)$ is the posterior probability, representing the probability of hypothesis H given evidence E. $P(E|H)$ is the conditional probability of evidence E given hypothesis H is true. $P(H)$ is the prior probability, indicating the initial probability of hypothesis H before considering the evidence. Lastly, $P(E)$ represents the total probability of evidence E.

By converting the observed spike patterns into predictions or estimations of the original

stimuli or behaviors, the decoder can decode the activity of single neurons or neural populations [133]. For example, a Bayesian decoder has been applied to predict the most probable locations of the rat given the ensemble firing patterns of hippocampal place cells [134]. Bayesian decoders establish a relationship between a variable of interest (such as a rat's location) and the firing rates of sorted spikes or the characteristics of the unsorted spike waveforms. Once this relationship is established, the Bayesian method is employed to estimate the variable of interest from the observed neural activity [135, 136].

Bayesian decoders can take as input either sorted or unsorted spikes. Sorted spikes are classified to specific neurons, clearly identifying their source. In contrast, unsorted spikes come from multiple neurons without distinct identification. The decoders establish a connection between a particular variable of interest (for instance, a rat's location) and either the firing rates of the sorted spikes or the features of the unsorted spike waveforms. Upon defining this relationship, the Bayesian approach is then employed to estimate the desired variable based on the recorded neural activity [135, 136]. It has been observed that decoders using unsorted spikes tend to perform better than those relying on sorted spikes [137].

2.13 Gaps in the Literature

Despite significant advancements in bioinspired algorithms, behavioral and neurophysiological studies, and neural recording technologies, there remain notable gaps in the existing literature. These gaps present opportunities for further research and investigation.

Even though there have been several bioinspired algorithms for mobile robot navigation and planning (see Section 2.2), there is a notable gap in the field. To the best of my knowl-

edge, no algorithm has been developed that draws inspiration from the cognitive processes observed in the brains of animals during complex locomotor tasks. This gap is partly because there have been limited studies on the cognitive process of animals during complex locomotor tasks such as jumping and ditching.

While place cells are known to encode the entire 3D space [64], most studies have been limited to rat navigation on the surfaces of experimental rigs, with a few exceptions like the recent work led by Buzsaki [138]. For instance, in the study of "hippocampal place-cell firing during movement in 3D space" by Knierim and McNaughton, even though the animals were walking on the inclined planes in 3D space, they were restricted to the 2D surface of the inclined planes [139]. During voluntary movements, rats typically walk on experimental surfaces or use their limbs to navigate vertical surfaces, such as pegboards [62]. Given a direct correspondence between a rat's location in 3D space and its position on a 2D surface in the aforementioned studies, it raises the question: Are the place cells truly encoding the 3D space, or are they only encoding the 2D surfaces? However, in this dissertation, when rats jump over gaps, they connect two topologically disconnected locations, a behavior beyond the conventional surface navigation commonly studied in prior research [140]. By comparing place cell activity during jumping and ditching trials and the fact that these trajectories have similar projections on the 2D surface of the experiment rig, it would clarify whether the place fields encode 2D surfaces or 3D spaces.

Furthermore, the interplay between the jumping behavior in rats and their neurophysiology requires further exploration. More specifically, the relationship between the theta rhythm and kinematic aspects of jumping is not well studied. Studies have shown a correlation between theta frequency and rhythmic locomotor behaviors [108, 141], and strong theta

rhythm has been observed during jumping [103]. A recent study has shown theta phase resting at the time of jumping [138]. Nevertheless, it remains unclear if there is a link between kinematically significant events like the time of takeoff or landing and specific phases of theta. Investigating the correlation between theta phase and jumping behavior could reveal novel insights into how the hippocampus and motor cortex interact during complex locomotor actions.

In previous studies, a correlation between the speed and theta frequency has been observed when the subjects ran on experiment rigs, with their speed being directly influenced by the movement of their limbs [103, 142]. However, it is unclear from the prior studies if the correlation between speed and theta frequency is due to the fact that limb movement is correlated with both speed and the theta frequency [108]. During the aerial phase of a jump, the previously mentioned correlation between limb movement and speed no longer applies. Thus, a jumping experiment provides a unique context to explore the relationship between speed and theta frequency, independent of the limb movement.

There have been limited neurophysiological studies on animals engaged in jumping behavior. In the majority of these studies, a negative reinforcement paradigm was employed, where rats were required to jump in order to avoid electric shocks [103, 104, 143, 144]. Only one recent study utilized a positive reinforcement approach [138]. Furthermore, none of the previous studies have given an alternative choice to the animal other than jumping. By giving the option to the animal to choose between jumping and ditching, the animal would potentially show decision making before jumping behavior. Moreover, VTE, splitter phenomenon, and retrospective and prospective coding during complex locomotor behaviors have not been studied before.

2.14 Summary

This chapter's literature review has highlighted the significance of the neurophysiological study of rats as model organisms for navigational tasks. The hippocampus, regarded as the cognitive map, is crucial in spatial representation. Place cells can capture current, retrospective, and prospective information (e.g., splitter cells) and can alternate between potential future trajectories during vicarious trial and error. The hippocampus utilizes the cognitive map as a foundation for memory formation and decision-making processes. Neural recording technologies and decoding tools have enabled the observation and analysis of neural activity, providing valuable insights into the brain's functioning during agile and complex locomotor behaviors.

Behavioral-based robotics and bioinspired algorithms have effectively used neural models from animal brains for navigation. The behavioral and neurophysiological study of the subjects during complex locomotor tasks helps advance our understanding of complex locomotor behaviors and the underlying neural processes.

However, there are still notable gaps in the literature, particularly in understanding the relationship between hippocampal activity and decision making during complex locomotor behaviors such as jumping. Additionally, the connection between kinematic aspects of jumps and hippocampal activity requires further investigation. Addressing these gaps will enhance our comprehension of the brain's role in controlling complex motor behaviors, contributing to both neuroscience and bioinspired computing. By building on the foundation of existing knowledge, this dissertation aims to explore these gaps and provide a new perspective on the neural mechanisms underlying animal behaviors, ultimately contributing to advancements

in both neuroscience and robotics.

Chapter 3

Methods

This chapter describes the methodology utilized in the research. It begins with an overview of the experimental paradigm, followed by a discussion of the animal subjects selected for the study and their respective training procedures. Details about the silicon probe implantation procedure are then provided. The chapter then describes the experimental rig and the data acquisition methods used to record neural data, camera images, and force data, giving an understanding of the hardware setup essential for data collection. This is followed by a section on the real-time control used during the experiment and the subsequent data analysis process. The data analysis section includes animal tracking, kinematic analysis, and neural analysis. Neural data analysis comprises neuronal spike analysis and local field potential analysis. The chapter concludes with the development process for a Bayesian decoder, a tool utilized for neural and behavioral analysis in this dissertation.

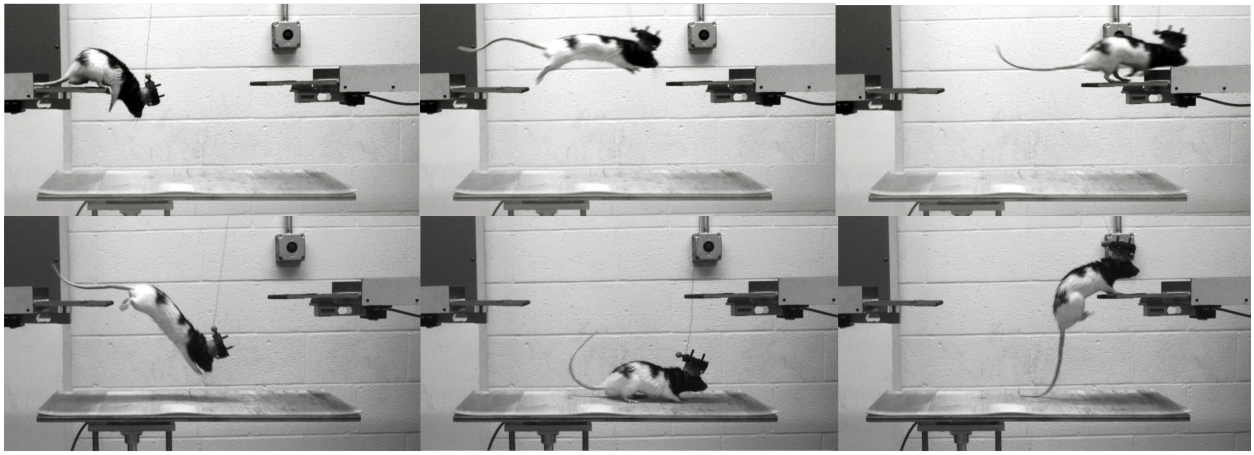

Figure 3.1: The top row depicts a rat jumping over the gap, while the bottom row illustrates the same rat 'ditching' the gap—jumping into and then out of the gap. Rats show a similar body posture before initiating both jumping and ditching.

3.1 Experimental Procedures

Rats were presented with a behavioral paradigm involving the navigation of a linear track with an adjustable gap in the middle (refer to Section 3.2 for more detailed information). Food rewards were dispensed at each end of the track, thereby motivating the food-deprived rats to traverse the gap to get their reward. In doing so, the rats had the choice of either 'jumping' over the gap or 'ditching', a term coined for this study to describe the behavior of descending into the gap and subsequently jumping out of it (see Figure 3.1). Through this behavioral paradigm, rats are challenged to perform complex locomotor behaviors to get to the reward.

3.1.1 Animal Subjects

The research subjects comprised four male Long Evans (Blue Spruce) rats, aged 6-7 months and weighing between 300-400 g at the time of implantation. These rats were

chosen for their well-documented cognitive abilities and proficiency in performing complex behaviors [19]. All animal care, training, and housing procedures were conducted in strict compliance with the protocols approved by the Institutional Animal Care and Use Committee (IACUC) at Johns Hopkins University.

Prior to the main experiment, the rats underwent a comprehensive training regime. During the training phase, the subjects were housed in wheeled cages (Scurry Rat Activity Wheel with Living Chamber, Lafayette Instrument, Inc., Lafayette, IN, USA) to encourage physical activity. They were moved to regular cages after surgery to reduce the risk of damaging the implantation. The initial training phase allowed the rats to explore, climb, and jump within a 64 cm x 43 cm x 132 cm cage (52-inch cage, Yaheetech, Shenzhen, China), preparing them for the jumping and ditching task.

Subsequently, in order to motivate the rats to navigate the linear track for the food reward, subjects were food deprived to 80%-85% of their baseline weight. The food reward consisted of dustless precision pellets (Bio-Serv, Flemington, NJ, USA) or Froot Loops cereal (Kellogg's, Battle Creek, MI, USA). In early training sessions, the gap was closed, and the subjects were running back and forth along the linear track to retrieve food rewards positioned at both ends of the track. The gap length was progressively increased until the rats consistently jumped 30 centimeters or longer. Upon reaching this stage, their diet was returned to ad libitum feeding in preparation for the surgery.

3.1.2 Animal Surgery

A two-step surgical procedure was designed to enhance the likelihood of successful silicon probe implantation in animal subjects. The first step was a craniotomy and durectomy surgery. It involved anesthetizing the animal using isoflurane gas along with preoperative intraperitoneal injection (IP) of Ketamine and Xylazine[1] to drill the skull and cut the dura mater. The opening was then sealed by layers of Dura-Gel, a dural sealant (Integra Lifesciences, Plainsboro, New Jersey, USA), Vaseline, and Kwik-Sil (World Precision Instruments, Sarasota, Florida, USA). Postoperatively, the rat was given subcutaneous (SC) injections of Buprenorphine and Dexamethasone[2].

After a recuperation period of 10-15 days, which included retraining the rat, the second step was implantation surgery. It involved the same anesthesia process above, and after removing the protective layers, a 4-shank Neuropixel 2.0 silicon probe was implanted into the durectomy site. The target implantation coordinates, relative to the bregma[3] were -4.5 mm anterior-posterior (AP), -3.25 mm mediolateral (ML), and deeper than 4.5 mm dorsoventral (DV). However, due to factors such as intervening arteries, the actual coordinates slightly deviated from these target numbers [146].

After securing the probe holder to the skull, the opening was again covered with the same materials as the previous surgery. Since the second surgery had minimal tissue damage, postoperative drug injections were unnecessary. The animal subjects were usually ready for the experiments as early as the next day.

[1] These agents work synergistically, where Ketamine provides anesthesia while Xylazine offers muscle relaxation and additional sedation to ensure deep and stable anesthesia during the procedure [145].

[2] These medications were administered to manage pain and reduce inflammation following the surgery.

[3] An anatomical landmark on the skull.

3.1.3 Experimental Paradigm

After one or two days of retraining, the subjects were ready for the experiment. The subjects were given food rewards at each end of the linear track after successfully crossing the gap. Each traverse from one end to another is called a 'lap' and can be leftward or rightward, depending on the direction of the gap crossing. The animals alternated between the two reward sites without any cues from the experimenters. They almost always went to the correct reward spot. In rare cases, when they mistakenly went to the wrong spot, especially during ditching trials, they were not given any food reward.

Four sets of experiments were performed by each subject[1]: jumping only, ditching only, titration, and hysteresis. The first experiment set was jumping, during which the rats, trained exclusively for jumping and unfamiliar with ditching, jumped their longest distances, as the subjects did not yet perceive ditching as an alternative. After that, they were acclimated to the ditch and trained for one or two days for ditching. After introducing the ditch, the animals opted for ditching at long distances. Subsequently, they were recorded for a ditching experiment at a long gap with a gap depth of around 20 cm.

After they got used to both jumping and ditching, the most crucial experiment was performed: titration. The idea was to keep the gap depth constant for the whole session and change the gap length in such a way as to maximize decision making and avoid habitual behavior, as illustrated in Figure 3.2. When a rat chose to jump in both directions, the gap length was increased, and when it chose to ditch in both directions, the length was decreased. When the decision of the animal was mixed in different directions, the length continued increasing or decreasing based on the previous alteration. The length adjustment

[1]Except Rat 1055

Table 3.1: Summary of Selected Experiments

Rat ID	Date	Experiment	Length (cm)		Depth (cm)	Brain Region	No. Laps
			Min	Max			
980	2021-12-13	jumping only	33	33	30	CA1/CA3	54
	2021-12-16	ditching only	33	33	22	CA1/CA3	126
	2021-12-21	titration	18	37	22	CA1/CA3	184
	2021-12-20	hysteresis	15	38	23	CA1/CA3	161
1055	2022-11-06	jumping only	20	41	30	CA1	171
	2022-11-09	titration	20	51	25	CA1/CA3	226
1068	2022-12-12	jumping only	61	61	30	CA1/CA3	216
	2022-12-13	ditching only	61	61	27	CA1/CA3	97
	2022-12-20	titration	36	64	27	CA1/CA3	241
	2022-12-19	hysteresis	41	71	27	CA1/CA3	248
1079	2023-03-28	jumping only	30	51	30	CA1/CA3	170
	2023-04-03	ditching only	51	51	23	CA1/CA3	227
	2023-04-05	titration	25	51	27	CA1/CA3	208
	2023-04-06	hysteresis	30	56	28	CA1/CA3	230

made it harder for the animal at each lap to repeat its previous choice on subsequent laps.

The final experiment was hysteresis, during which the gap length was constantly increased from a minimum value to a maximum value and then decreased. The maximum and minimum range of the gap length and the increment size were determined based on the performance of the subjects in the experiments of previous days. This cycle of increase and decrease was repeated four to seven times during a session, depending on the performance of the rat. This experiment was used to investigate the effect of history on decision making. A hysteresis analysis shows how the history of choices impacts the current decision to jump or ditch. As illustrated in Figure 3.3, the gap length was increased until it reached the maximum limit, then decreased until it reached the minimum limit, and the process repeated until the end of the experiment.

Table 3.1 provides detailed information about the selected experiments conducted on the subjects, including the date, minimum and maximum gap lengths, gap depth, brain region

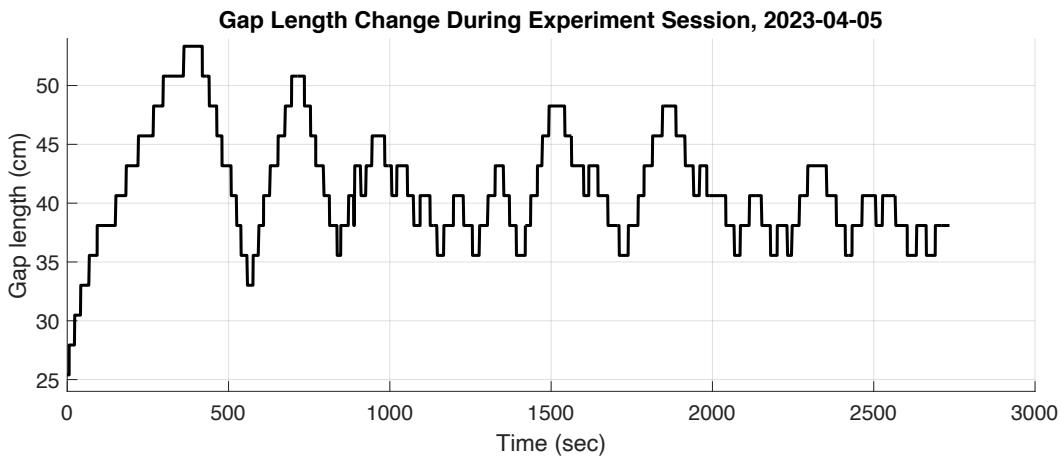

Figure 3.2: Titration experiment: gap length changed between 25 and 55 centimeters with a 1.25-centimeter step size. The gap length increased or decreased based on the decision of the subject. The gap length changed after one rightward and one leftward lap. It increased if the decision of the animal was jumping in both directions and decreased if the decision was ditching in both directions. Otherwise, the length continued increasing or decreasing based on the prior change.

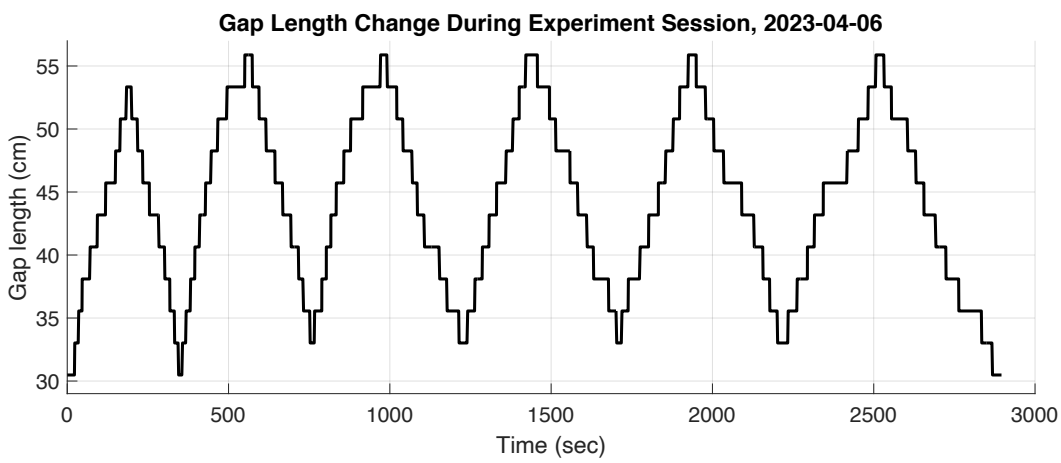

Figure 3.3: Hysteresis experiment: gap length changes between 30 and 55 centimeters with a 2.5-centimeter step size. The gap length increased or decreased by a known increment size until it reached the predefined maximum and minimum range. The gap length changed after one rightward and one leftward lap.

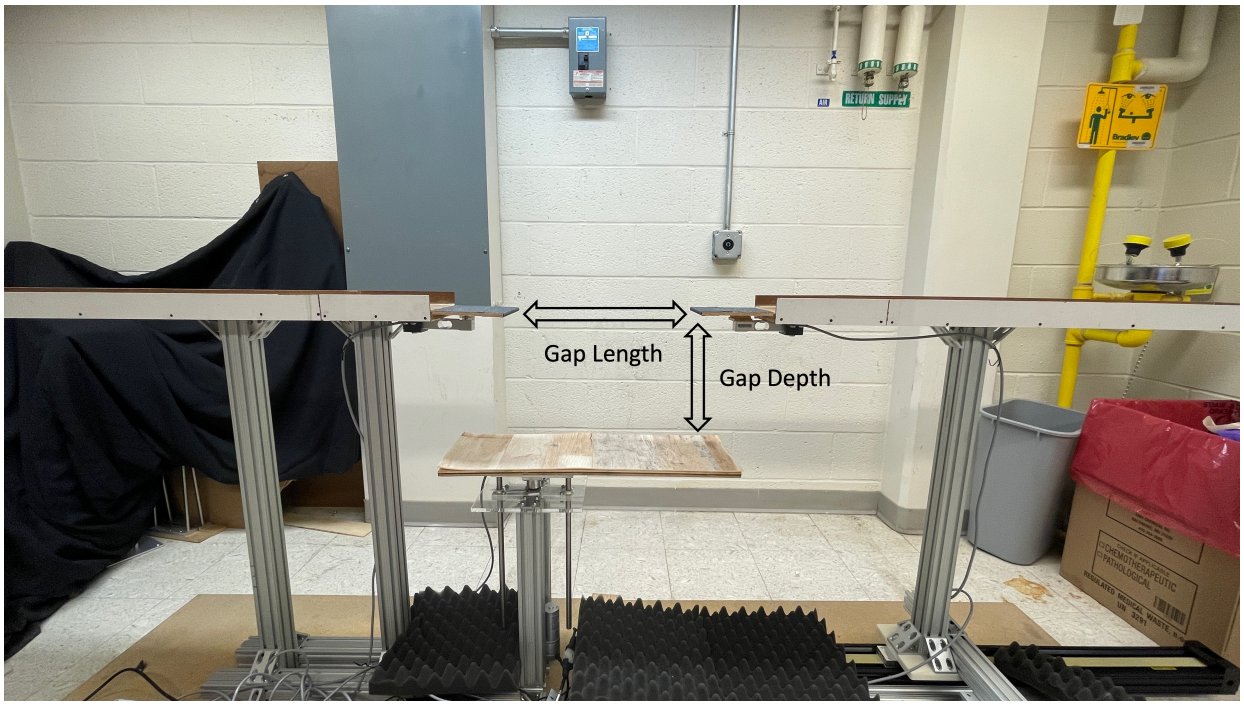

Figure 3.4: The experiment rig comprised two elevated linear tracks and the gap between them. Two remote-controlled linear actuators specify the length and depth of the gap. The photo was taken from the standpoint of the side camera; another camera records the experiments from the top.

involved, and the number of directional (either rightward or leftward) laps completed. CA1 and CA3 are subregions of the hippocampus where place cells are commonly found [147].

3.2 Experimental Setup

The experiment rig was designed with the specific aim of inducing decision-making behavior in rats. The adjustable gap served as the key feature to provoke this behavior, compelling the subjects to choose between jumping or ditching to traverse the gap. As illustrated in Figure 3.4, the experiment rig consisted of two elevated linear tracks known as 'runways'. They were constructed from wood with the size of 3/4 in x 5.5 in x 4 ft (approx. 2 cm x 14 cm x 120 cm). Thin boards were used to create shallow walls to prevent unintended falls.

The gap bottom was constructed from plywood, measuring 1/4 in x 8 in x 24 in (approx. 6 mm x 20 cm x 60 cm). A layer of Restored Rosewood Wood Residential/Light Commercial Vinyl Sheet (Lifeproof, Calhoun, GA, USA) was glued to the top layer of wood pieces that were in contact with the animal. This vinyl sheet layer was not only water-proof but also provided better traction and reduced the risk of slipping for the animals. To maintain hygiene, the surfaces were cleaned and sanitized with Ethanol before and after the experiments based on the protocol.

In the gap region, the linear tracks were connected to two thin boards, named 'launch pads', which were used for jumping and landing. The launch pads were made of 1/4 in x 5.5 in x 6 in (approx. 6 mm x 14 cm x 15 cm) oak board (Weaber, Inc., Lebanon, PA, USA). These oak boards were chosen after thoroughly testing the natural frequencies of boards made from different materials and thicknesses. The tests also indicated that the animals could effectively jump from and to these boards. The top and sides of the launch pads were covered with anti-slip safety tape (LifeGrip Stay on Track, LLC, Lehigh Acres, FL, USA) to reduce the risk of rats stumbling or slipping and to increase their grip needed for some behaviors (such as pull-ups when getting out of the gap).

The overall structure and legs of the experiment rig were crafted from 80/20 T-slot aluminum pieces (80/20 Inc., Columbia City, IN, USA). Acoustic foam panels were placed on the floor and the base of the rig to cushion potential falls, ensuring maximum safety for the rats during the experiments.

The schematic of the entire experimental setup is illustrated in Figure 3.5. Sensors and actuators, along with hardware and software devices, are shown in the figure. The arrows show the direction of communications between different devices. Green arrows show the con-

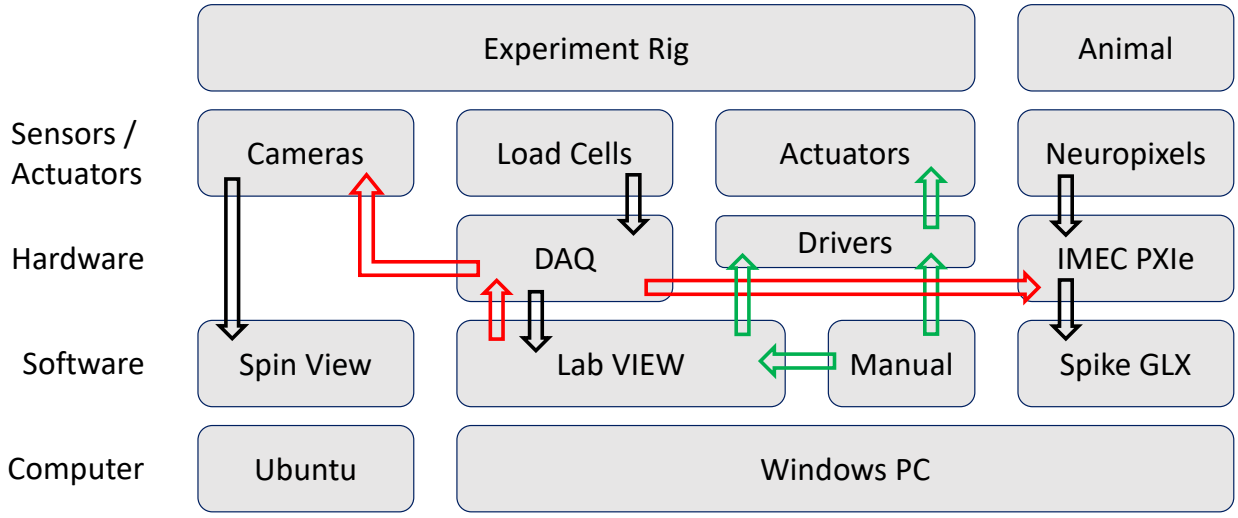

Figure 3.5: Detailed schematic of the experiment setup, highlighting device interactions. Green arrows represent control signals, black for data streaming, and red ensures synchronization among devices.

trol signals, black arrows show the stream of data, and red signals work as a synchronization between all the devices. The individual pieces will be discussed in the following sections.

3.2.1 Actuators

The design of the linear track required precise control over the depth and length of the gap, for which two types of actuators were incorporated into the experiment rig. The first actuator, an FA-OS-35-12-X linear actuator, along with a 2-channel remote control system (Progressive Automations, Inc., Delta, BC, Canada), was utilized to adjust the gap depth. The remote-controlled actuator allowed manual variation in the gap depth without disturbing the ongoing experiment. The actuator could move the ditch bottom up and down with a travel distance of approximately 30 centimeters, creating different gap depths. It was only in operation when animals were not on the ditch platform.

The second actuator was a belt-driven BiSlide assembly controlled via a corresponding

VXM controller (Velmex, Inc., Bloomfield, NY, USA). The primary role of this actuator was to adjust the length of the gap with a travel distance of 1 meter. A range of gap lengths was achieved by adjusting the right platform of the track back and forth. The actuator was controlled by a 2-button keyfob RF remote control and a simple RF M4 receiver (Adafruit Industries, LLC, New York, NY, USA), providing the flexibility to experiment with various gap lengths while maintaining a minimal intervention approach. This feature preserved the natural behavior of the rats and was beneficial during the titration and hysteresis experiments (see Section 3.1.3). This actuator only moved the right platform, and the left platform was stationary during the experiment, as depicted in Figure 3.4. The adjustments were happening only when the subjects were on the stationary platform. The length and depth of the gap could be efficiently controlled with these two actuators, thereby creating a dynamic environment suited for the study of place cell activity during different locomotor challenges.

3.2.2 Rat Cap and Marker Crown

To track the animals with high precision and robustness, a 3D-printed marker crown was utilized as described in [148]. The crown housed a constellation of retroreflective markers (OptiTrack, Corvallis, Oregon, USA) of various sizes (3 mm facial, 7.9 mm, and 12.7 mm). It was magnetically attached to the 'rat cap' during the experiments. The rat cap housed the silicon probe and the necessary electronics. It was permanently attached to the skull during the surgery, ensuring a consistent relative position between the crown and the head of the animal. The rat cap design was heavily influenced by prior work in Buzsáki's lab [149]. Figure 3.6 illustrates the crown marker and rat cap.

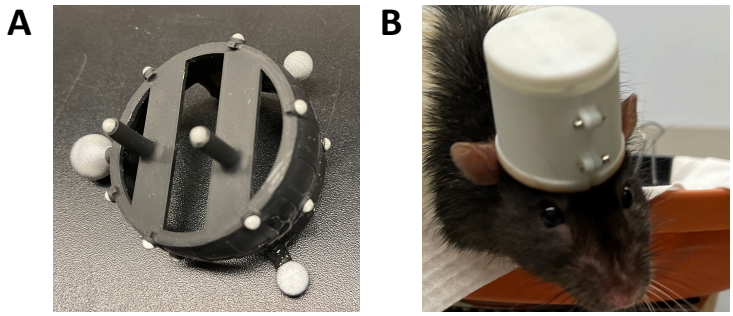

Figure 3.6: (A) 3D-printed marker crown featuring retroreflective markers of different sizes. (B) The rat cap is surgically attached to the skull of the animal.

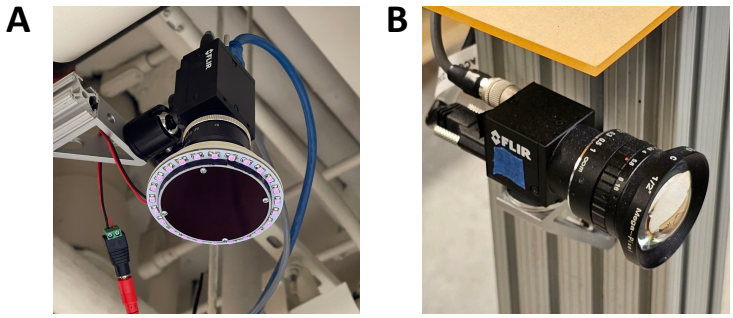

Figure 3.7: Tracking system configuration. (A) Top-view camera equipped with an IR LED ring and an IR filter. (B) Side-view camera setup. Both cameras operate using external triggers.

3.2.3 Cameras

As displayed in Figure 3.7, the tracking setup used a two-camera system for optimal perspective capture, including a top-view and a side-view camera and a specially designed marker crown to aid in the pose tracking of the rats. For the top-view perspective, a NIR (near-infrared) GS3-U3-41C6NIR-C 4 MP camera (FLIR Systems, Inc., Wilsonville, OR, USA) paired with an LM6HC 1” 6mm F1.8 Manual Iris C-Mount lens (Kowa Company Ltd., Tokyo, Japan), was used. This combination provided wide-angle coverage, ensuring the entire experimental rig was within view.

A ring LED with QBLP670-IR3 NIR LEDs (QT Brightek, San Jose, CA, USA) surrounded the camera to enhance visibility. These LEDs emitted light at an 850 nm wavelength

within the NIR spectrum. A NIR filter was mounted in front of the lens. This filter blocked visible light, allowing only NIR light to pass through and reach the camera sensor. The reflection of the NIR light from LEDs to the markers were the only beams passing through the filter camera, ensuring a sharp image of markers on a black background.

The side-view images were recorded using a mono-color BFS-U3-23S3M-C camera from FLIR Systems, Inc., paired with an LMVZ4411 1/1.8" 4.4-11 mm Varifocal lens from Kowa Company Ltd. This setup effectively covered the areas within the gap region, capturing the rats' movements during jumping and ditching.

Both cameras were externally triggered by signals from the DAQ, adjusting their frame rates dynamically to optimize memory usage. Whenever the rat entered the gap region, force sensors (see Section 3.2.4) detected its presence. Subsequently, the frame rate increased to capture the movement of the animal with higher detail. The top and side cameras recorded at high speeds of 300 fps and 200 fps, respectively[1]. Both cameras returned to a tenth of these speeds when rats exited the gap region.

The nominal camera speed is the rate at which the camera can capture images across its entire sensor. Nevertheless, the camera can function at higher speeds when the imaging area is reduced, and fewer pixels need to be digitized. The aforementioned speeds were achieved by choosing the appropriate region of interest (ROI) to be captured.

Videos from both cameras were recorded through SpinView 2.4 software (FLIR Systems, Inc., Wilsonville, OR, USA). To achieve high-speed recording and data transmission, raw frames were stored on a separate computer, distinct from the neural recording PC (refer to Section 3.2.6 for further details).

[1]Top camera images were used by the high precision pose tracker, necessitating a higher frame rate.

Table 3.2: Specification of PW6D single point load cell

Specification	**PW6D**
Accuracy class	C3 Multi Range (MR)
Maximum capacity	5 kg
Sensitivity (Cn)	2 ± 0.2 mV/V
Natural frequency, approx	390 Hz
Non-linearity	±0.0166% of Cn
Cable length	3 m (6 wire)
Material of measuring body	Aluminum
Nominal (rated) displacement at Emax, approx	< 0.18 mm

3.2.4 Force Sensors

As explained in Chapter 1, in order to record the ground reaction forces of the animal during preparation, takeoff, and landing to test the correlation with neural signals, force sensors were added to the experiment rig. The experiment rig was equipped with PW6D single-point load cells (HBK - Hottinger, Brüel & Kjær, Nærum, Denmark) mounted under both launch pads. The specification for the load cell is presented in Table 3.2. An additional load cell was placed under the ditch bottom. These sensors facilitated precise measurement of the force exerted by the rat during critical phases of the jumping or ditching process. These phases included the preparation phase, where the rat gathers momentum to jump across the gap or descend into the ditch, and the landing phase, where the rat either lands on the other side of the gap or at the bottom of the ditch.

The custom-made load cells were equipped with a shielded cable, 3 m in length, ensuring uninterrupted and noise-free data transmission. The voltage generated by the load cells, proportional to the force exerted by the rat, was then amplified by a BRT RW-GT01A DIN Rail-mounted load cell amplifier (Brightwin Electronics, Shenzhen, China). The amplified signals were fed into the analog inputs of the DAQ (see Section 3.2.5 for further details),

facilitating real-time recording and monitoring of the force exerted by the rats.

3.2.5 Data Acquisition and Control

LabVIEW 2020 software (NI, Austin, TX, USA) was used to control and monitor the experimental setup. The system was interfaced with the 782522-01 NI PXIe-PCIe8381 cable to PCIe-6259. This interface provided high-speed, direct control of the PXI system from a desktop or server and served as the bridge between the desktop and PXI systems.

The 781052-01 PXIe-6341 (NI Corporation, Austin, TX, USA) was integrated into the setup. An X Series Data Acquisition System (DAQ) included 16 analog inputs and two analog outputs. This DAQ was the primary data collection and control device, interfacing the physical measurements with the controlling software. Analog inputs were utilized to record load cell data and the remote control R4 receiver (see Sections 3.2.4 and 3.3.2). Two analog outputs were used for synchronization between the PCIe-6259 DAQ, cameras, and the IMEC PXIe acquisition module (see Sections 3.2.3 and 3.3.2).

3.2.6 Experiment Computers

The experimental setup leveraged the computational power of two high-performance PCs, each tailored to handle specific tasks essential to this study. The primary PC was designated for running SpikeGLX software for neural data acquisition and real-time visualization, as well as LabVIEW software for experimental control and monitoring. This PC was equipped with a Corei9-11900K processor running at 3.50GHz (Intel Corporation, Santa Clara, CA, USA). The system had 64GB of T-Force Delta DDR4 memory (TEAMGROUP Inc., Taipei,

Taiwan). Storage included a 1TB 980 PRO SSD with PCIe 4.0 NVMe Gen 4 interface and a 500GB 980 SSD with PCIe 3.0x4 NVMe M.2 Gen 3 interface (SAMSUNG Electronics Co., Ltd., Seoul, South Korea). The PC utilized a GeForce GTX 1660 graphics card (NVIDIA Corporation, Santa Clara, CA, USA), and it ran on the Windows 10 Enterprise N (64-bit) operating system (Microsoft Corporation, Redmond, WA, USA).

The secondary computer was exclusively set up to acquire and store high-speed, high-resolution video data from the two cameras utilized in the experiment setup. This Linux-based system (Ubuntu 18.04 operating system, Canonical Ltd., London, United Kingdom) ran on a Core i9-9900K processor at 3.60 GHz (Intel Corporation, Santa Clara, CA, USA) and 64 GB of Ripjaws V Series DDR4-3200 memory (G.Skill International Enterprise Co., Ltd., Taipei, Taiwan). A 2TB 980 SSD with PCIe 3.0x4 NVMe M.2 Gen 3 interface (SAMSUNG Electronics Co., Ltd., Seoul, South Korea) provided storage.

Following the completion of the experiment sessions, the generated raw data was preserved in multiple locations. It was first uploaded to the cloud service, providing easy access from any internet-connected device. Simultaneously, the data was copied to a Network Attached Storage (NAS) system with four hard drives arranged in a RAID 1 configuration, offering hardware failure protection. In addition, for offline accessibility and further redundancy, the data was also stored on external hard drives.

3.3 Neurophysiological Recording Setup

The neurophysiological recording setup was a critical component of the study. It included the Neuropixels 2.0 probes and hardware and software setup for recording neural activity.

The design of the neural recording setup was geared towards ensuring optimal data acquisition while simultaneously promoting conditions conducive to the natural behaviors of the rats.

3.3.1 Neuropixels 2.0 Probes

Neuropixels 2.0 probes by IMEC (Interuniversity Microelectronics Centre, Leuven, Belgium) were utilized to record the neural activity of the rats. These silicon probes offered simultaneous recording from 384 (out of 5120) recording sites across four shanks. Their lightweight, low profile and high number of channels made them ideal for studying place cells during agile behaviors such as jumping (see Table A.1 for comparison of different neural data acquisition devices).

The preparation process for these probes involved gluing a dovetail mount for connecting to a metal holder, sharpening the shanks, and testing the connectivity inside saline. After experiments and explantation, the shanks were cleaned by a Tergazyme enzyme-active detergent (Alconox, Inc., White Plains, New York, USA).

3.3.2 Neural Data Acquisition Hardware

The primary components used in the neural data acquisition process included the PXIe Chassis, an MXI-Express interface, and a custom-made IMEC PXIe Acquisition Module.

The NI PXIe-1071 PXIe Chassis (NI Corporation, Austin, TX, USA) served as the housing unit for PXIe modules. Its high-performance backplane offered robust timing and synchronization capabilities. This chassis was crucial for maintaining the precise timing required

in recording neural activity, thereby ensuring the reliability of the data.

The MXI-Express interface, comprising the NI PCIe-8381 and PXIe-8381 from NI, provided a high-bandwidth, direct connection to the PC.

Lastly, the PXIe Acquisition Module by IMEC (Interuniversity Microelectronics Centre, Leuven, Belgium), a custom-made Printed Circuit Board (PCB) module with dual Field-Programmable Gate Arrays (FPGAs), handled probe configuration, data acquisition at a sampling rate of 30 kHz, and transmission. This unit ensured efficient data collection from the Neuropixels 2.0 probes and swift data transfer to the PC via the PCIe interface, thereby enabling real-time signal processing and enhancing the overall efficiency of data handling.

3.3.3 Neural Data Acquisition Software

SpikeGLX software (Version 20220101, Imec phase30 v3.51) was used for real-time visualization and acquisition of neural data from the Neuropixels 2.0 probe [150]. This software platform facilitated data acquisition, selection of channels of interest, and filtering of high-density electrophysiological data and also featured an auditory functionality. This feature enabled the experimenters to listen to the selected signal during the experiment, providing a more engaging and intuitive method than visualization, as the human ear is often more sensitive to frequency content than the eye. A snapshot of SpikeGLX in operation during the data acquisition process from the hippocampus of a rat is demonstrated in Figure 3.8.

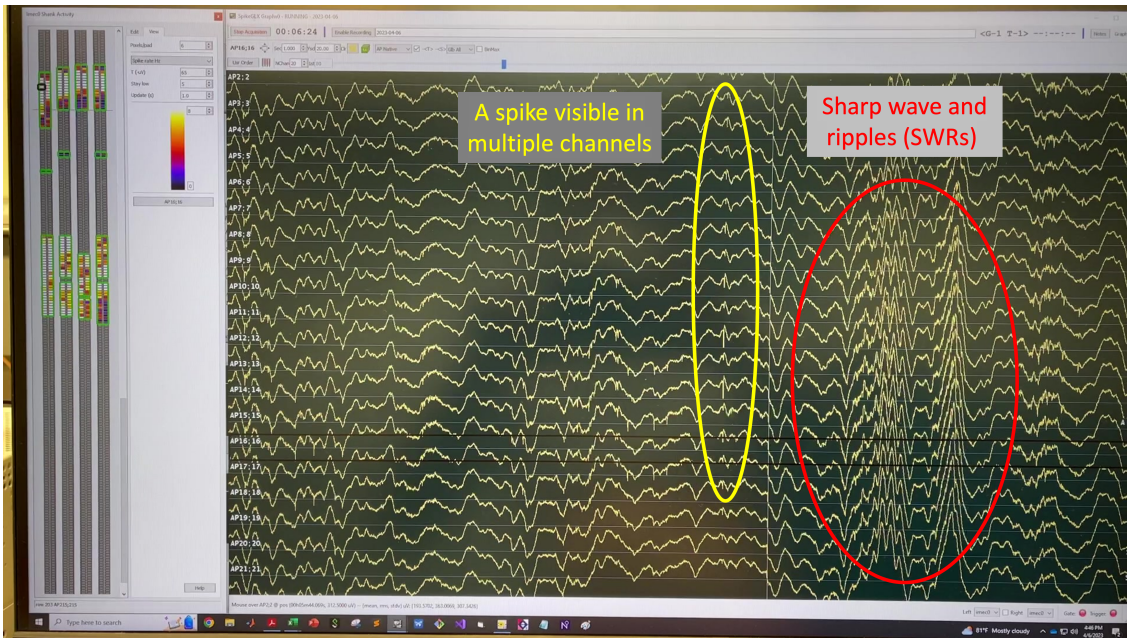

Figure 3.8: A snapshot of SpikeGLX engaged in real-time visualization and recording of neural data during an experiment. The figure demonstrates simultaneous recordings from multiple adjacent sites. Noticeable in the middle of the image are individual unit activities. In contrast, the activity known as a sharp wave ripple, a distinctive feature of the hippocampal CA1 layer, is visible on the right side of the image (for more details, see Section 2.8).

3.4 Data Analysis

With the data effectively acquired, the next step in the process involved detailed analysis of this data, as described in this section. A combination of MATLAB 2021a (MathWorks, Inc., Natick, MA, USA) and Python 3.6[1] was utilized for data analysis. These powerful computational tools enabled a comprehensive and detailed analysis of the collected data.

3.4.1 Animal Tracking

3D pose tracking of the rats was performed using a marker-based system that specifically targeted the head of the animal. As depicted in Figure 3.9, this system used a single top-view

[1]Employing libraries such as numpy, scipy, matplotlib, time, sys, os, multiprocessing, and glob.

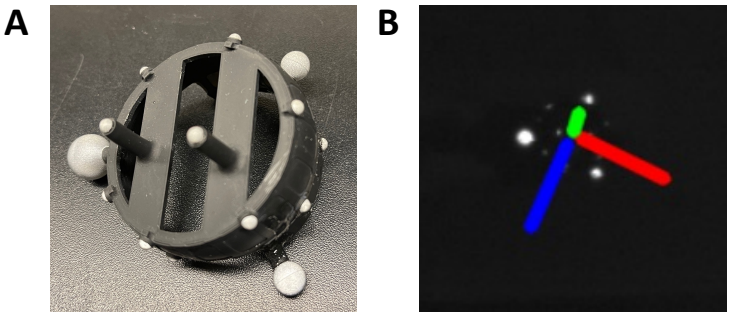

Figure 3.9: Tracking system (A) 3D-printed marker crown featuring retroreflective markers of different sizes. (B) Example of a sample frame from the top-view camera and the superimposed pose estimation results obtained using the marker tracker.

camera with a wide field of view to enable high-accuracy tracking of the six-degree-of-freedom position and orientation of the marker crown mounted on the rat cap (see Section 3.2.3 for more information). It has been demonstrated to accurately identify rat head position and orientation with subcentimeter precision, providing robust measurements of rodent head motions in a wide range of orientations [148]. This tracking was essential, as it allowed for accurate measurement of the rats' activity during the execution of complex maneuvers.

Another tracker was also developed in C++ by using STL and OpenCV [151] libraries to track the position of the rat in the 2D image plane using top-view camera images and to track the variable gap length during the experiment using the side-view camera images. The tracker also extracted the metadata of the frames for more precise synchronization.

3.4.2 Behavioral Data Analysis

The behavioral and kinematic data were analyzed to understand the mechanical principles underlying the complex locomotor behaviors of the rat. This involved calculating head-bobbing frequency, linear and angular velocities and accelerations, and determining parameters such as time of flight and ground reaction forces, which provided valuable in-

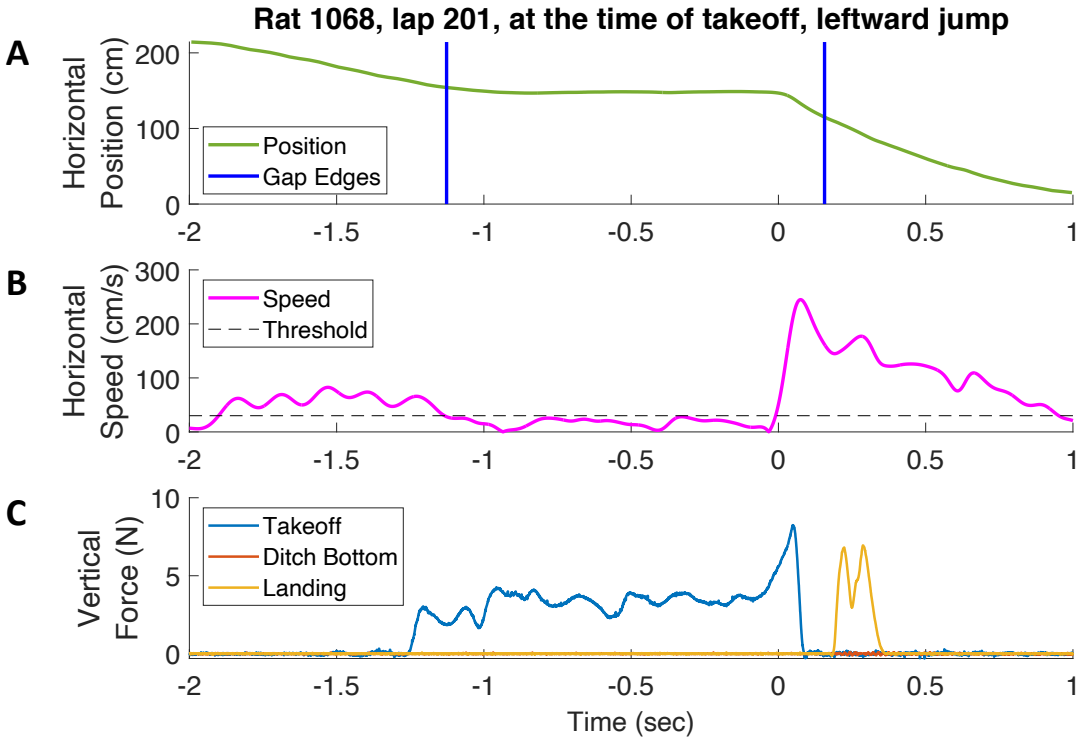

Figure 3.10: Demonstration of position, speed, and force on launchpads before, during, and after a representative jump. (A) The horizontal position (no filter) is plotted in a green curve. The moments that the head of the animal is in the gap region are shown by blue vertical bars. (B) The horizontal speed (filtered 0.01-10 Hz) is plotted in magenta. The speed threshold (30 cm/s) for detection of the initiation of the takeoff is shown with the black dashed line. (C) Vertical forces (notch filtered, between 20-60 Hz) applied to the launchpads and the ditch bottom are plotted. Since the rat does not walk on the ditch bottom, the corresponding force is zero.

sights into the jumping and ditching behaviors. Figure 3.10 shows the position, speed, and ground reaction force of an animal during a representative jumping lap.

3.4.2.1 Head Bobbing Analysis

To understand the behavior of animals during the preparatory phase preceding a jump, the analysis of the characteristic behavior of head bobbing became pivotal. As illustrated in Figure 3.11, the detection mechanism identifies moments where the animal's head is situated within the gap region prior to takeoff. The pitch angle, filtered between 0.5-10 Hz, is plotted

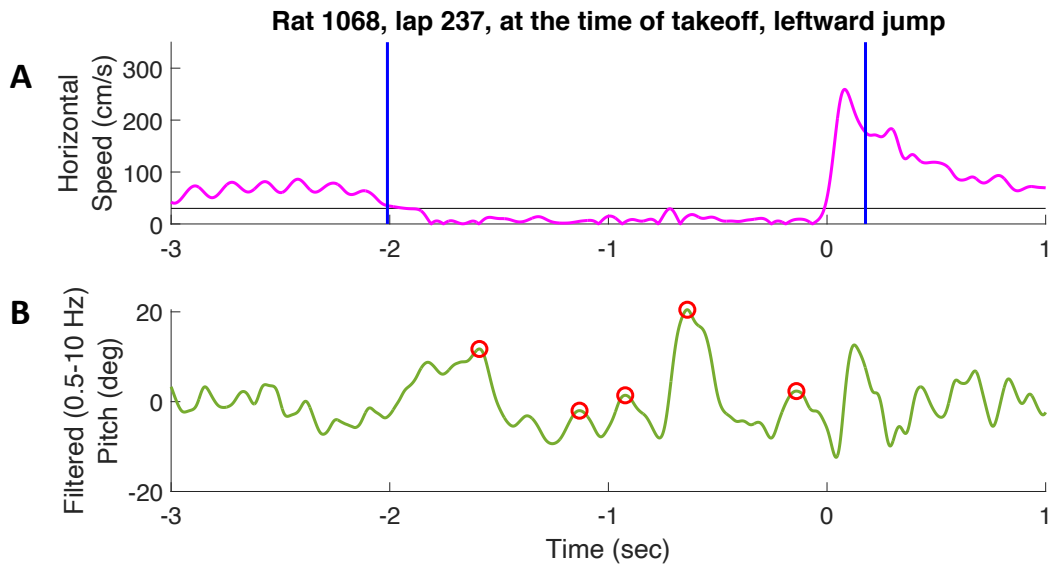

Figure 3.11: Detection of head bobbing during the preparation time before jumping. Head bobbing is considered when the animal's head is in the gap region and before the time of takeoff. (A) The horizontal speed (filtered 0.01-10 Hz) is plotted in magenta. The moments that the head of the animal is in the gap region are shown by blue vertical bars. (B) The pitch angle (filtered 0.5-10 Hz) is plotted in light green. The peaks are detected as head-bobbing incidents.

in light green. The red markers indicate peaks as instances of head bobbing. In the figure, the animal demonstrated 5 head bobs within a short span of 2 seconds, resulting in a head-bobbing frequency of 2.5 Hz. This head-bobbing frequency is an anticipatory mechanism that animals demonstrate before jumping and ditching, which will be discussed in the following chapter.

3.4.2.2 Ground Reaction Force

Ground reaction forces (GRFs) were captured using load cells (see Section 3.2.4) placed strategically at the launch and landing pads. As the rats initiated a jump, the force exerted on the launch pad significantly increased, detected as a spike in the output of the corresponding load cell. Similarly, a force increase was also observed at the moment of landing. Depending

on the length of the jump gap, this force increase exhibited either a single peak (unimodal) or a dual peak (bimodal). The latter reflected the time delay between the rat's forelegs and hindlegs touching down.

Figure 3.10 illustrates the GRFs recorded by the load cells on both the launch and landing pads. The times are relative to the time of takeoff. In the third subplot from the top, the yellow signal represents the GRF at the launch pad, while the blue signal depicts a single peak GRF at the landing pad. By tracking these ground reaction forces, biomechanical metrics such as maximum energy and the time of flight can be calculated, and more insights into the kinematics and kinetics of jumping and ditching behaviors can be provided.

3.4.2.3 Time of Flight

The estimation of the time of flight is a crucial element in understanding the jumping behavior of Long-Evans rats. This measure provides valuable information about the duration of the aerial phase, a key parameter in assessing the kinematic features of the leap. The time of takeoff was identified when the force on the launch pad rapidly dropped to zero, indicating that the rat had entered the aerial phase of the jump. The force remained close to zero during the flight and suddenly increased upon landing, providing a precise estimation of the landing time. The difference between takeoff and landing times accurately determined the time of flight.

3.4.3 Neural Data Analysis

This research explores the neural activity of the hippocampus during navigational tasks. The process comprises spike sorting, firing rate analysis, and theta analysis, as will be explained in the following sections.

3.4.3.1 Spike Sorting

Upon recording the neural activity, the initial steps entailed automatic spike detection and manual spike sorting. Spike detection was performed by referencing[1], filtering the signals with a zero-lag Butterworth filter within the 600-6000 Hz range, thresholding, and peak detection.

Spike sorting was essential for accurately clustering spikes from each recorded unit, with each cluster representing distinct neural firing patterns. These patterns were quantified using metrics, one such being the peak voltage of the spike. Since a unit's activity was usually captured across multiple recording sites, projecting these metrics from different sites aided in manually clustering the data, isolating similar spikes.

Despite the possibility of a unit encompassing data from multiple cells, adopting several techniques, such as inspecting individual spike shapes and examining the distribution of inter-spike intervals, reduced the chance of cross-contamination considerably. This ensured the preservation of the data's integrity and reliability. However, it is worth noting that if the data exhibited a high noise level or the metrics fell within this noise level, the reliability of the clusters could have been compromised.

[1]Post referencing was done by local or global common average referencing (CAR).

Table 3.3: Summary of the number of clustered units and place fields in the Titration experiment session for each rat.

Rat ID	No. Clusters	Direction	No. Place Fields		No. Laps
			CA1	CA3	
980	47	Rightward	23	2	92
		Leftward	32	3	91
1055	7	Rightward	5	0	113
		Leftward	6	0	112
1068	50	Rightward	20	14	120
		Leftward	13	12	121

The neural statistics resulting from spike-sorting are outlined in Table 3.3. This table provides information about the number of clustered units and place fields during the Titration experiment session for three subjects. While data was collected from four rats, the analysis presented in this dissertation includes data from three of those subjects.

3.4.3.2 Measuring Firing Rates

The clustered neural data underwent further analysis to calculate the firing rates of place cells during different behaviors. Occupancy[1] was calculated using a spatial histogram for the linear track with 3 cm bins. The number of spikes per bin was calculated using a similar histogram. The firing rate was calculated as the ratio of these two quantities at each bin. A speed threshold was used to exclude the spikes from the moments the subjects were idle if they were not in the vicinity of the gaps. For each cell, eight different firing rates were calculated. These rates were separately determined for leftward and rightward laps, stationary and moving frames of reference, and finally, for the different actions, namely jumping and ditching.

[1] cumulative time in a given location

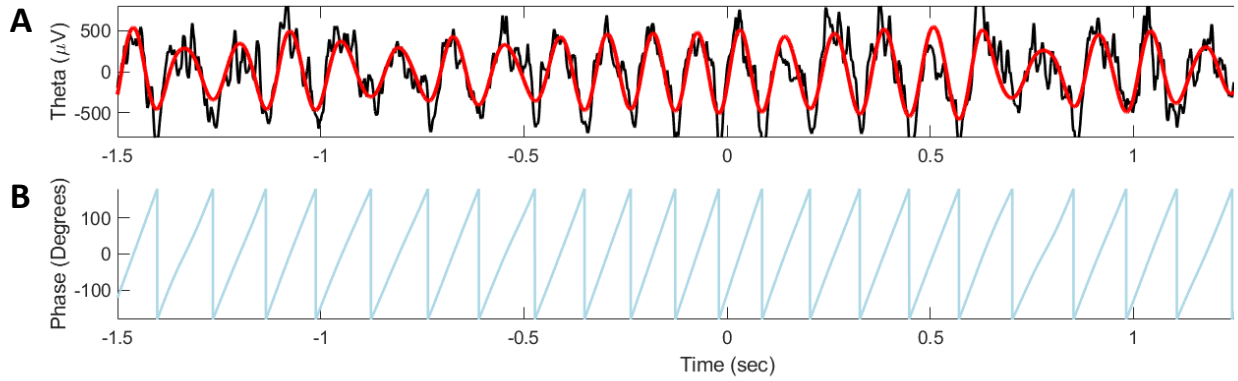

Figure 3.12: LFP and the associated theta rhythm during a representative jumping trial. Time is relative to the time of takeoff. (A) LFP is depicted in black, while the theta rhythm, shown in red, represents the zero-lag filter of the LFP between 6-12 Hz. (B) The theta phase corresponding to the theta rhythm is extracted using the Hilbert transform.

3.4.3.3 Theta Analysis

As mentioned in Section 2.8, theta rhythm is a characteristic EEG pattern in the hippocampus [152]. This section focuses on analyzing the theta rhythm from the recordings, especially from the hippocampal fissure, a location known to produce prominent theta activity in rats. Figure 3.12 shows the LFP, the theta rhythm, and the theta phase around the time of takeoff within a representative jumping trial.

Raw voltage recordings from the probe sites were utilized, with a Butterworth filter of order two applied in MATLAB. The zero-phase bandpass filter was specifically designed to isolate the frequency range of theta rhythm (6-12 Hz for rats, see Section 2.8). This filtering process enabled the extraction of the theta component from the raw signal, reducing noise and other unwanted neural activity.

After applying the Hilbert transform to the theta signal and forming the analytic signal (see Appendix A.2), it became possible to extract the instantaneous phase and amplitude of the theta rhythm, which was critical for subsequent analyses. Among the multiple recording

sites, the one with the highest theta amplitude was chosen as the reference. This site had the highest signal-to-noise ratio (SNR) for theta rhythm, thereby ensuring the quality of the analysis. Usually, this site was the closest one to the hippocampal fissure.

3.4.3.4 Theta Phase Analysis

To study the presence and implications of theta phase precession during jumping behavior, the theta phase was initially calculated using the Hilbert transform. This process is explained in greater detail in Section 3.4.3.3. The wavelet transform was also employed as an alternative method to extract the phase of theta. However, since both methods yielded similar results, the Hilbert transform method was chosen for the analysis. By plotting the phase of theta at the time corresponding to a cell firing versus the position of the rat (or versus the relative time with respect to an event) at that instance, it can be observed if the location (or the relative time) is encoded in the phase of cell firing, indicating the presence of theta phase precession.

Given the cyclic nature of theta phase, traditional methods like Pearson correlation, which are effective for linear-linear correlations, are not suitable for quantifying theta phase precession. Kempter et al. proposed a novel technique that provides a more reliable method for assessing circular-linear associations [153]. CircStat, a Matlab toolbox designed for circular statistics, was utilized to compute circular-linear correlations and the associated p-values for theta phase precession [154].

3.4.3.5 Theta Frequency Analysis

As described above, the hippocampus exhibits theta rhythm, a neural oscillation in the frequency range of 6-12 Hz for rats. The instantaneous phase of theta (see Section 3.4.3.3) during the time of flight (see Section 3.4.2.3) for each jump was first determined to calculate the average frequency of theta during jumping. The phase was subsequently unwrapped to measure the cumulative phase change during the jump. The number of cycles was obtained by dividing the total phase change by 360°, and the average frequency was calculated as the reciprocal of the number of cycles. This method reliably computes instantaneous and average frequency when the frequency of the signal varies.

3.4.4 Development of the Bayesian Decoder

A Bayesian decoder was designed to predict a rat's behavior by analyzing the firing rate of the hippocampal place cells in the time interval of 3 to 0.5 seconds preceding takeoff. This decoder, described in Algorithm 1, employed Bayesian statistics principles to draw predictions. The algorithm started by loading the clustered neural data and specifying the direction of the rat's traversal of the gap at each lap. Each lap is labeled as either 'jump' or 'ditch' based on the final decision of the rat. The decoder shuffled the data and assigned 60% of it for training and used the remaining 40% for validation.

This data was subsequently utilized to calculate the prior probabilities of two possible rat behaviors: 'jump' and 'ditch'. Using a Bayesian approach, the algorithm computed the mean and covariance for each behavior category to form a statistical model. This model was then used to calculate each behavioral category's likelihood and posterior probability, given the

observed neural activity, a process known as applying Bayes' rule. The behavior associated with the highest posterior probability was selected as the prediction for each data point in the validation set. The algorithm then calculated metrics such as accuracy and precision to evaluate the performance of the decoder. For more information about these statistical metrics, refer to Appendix B.1.

To get the distribution of the metrics, the shuffling process explained above was repeated for the Bayesian decoder and the random decoder. Bootstrapping (resampling with replacement) was employed for 1000 iterations to compute the distribution of accuracies. The random decoder only used prior probabilities to predict the outcome. Since samples of each distribution were not independent, a t-test was not considered appropriate for demonstrating the significance of the Bayesian decoder. Therefore, alternative metrics, such as effect size, were calculated that were independent of the sample size. A conservative metric was utilized by calculating the p-value from the z-score of the distribution of the accuracy differences. This distribution is derived by subtracting the accuracy of the random decoder from that of the Bayesian decoder for each sampling. If the p-value for negative numbers was below 0.05, the accuracy of the Bayesian decoder was considered to be significantly higher than that of the random decoder.

Chapter 4

Behavioral and Neural Correlates of Jumping and Ditching

This chapter investigates the behavioral and neural correlates of jumping and ditching behaviors displayed by Long-Evans rats when faced with an adjustable gap on a linear track. These locomotor behaviors, characterized by distinct behavioral and neural patterns, are analyzed to study the decision-making processes in the rats. Psychometric analysis provides a probabilistic understanding of the choice behavior under different conditions. Specifically, a hysteresis analysis shows the history-dependent nature of decision making during complex locomotor tasks. Further, the chapter explores the intriguing neural encoding underlying these behaviors, emphasizing the firing patterns of place cells in the hippocampus. Collectively, these findings deepen our comprehension of the sophisticated interplay between behavior and neural activity in spatial navigation tasks.

4.1 Behavioral Analysis

In the context of the locomotor behaviors of rats, the behavioral characteristics associated with jumping and ditching were analyzed. The jumping behavior typically consisted of a leap over the adjustable gap in the linear track. On the other hand, ditching behavior was characterized by the rat jumping into the gap and then making a subsequent leap out of it to traverse the gap. Depending on the depth of the gap, the animal may clamber in and out of it. Differences in behavioral patterns, reaction times, and success rates between these two behaviors were studied and will be reported in this section.

4.1.1 Psychometric Function

The psychometric analysis provided insight into the decision-making process of the animals when confronted with the choice of jumping or ditching to cross the gap. The decision to jump or ditch was monitored as gap lengths varied within experiments. At a given gap length, the number of jumps is divided by the number of passages to estimate the probability of jumping for that length. A sigmoid function is fitted to the data points to evaluate the psychometric function of the rat, offering a probabilistic understanding of the choice behavior under risky circumstances. Given the directionally sensitive behavior of the rats, leftward and rightward passages were analyzed separately. Figure 4.1 presents psychometric functions for different directions and conditions.

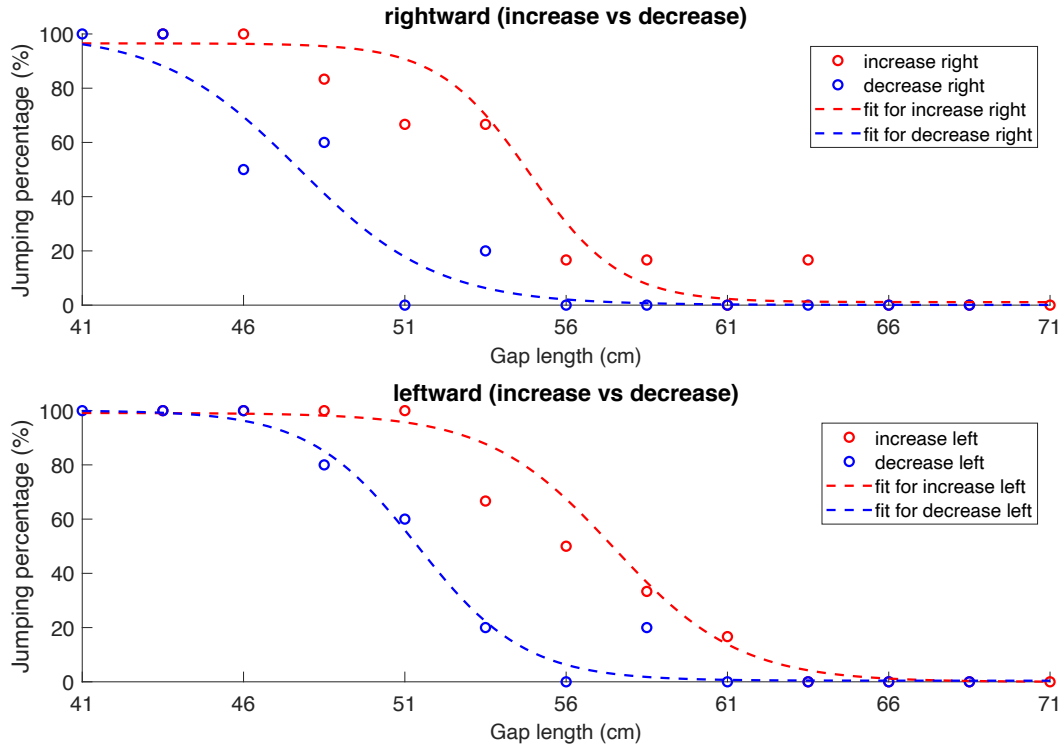

Figure 4.1: Psychometric functions for incremental and decremental changes of the gap length lead to a hysteresis loop. This figure shows both leftward and rightward direction results for one experiment session. The blue and red psychometric functions correspond to the decremental and incremental changes in gap length, respectively.

4.1.2 Hysteresis Effect

Hysteresis is a phenomenon observed when the increasing and decreasing psychometric functions do not exactly coincide. This implies that the response to a given gap length can differ depending on the previous progression of gap lengths, i.e., whether the gap length has increased or decreased relative to the prior trial. The hysteresis analyses help in understanding how rats' decisions, when confronted with the adjustable gap, are influenced by their past experiences.

Figure 4.1 depicts hysteresis plots for both leftward and rightward laps. The blue and red psychometric functions correspond to the decremental and incremental changes in gap length,

respectively. The area between these two functions represents the hysteresis effect. For example, in leftward trials, the rat's probability of jumping a 56-cm gap varied substantially depending on the prior distance; it was near zero if the preceding gap was 58.5 cm, yet approached 70% if the previous gap was 53.5 cm.

The hysteresis effect can be quantified as the bias, calculated by measuring the area between the increasing and decreasing psychometric functions. The 'signed area of the hysteresis loop' is obtained by integrating the psychometric function across gap lengths and subtracting the area under the decreasing psychometric function from the increasing one. A positive value indicates a larger area under the increasing psychometric function, suggesting a shift towards larger gap lengths in the hysteresis effect. The magnitude of the area shows the amount of shift in the unit of gap length. This metric can be used not only for hysteresis experiments but also for titration experiments to show the history-dependency of the decision making.

Table 4.1 presents the areas calculated for each rat and experimental session that included both jumping and ditching behaviors. Dates marked with an asterisk (*) denote sessions where a hysteresis experiment was conducted, while all other sessions involve titration experiments. The signed area of the hysteresis loop across all the sessions (both titration and hysteresis, for three subjects) was significantly positive ($p = 5.1 \times 10^{-4}$, binomial test). This statistical evidence indicates that the increasing psychometric function is significantly shifted towards larger gap lengths.

Table 4.1: Signed area of the hysteresis loop. Dates marked with an asterisk (*) indicate hysteresis experiment sessions, while others are titration experiment sessions.

Rat ID	Date	Signed Area of the Hysteresis Loop (cm)	
		Rightward Trials	Leftward Trials
1055	2022-11-07	2.16	0.12
	2022-11-08	2.92	1.01
	2022-11-09	2.93	0.09
	2022-11-10	0.57	-0.24
1068	2022-12-15*	3.21	3.12
	2022-12-16	3.94	3.70
	2022-12-17	3.31	2.64
	2022-12-18	0.62	0.60
	2022-12-19*	2.68	2.34
	2022-12-20	1.11	1.98
	2022-12-21	2.30	-0.77
	2022-12-22	0.93	-1.79
1079	2023-04-04	0.83	-0.14
	2023-04-05	0.78	1.06
	2023-04-06*	0.16	-0.48
	2023-04-07	-0.15	-0.47
	2023-04-10	0.49	2.10

4.1.3 Head bobbing

Rats exhibited a characteristic behavior termed head bobbing, especially pronounced when preparing for a jump. This behavior is not restricted to the rapid up-and-down movement of the head but also includes subtle shifts and adjustments of the entire body.

To further investigate this behavior, the frequency of head-bobs was quantified by counting the peaks in the pitch angle of the animal head after filtering the pose tracking data (see Section 3.4.2.1 for more details). Figure 4.2 illustrates this distribution for Rat 1068 during a session across both jumping and ditching trials. Notably, there is a significant increase in head-bobbing frequency before jumping compared to ditching trials.

Table 4.2 compares head-bobbing frequencies for different rats during both jumping and ditching actions. The results consistently show a significant increase in the head bobbing

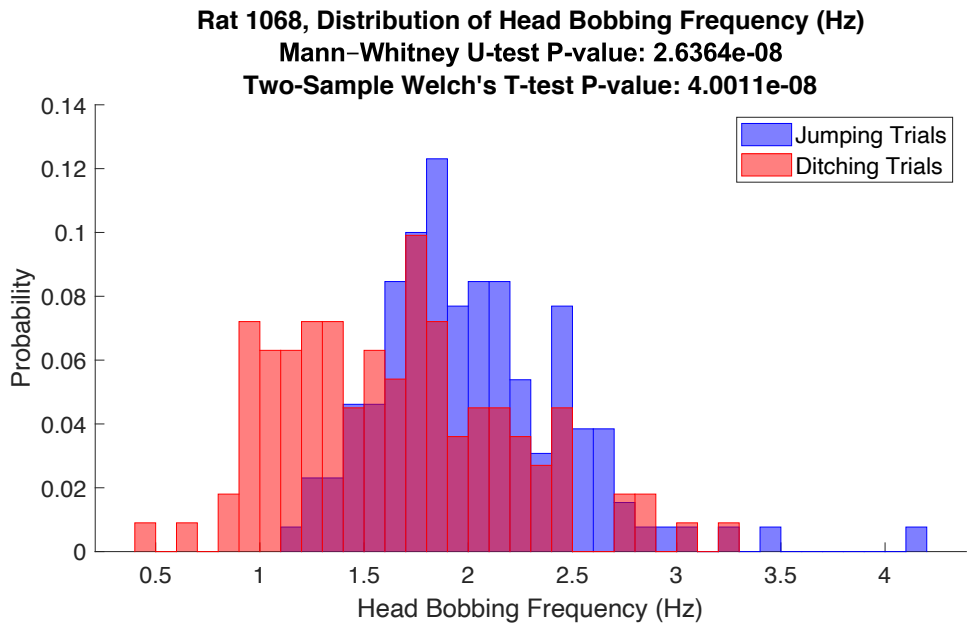

Figure 4.2: Histogram illustrating the distribution of head-bobbing frequencies for rat no. 1068 during a single session across both jumping and ditching trials. The frequency of head bobbing is significantly higher preceding a jump than a ditch. The frequency was determined as the number of head bobs per unit of time spent by the rat at the decision point before initiating movement.

frequency before jumping trials. The analysis also found no significant correlation between head bobbing frequency and gap length in all three animals, with p-values of 0.51, 0.89, and 0.22 (for rat no. 980, 1055, and 1068, respectively).

4.2 Neural Correlates of Jumping

Beyond behavior, this research probed the neural activity underlying jumping and ditching behaviors. Although the specific emphasis of this section is on the activity of place cells in the hippocampus, there was another interesting phenomenon that did not originate from the hippocampus but was observable in the hippocampal recordings. Figure 4.3 illustrates the neural activity during jumping and ditching trials. Takeoff time is detected when the

Table 4.2: Comparison of head bobbing frequencies for different rats before jumping and ditching. Two-sample Welch's T-test results, number of jumps and ditches, and the mean head bobbing frequency (with standard error of the mean, SEM) for different rats before jumps and ditches. Results show a significant increase in the head bobbing frequency before jumping trials.

Rat ID	Number of Trials		Mean Head Bobbing Frequency ± SEM		P-value
	Jumping	Ditching	Before Jumping	Before Ditching	
980	86	97	2.50 ± 0.04	1.50 ± 0.09	6.44×10^{-18}
1055	116	109	1.84 ± 0.05	1.62 ± 0.08	0.0193
1068	130	111	2.03 ± 0.04	1.66 ± 0.05	4.00×10^{-08}

speed surpasses a specific threshold before jumping or ditching.

The LFP (see Section 2.8 for more information) for each jumping or ditching trial is extracted and then aligned based on the takeoff time within that trial. Then all the LFPs are averaged for jumping and ditching trials separately to see if there is any common LFP activity before the takeoff. If there is an activity that is correlated with the time of takeoff, it will be pronounced with this illustration. A similar result was observed for other animals in other sessions. In order to test the correlation of theta phase with time of takeoff and other kinematically important times, statistical analysis was conducted in Section 4.2.3.

4.2.1 Theta Phase Precession

As explained in detail in Section 2.9, theta phase precession is a notable phenomenon in hippocampal activity. Figure 4.4 depicts theta phase precession for a rat on the runway as the animal ran toward the food reward. The methods utilized to analyze this phenomenon are described in Section 4.2.2.

In the context of jumping behavior, a hypothesis was formulated that the firing of place cells, and consequently, the occurrence of theta phase precession, would be influenced by the

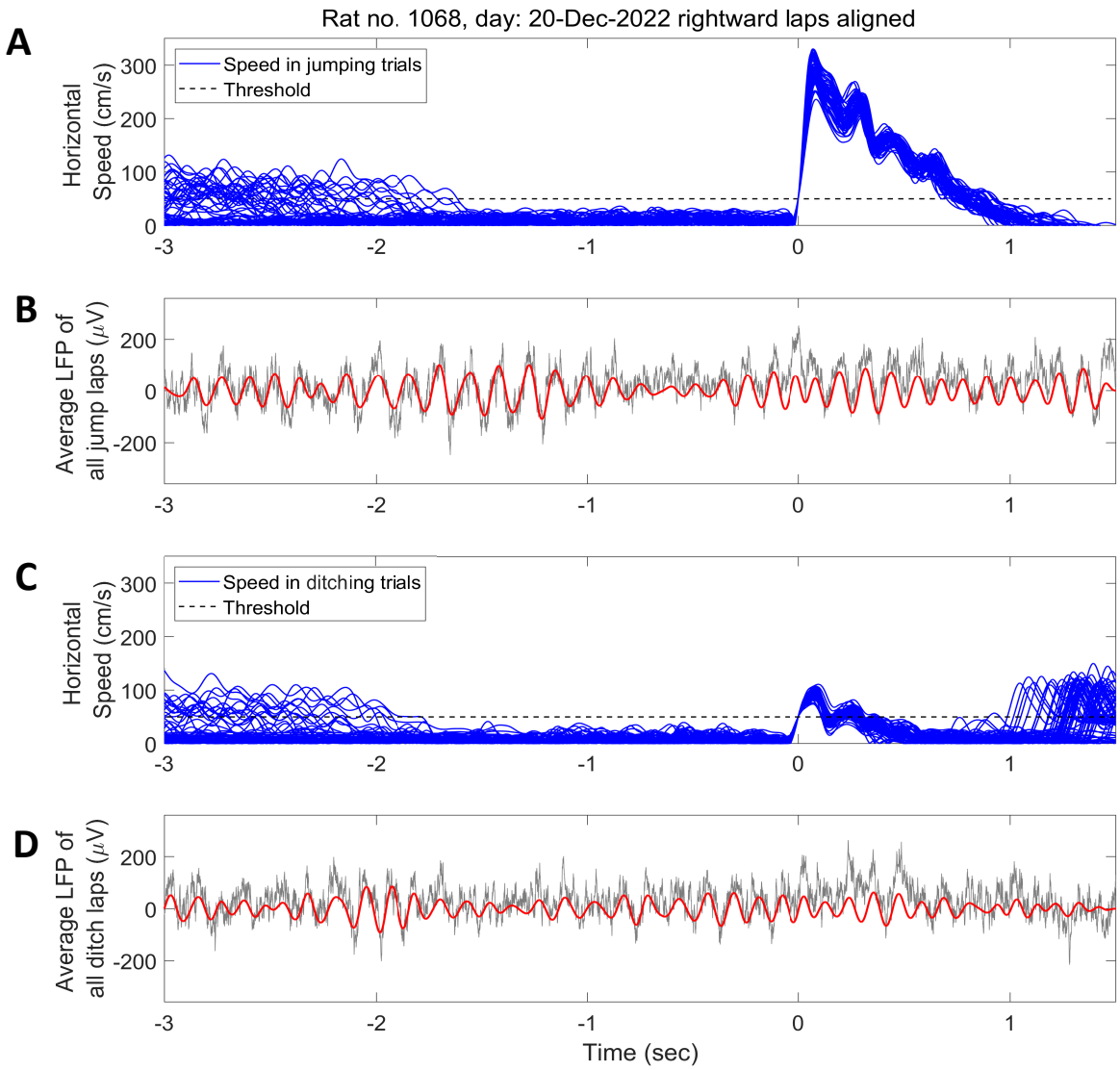

Figure 4.3: The LFP plots show the local field potential for one recording site averaged across all laps. Time is relative to the time of takeoff, which is detected when the speed crosses a threshold right before jumping or ditching at each trial. (A) The horizontal speed of the head of the animal overlayed for all jumping trials within a session. (B) Mean LFP across all jumping trials. (C) The horizontal speed for all ditching trials. (D) Mean LFP across all ditching trials.

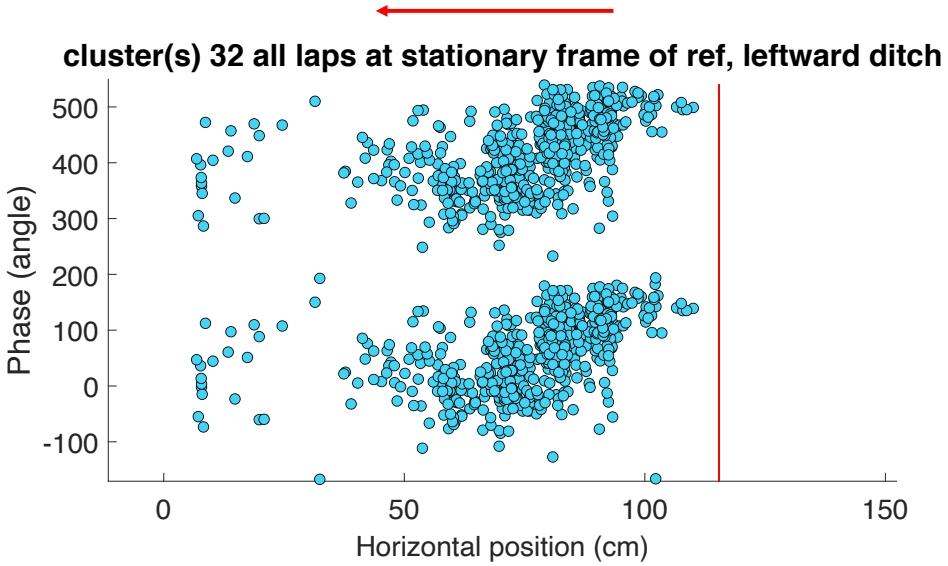

Figure 4.4: This figure illustrates the relationship between the theta phase of a place cell (no. 32) and the position of the rat as the animal is running on the runway toward the food reward after all ditching trials. Blue markers represent the theta phase and position of the rat when the cell fired. A clear pattern of phase precession can be observed as the animal crosses the gap by jumping. The red vertical lines show the edges of the adjustable gap for each ditching trial. To better visualize the wrapped cyclic nature of the theta phase and its correlation with position, the phase precession is plotted over two complete phase cycles. The animal runs from right to left, as indicated by the direction of the arrow.

animal's position and time during jumping. To investigate these relationships, two distinct analyses were conducted.

First, the relation between theta phase precession and the position of the animal during jumping was examined. Figure 4.5 illustrates an example that indicates that the phase precession is strongly associated with the position of the rat, showing a downward trend for the theta phase as the animal jumps.

Next, the relationship between theta phase precession and time during jumping and ditching trials was evaluated. As an example, Figure 4.6 displays the same cell shown in Figure 5.4 with respect to time, where time is relative to the time of takeoff. A correlated phase precession was observed as the rat jumped. However, since space and time are highly correlated during jumping, it is difficult to know if the cell encoding time or space or a combination of both of them by only looking at the phase precession plots (Figure 4.5 and 4.6). It is important to note that these correlations happen even though the gap length changes and the jumping distances and times vary accordingly.

The circular-linear correlation analysis explained in Section 3.4.3.4 revealed the existence of theta phase precession for most place cells. The results for all subjects are visually represented in Figure 4.7. There was a stronger correlation between theta phase and position than with time. A small percentage of fields showed no significant alignment with either time or position.

These findings are in line with the findings of previous studies of animals running on linear tracks [110]. They underline the multi-dimensional nature of hippocampal theta oscillations in encoding spatial-temporal information, particularly during complex locomotor behaviors like jumping.

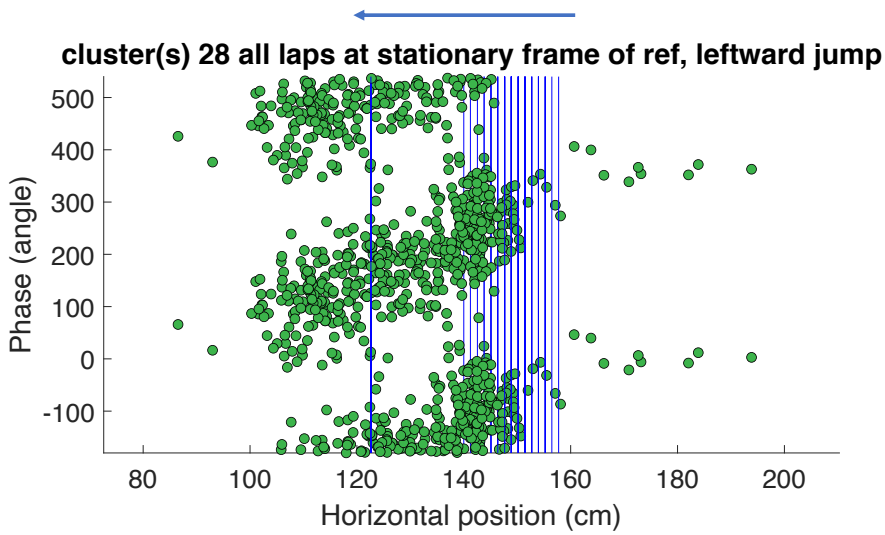

Figure 4.5: This figure illustrates the relationship between the theta phase of a place cell (no. 28) and an animal's position during a jump. Green markers represent the theta phase and position of the rat when the cell fired. A clear pattern of phase precession can be observed as the animal crosses the gap by jumping. The blue vertical lines show the edges of the adjustable gap for each jumping trial. To better visualize the wrapped cyclic nature of the theta phase and its correlation with position, the phase precession is plotted over two complete phase cycles. The animal jumps from right to left, as indicated by the direction of the arrow.

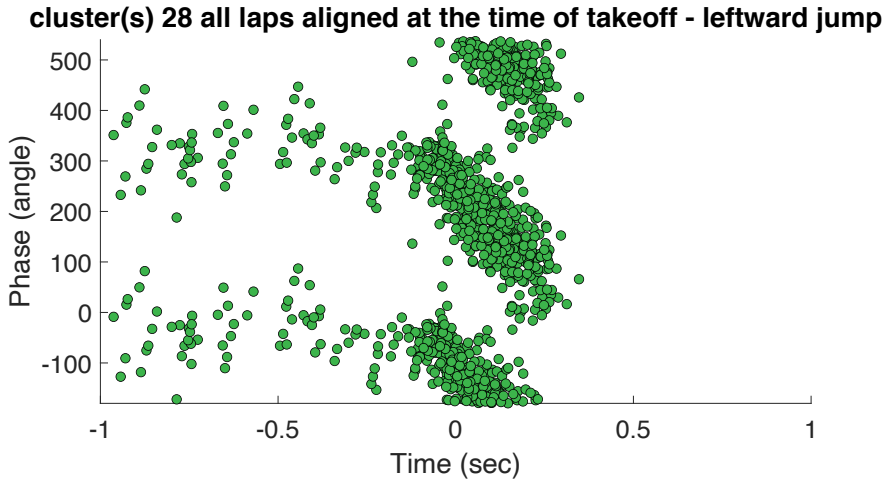

Figure 4.6: This figure demonstrates the relationship between theta phase precession and the time as a rat jumps. This cell (no. 28) is the same as the one shown in Figure 4.5. Time is relative to the time of takeoff at each trial. To better visualize the wrapped cyclic nature of the theta phase and its correlation with time, the phase precession is plotted over two complete phase cycles. The figure reveals a phase precession as time evolves across all trials.

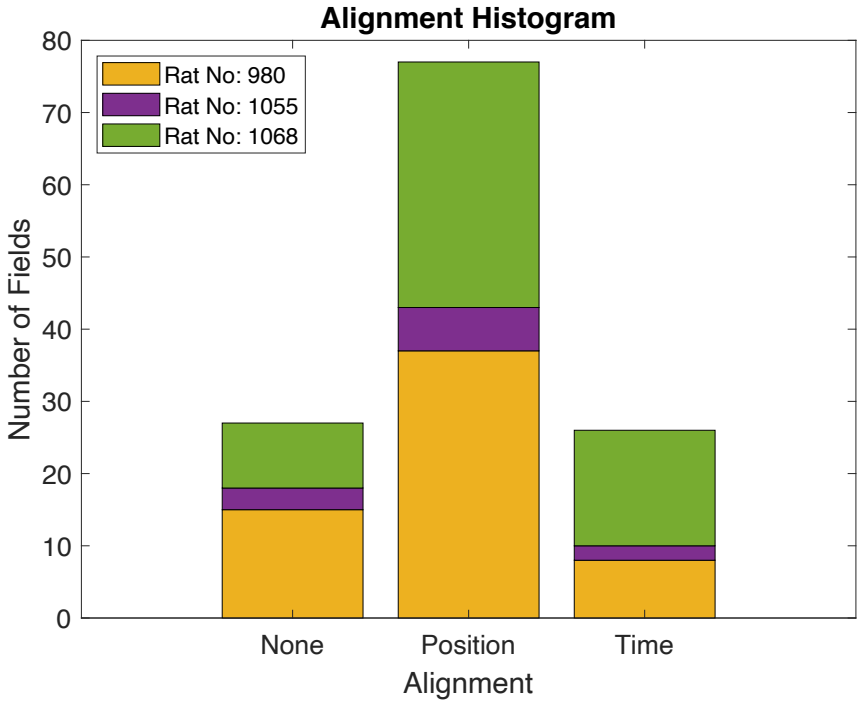

Figure 4.7: Statistics illustrating the correlation of theta phase with respect to position and time for all subjects. Fields with significant correlations ($p < 0.05$) and a higher correlation with the position are marked as 'position', while those with a stronger correlation with time are marked as 'time'. Fields with no significant correlation ($p > 0.05$) are labeled as 'none'.

Table 4.3: Pearson correlation coefficients, number of jumps, and the corresponding p-values for different rats in one experiment session. The average theta frequency is significantly correlated with the average speed of the rats during jumping.

Rat ID	No. of Jumps	Correlation Coefficient	P-value
980	86	0.428	4.01×10^{-5}
1055	114	0.594	3.21×10^{-12}
1068	130	0.581	4.09×10^{-13}

4.2.2 Theta Frequency Versus Speed

Previous research works show a correlation between the frequency of the theta rhythm and running speed in rats [103]. This study extends these findings by demonstrating this correlation holds even during complex locomotor behaviors such as jumping. The procedure to calculate the average frequency of theta during jumping is explained in Section 3.4.3.5. This method reliably averages frequency when the signal frequency changes over time.

As shown in Figure 4.8, there is a clear correlation between theta frequency and the speed of rats as they jump over gaps of different lengths. Data were collected from three rats, and a consistent linear increase in theta frequency was found as the jumping speed increased.

Table 4.3 highlights that the frequency of the theta rhythm is significantly correlated to the movement speed of an animal, even during moments when the animal is airborne. Interestingly, during these airborne periods, the speed is not directly influenced by the motor actions of the rat but predominantly by its projectile movement. These findings suggest the idea that the theta frequency is correlated with the speed and not the motor actions of the animal.

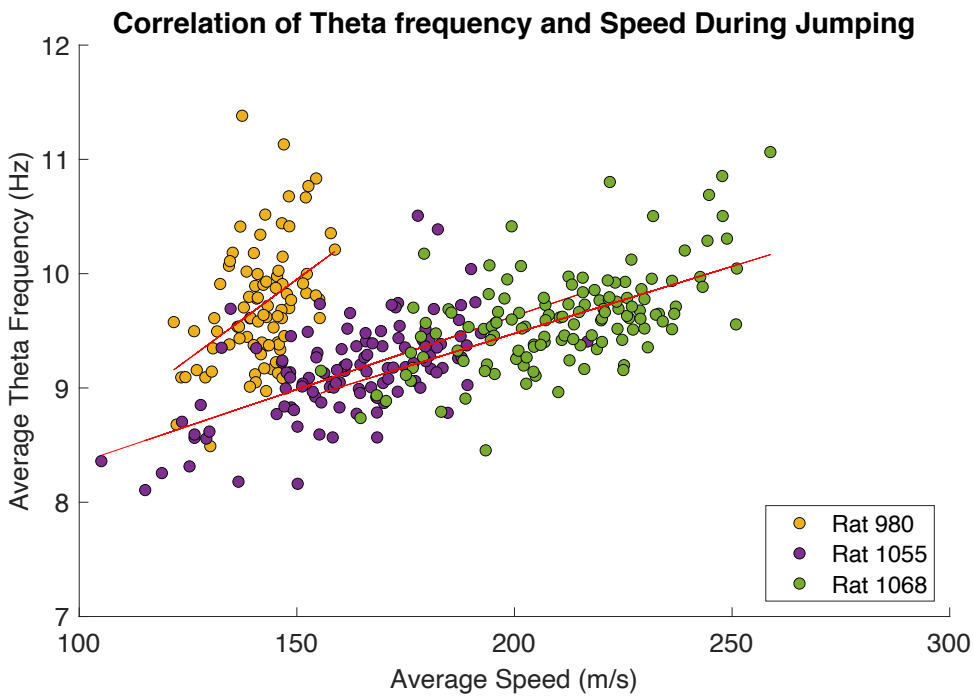

Figure 4.8: This plot represents the correlation between the theta frequency and the speed of the rats as they jump over gaps of different lengths. Theta frequency and speed are averaged across the time of flight at each trial. The data from three rats show a consistent linear increase in theta frequency as the speed of jumping increases.

4.2.3 Correlation of Theta Phase with Action

As explained in Section 2.8, studies have shown a correlation between locomotion and theta rhythm. This led to the hypothesis that jumping behavior might be correlated with theta rhythm and, more specifically, that jumping kinematics might be correlated with a particular phase of the theta cycle. To evaluate this hypothesis, the theta phase distribution at several kinematically crucial moments, such as takeoff and landing times, was examined. The distribution of theta phase at these moments was visualized using polar coordinates (Figure 4.9). Rayleigh test (see Section C.7 for more information) was implemented to check whether the distributions are biased toward a specific phase or they are uniform. No specific correlation between the theta phase and these important moments was identified in the analysis for any of the subjects in any session ($p > 0.05$ for all tests).

4.2.4 Theta Frequency and Kinematic Phases

Figure 4.10 shows different kinematic phases of locomotion during one jumping trial. The initial phase is 'running' when the subject runs toward the gap. Following this, in the 'preparation' phase, the animal is situated on the launchpad with its head inside the gap, yet the takeoff initiation has not begun. Subsequent to this is the 'takeoff' phase, defined by the time span starting 50 ms before the moment the speed threshold is surpassed and concluding when there is an absence of force on the takeoff platform. This is succeeded by the 'aerial phase', characterized by a lack of force on any platform. The concluding phase is 'landing and running', occurring when the animal touches down and runs towards the food reward.

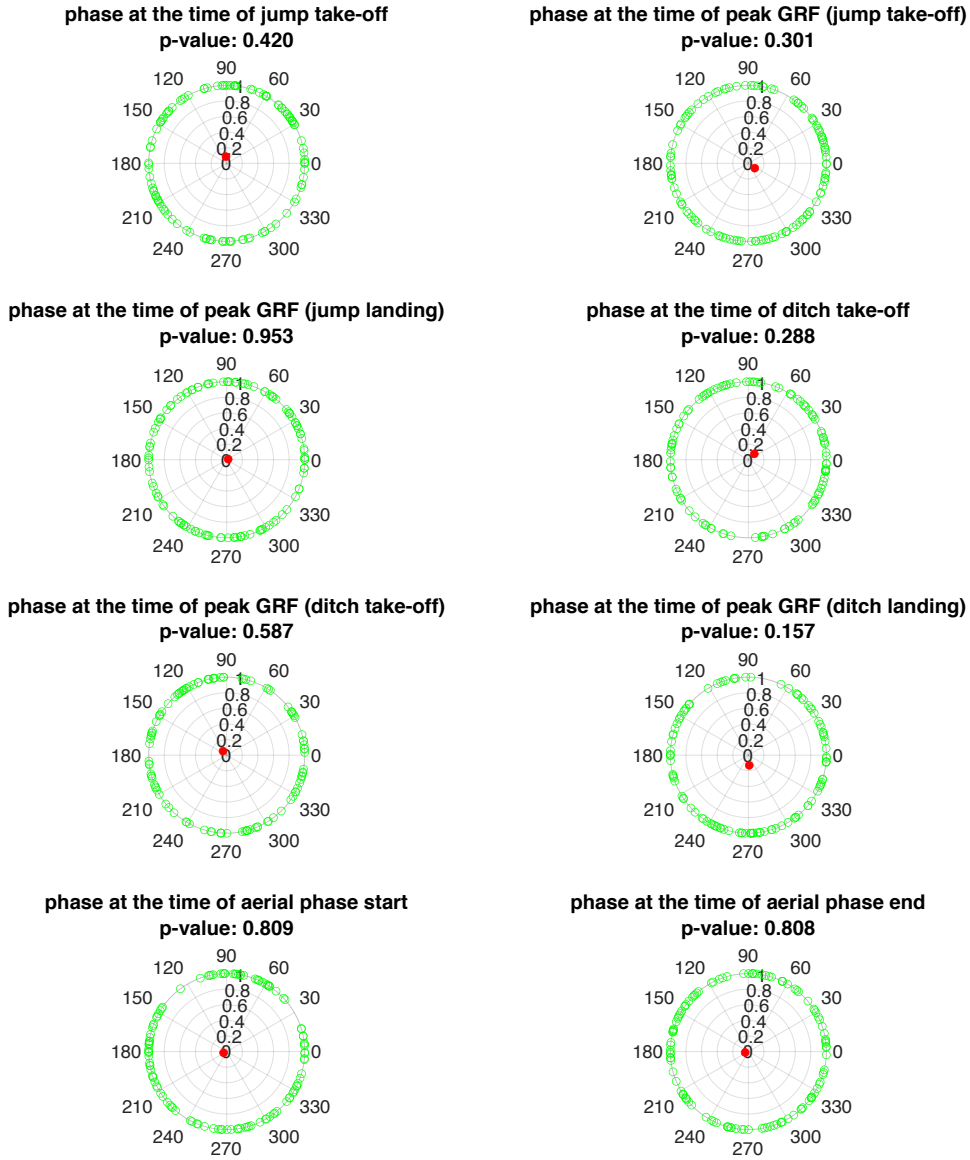

Figure 4.9: The distribution of the theta phase at different kinematically important moments in polar coordinates. All the data shown here are for one animal during one experiment session. Green markers show the phase of theta in the time of interest for each lap in the session. The red markers illustrate the vector mean of these phases for each plot (Rayleigh test, see Section C.7). As evident from the plots, the red markers are close to the origin. P-values for all the cases show that the theta phase is uniformly distributed rather than occurring at a specific phase.

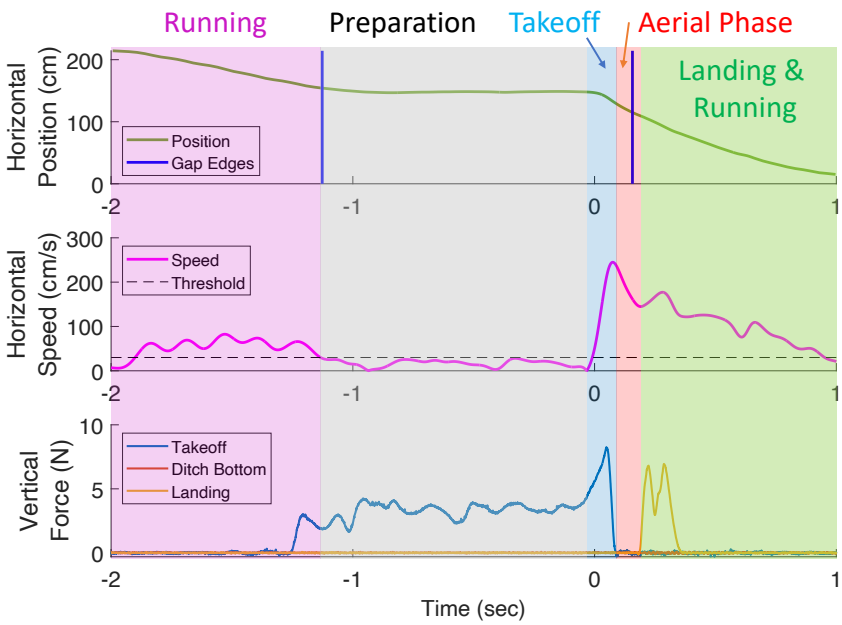

Figure 4.10: This figure depicts the same plots as those in Figure 3.10, with distinct colors superimposed to visually represent various kinematic phases observed during a representative jumping trial.

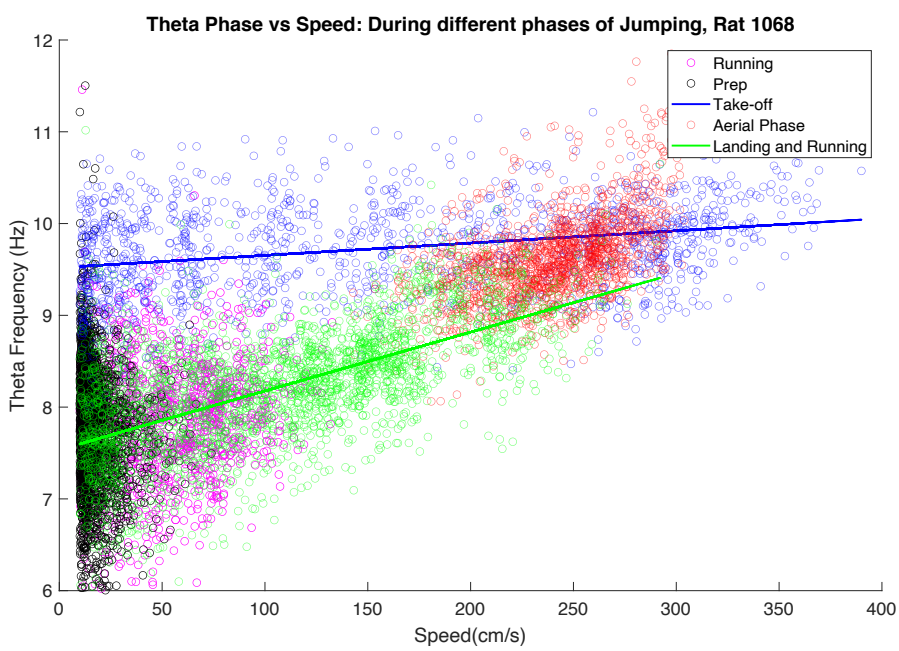

Figure 4.11: The correlation between the instantaneous theta frequency and the instantaneous speed during different kinematic phases of locomotion for all the jumps in an experiment session. Notably, the theta frequency is almost constant during a large range of speeds during takeoff. The color code is similar to Figure 4.10.

Figure 4.11 shows the relationship between the instantaneous theta frequency and speed for the aforementioned phases (The instantaneous theta frequency and speed are calculated in 10 ms interval, see Section 3.4.3.5 for more information). As shown in the figure, different phases follow a cyclical pattern around the triangle. A salient observation from the figure is the near-constancy of theta frequency over an extensive speed range during the takeoff. This phenomenon was observed for all three animals.

4.3 Discussion

This chapter explored the behaviors and the correlation between kinematics and neural activity in rats during complex locomotor actions of jumping and ditching. Findings from the psychometric function and hysteresis analysis provided insights into the decision-making processes.

On the behavioral front, psychometric analysis showed the history-dependency of animal decision making during a risk preference task of choosing between jumping and ditching, as the risk of jumping varied by changing the gap length. Rats were significantly more inclined to take the risk (jump) when the gap length gradually increased from low to high levels, as opposed to when it decreased. The novelty is that the risk assessment is based on complex locomotor behaviors involved at different gap lengths, not the reward contingency.

Additionally, the head-bobbing frequency of the rats was significantly higher before jumping trials than ditching ones, which can be a preparatory action for jumping or parallaxing to estimate the distance. Since the animals need more agility in jumping than ditching, muscular preparation and distance estimation are more important for jumping. Hence, the

exact role of this specific behavior remains an area of future exploration. In contrast to the earlier work involving gerbils [155], which found a correlation between pre-jumping head bobbing frequency and gap length, this study did not observe any such correlation.

On the neural level, the theta phase precession was observed to be associated spatially and temporally during jumping. The correlation between theta phase and position was higher than that with time for most fields. However, in some field the correlation of theta phase was higher with time, indicating the intricate spatiotemporal encoding of hippocampal place cells during complex locomotor tasks. Additionally, no correlation was observed between the phase of theta with several kinematically important moments, such as takeoff and landing times.

Furthermore, a significant correlation was observed between the theta frequency and the jumping speed of the animal during the aerial phase of jumping. This supports previous findings but extends them to the flight time. The novelty is that jumping is a unique occasion when the voluntary and natural movement of an animal is decoupled from the limb movement, which is known to be correlated with theta frequency [108]. Consequently, further investigation is needed to understand the mechanism behind the correlation of theta frequency and speed.

Last but not least, the theta frequency is almost constant during a large range of speeds during the takeoff phase of jumping. In other kinematic phases of jumping, such as the flight time or running phase, theta frequency is correlated with speed. However, during the preparation time, the theta phase increases in anticipation of the takeoff. As an animal rapidly accelerates and propels itself into the air, the theta frequency remains constant, capping at the maximum theta frequency for the animal.

Chapter 5

Firing Properties of Place Cells During Complex Locomotor Behaviors

This chapter investigates the firing properties of place cells in the hippocampus during complex locomotor behaviors, namely jumping and ditching. The focus is on the ability of these place cells to encode distinct 3D trajectories based on the actions of the animals. So, the trajectories are categorized into jumping and ditching trials based on the actions of the rats. Considering the prevalent directional characteristic of place cells, these trajectories are also categorized into leftward and rightward trials, determined by the direction in which the rat traverses the gap. Further details regarding the experiments can be found in Chapter 3. The study of dynamic encoding of spatial information during complex motor tasks adds to the understanding of how place cells contribute to spatial navigation.

5.1 Anchoring Frames of Reference

Place cells exhibit the capability to anchor their activity to distinct frames of reference [156]. As documented in a prior study, hippocampal neurons in rats shuttling between a fixed reward site and a movable reward site demonstrated a dynamic encoding behavior [157]. During that experiment, place fields near the fixed reward site maintained their firing patterns. In contrast, place fields closer to the movable reward site shifted their firing locations along with the site's movement. This suggests that the activity of the cells was anchored to a nearby or local frame of reference. In a review by Knierim and Hamilton, it was pointed out that in spatial tasks, animals' place-cell firings were more influenced by local cues and boundaries, with distal cues mainly setting the orientation of the internal spatial coordinate system and local cues determining its translation and scale [158].

A similar dichotomy was observed in the 'jumping and ditching' experimental setup. Some place cells aligned their activity with the stationary platform, the left platform in the experiments, while others aligned with the moving platform, the right platform in the experiments. As depicted in Figure 5.1, green and purple markers represent place fields corresponding to two distinct place cells. The green field, representing a place cell anchored to the stationary platform, maintains its position regardless of the moving platform's location. In contrast, the purple field, indicative of a place cell anchored to the moving platform, shifts its position along with the location of the moving platform.

To determine which platform the place fields were more closely aligned with, a two-sample f-test was utilized (as described in Section C.4). By comparing the firing rate distribution from both frames of reference, the frame with a significantly smaller standard deviation was

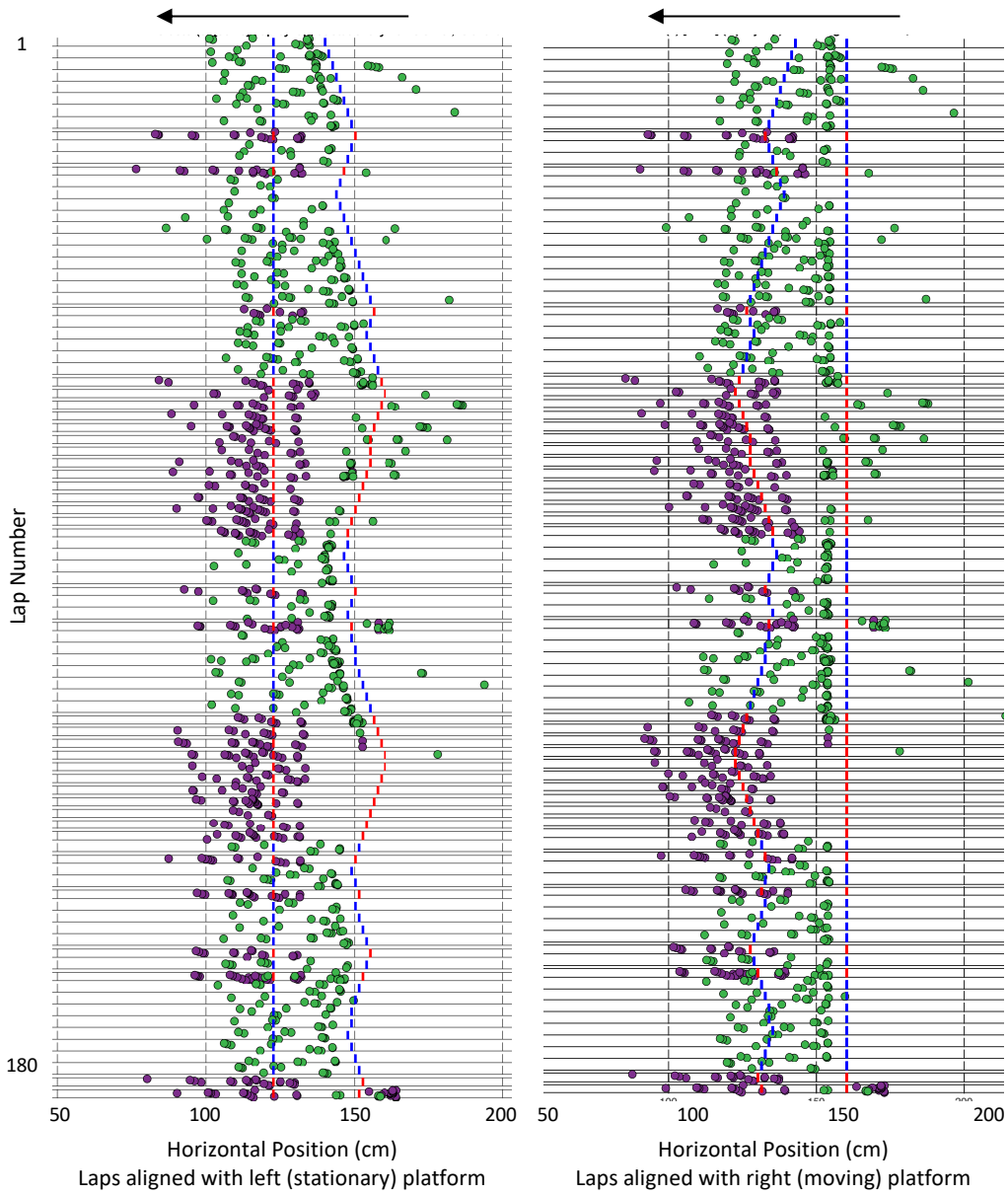

Figure 5.1: Illustration of two place fields anchoring to different frames of reference in an experiment session. The green and purple markers represent the firing locations for two distinct place cells during one experiment session. Both plots show the same data but are illustrated in different frames of reference - The left plot demonstrates alignment with the left (stationary) platform. In contrast, the right plot exhibits alignment with the right (moving) platform. The blue and red vertical lines show the edges of the adjustable gap for each jumping and ditching trial, respectively. The purple markers on the left plot maintain their position, indicating the place cell's alignment with the left platform. Conversely, the green markers align with the right platform. The direction of the rat's passage is from right to left, as the arrows indicate.

identified as the preferred alignment. Fields without a significant difference were labeled as ambiguous. Figure 5.2 shows an example of a place field more closely aligned with the stationary platform, indicated by the less spread-out distribution. Similarly, Figure 5.3 shows a place field more aligned with the moving platform. This dichotomy shows the ability of place cells to use different frames of reference for encoding, as indicated in the previous research.

The categorization of place fields based on the alignment for three subjects is shown in Figure 5.4. Only a fraction of place fields aligned significantly with stationary or moving frames of reference. Most place fields were not aligned significantly with either frame of reference, so they were categorized as ambiguous.

Observations indicate that place cells align with the stationary and moving platforms when animals are situated on or near them. Interestingly, during jumping, the cells were anchored to the platform from which the rat was taking off, not the landing platform. During ditching, however, the cells aligned with the takeoff platform while the rats were jumping into the gap and switched their alignment to the destination platform when the rats were jumping out of the gap. The place cell activity within the gap displayed mixed alignments.

5.2 Place Cell Activity During Jumping and Ditching

The activity of place cells was observed when the animals were jumping. Their activity was recorded while the animals were in midair, providing evidence that these place cells

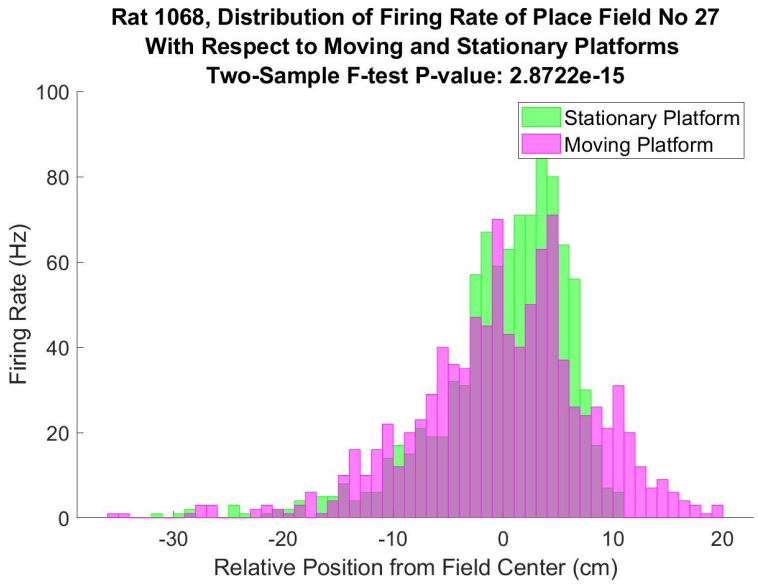

Figure 5.2: Distribution of firing rate in a place field (no. 27) for a rat in an experiment session. The distribution with respect to the stationary platform is plotted in light green, and the one with respect to the moving platform is plotted in magenta. The place field is significantly more aligned with the stationary platform.

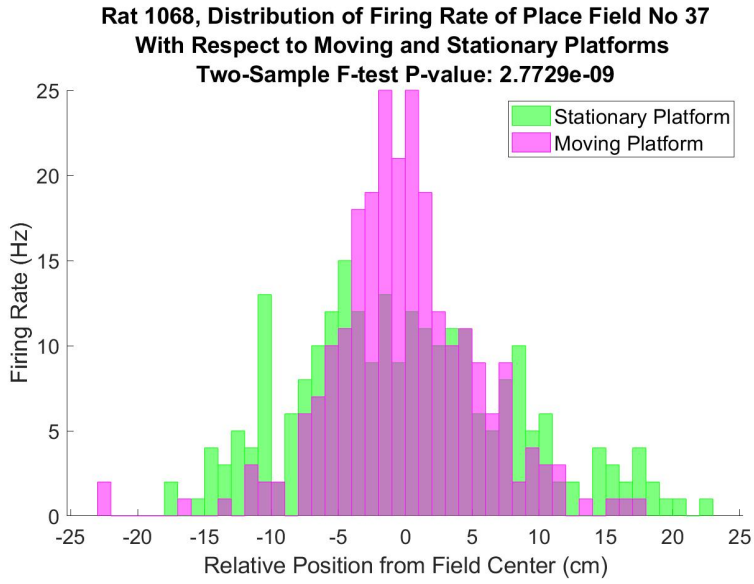

Figure 5.3: Distribution of firing rate in a place field (no. 37) for a rat in an experiment session. The distribution with respect to the stationary platform is plotted in light green, and the one with respect to the moving platform is plotted in magenta. The place field is significantly more aligned with the moving platform.

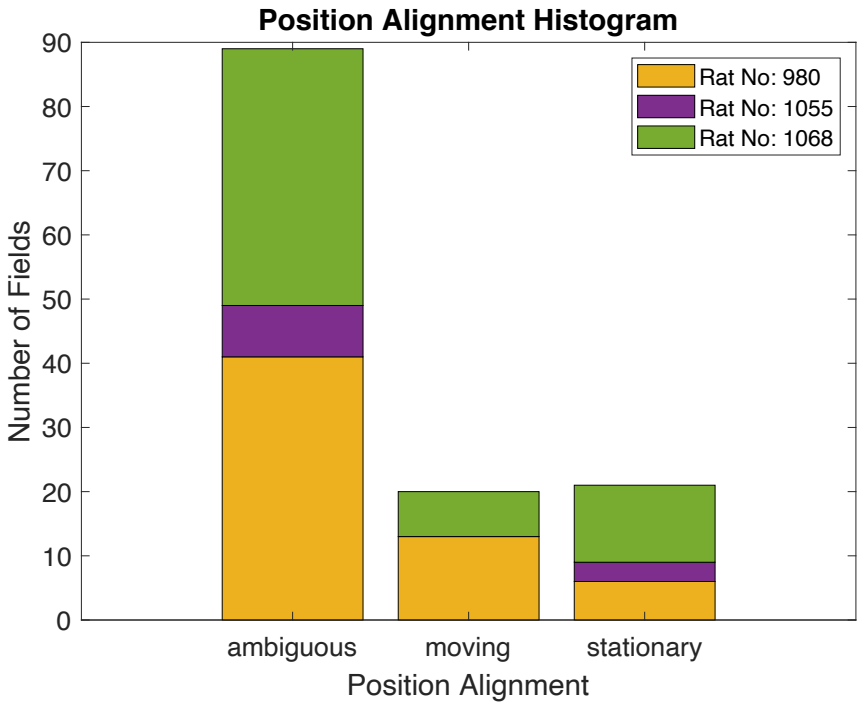

Figure 5.4: Illustration of place fields aligning with different frames of reference. Most fields were ambiguous, indicating that the distribution of the firing rates with respect to stationary and moving frames did not have a significantly different standard deviation ($p > 0.05$). Other fields showed more alignment with one of the platforms.

remain active even during the jump (See Figure 5.5). These observations were consistent with the previous findings, which also demonstrated place cell activity for rats during jumping in both negative reinforcement, such as jumping avoidance task [143], and also in positive reinforcement, such as liquid rewarding task [138]. Similarly, a subset of place cells remained active during ditching trials (See Figure 5.6).

5.3 Analysis of Trajectory Selectivity

The research exposed exciting aspects of the firing properties of place cells during Hysteresis and Titration experiments (refer to Section 3.1.3), in which animals performed both jumping and ditching. As animals traversed the gap, place cells displayed 'splitter-like' behavior instead of a uniform response to these different behaviors and trajectories. This suggests that these cells were encoding the trajectories associated with both jumping and ditching distinctly, even though they had similar 2D projections onto the experimental rig. Diverging firing patterns were observed depending on whether the rats jumped over the gap or took the ditching route. The selectivity for jumping and ditching is discussed in detail in the subsequent subsections.

5.3.1 Selectivity for Jumping

As shown in Figure 5.7, a subset of place cells showed strong selectivity for jumping. These cells exhibited distinct firing patterns when the rats chose to jump across the gap in the track. The firing rate of these cells significantly increased during the jump action.

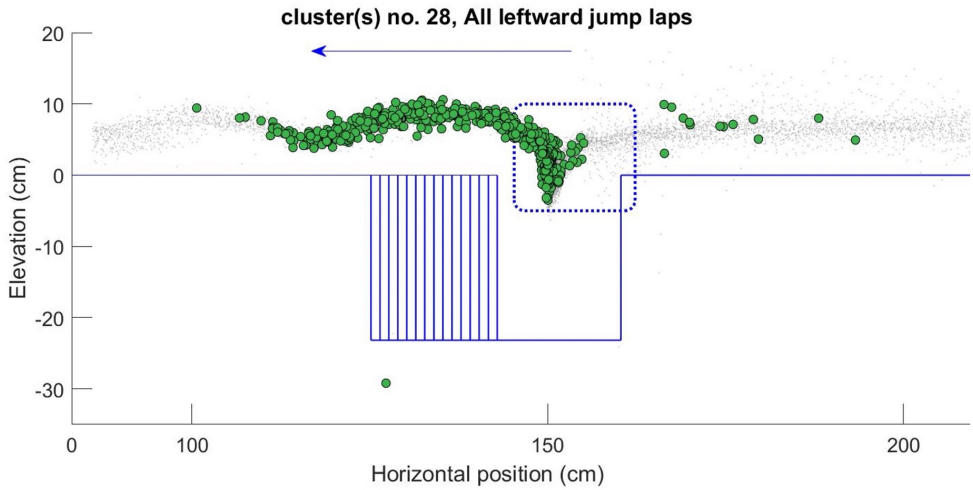

Figure 5.5: A side view picture of the place field of a cell (no. 28) that fires when the animal is in midair. Green markers show the location of the head of the animal when the cell fires. Gray dots show the occupancy of the rat, and the blue vertical lines show the edges of the adjustable gap for each jumping trial. The animal jumps from right to left, as indicated by the direction of the arrow.

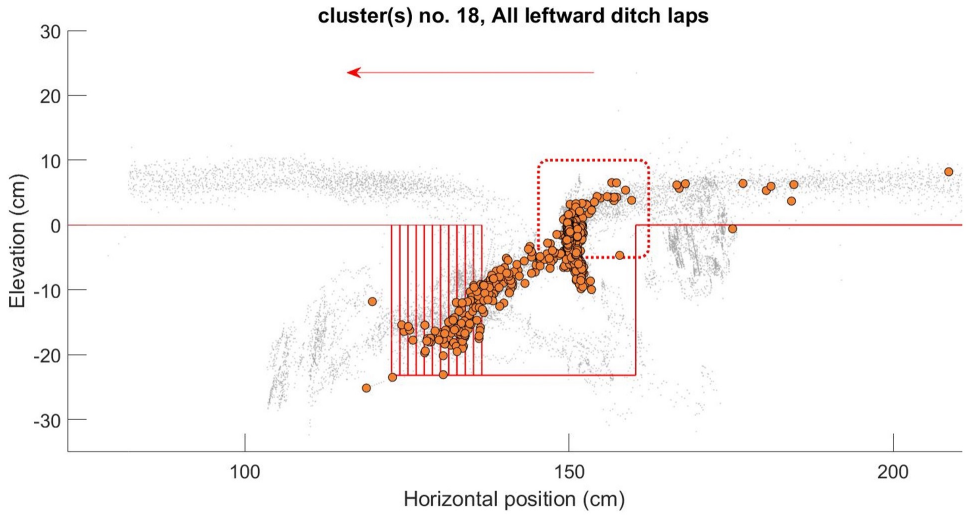

Figure 5.6: A side view picture of the place field of a cell (no. 18) that fires when the animal is free-falling into the gap. Orange markers show the location of the head of the animal when the cell fires. Gray dots show the occupancy of the rat, and the blue vertical lines show the edges of the adjustable gap for each jumping trial. The animal traverses from right to left, as indicated by the direction of the arrow.

In contrast, when the animal decided to ditch, either significantly less firing or no firing was observed in these cells, emphasizing the selective response to the jumping action or trajectory.

As evident from Figure 5.8, which represents the comparison of firing rates of the cell in Figure 5.7 during jumping and ditching trials, this category of place cells displayed a higher firing rate during the jumping trials, underscoring the selectivity of the cell for the jumping behavior (for calculation of firing rate see Section 3.4.3.2).

The statistical analysis explained in Section 5.5 also confirmed a significant association between the firing rates of these cells and the jumping behavior.

5.3.2 Selectivity for Ditching

In a manner mirroring the selective response to jumping, a different subset of place cells displayed a significant selectivity for ditching. As illustrated in Figure 5.9, these cells demonstrated firing patterns when the rats chose to traverse the gap by ditching, but they were almost silent during jumping.

The firing rates of these cells notably increased during the ditching, signaling their distinctive selective response to the ditching action or trajectory. However, during trials that the rat decided to jump, the firing rates of these particular cells were considerably lower or even completely absent. Figure 5.10 compares the cell's firing rates during ditching and jumping trials.

Furthermore, the statistical analysis detailed in Section 5.6 corroborates the substantial correlation between the higher firing rates of this category cells and the ditching behavior.

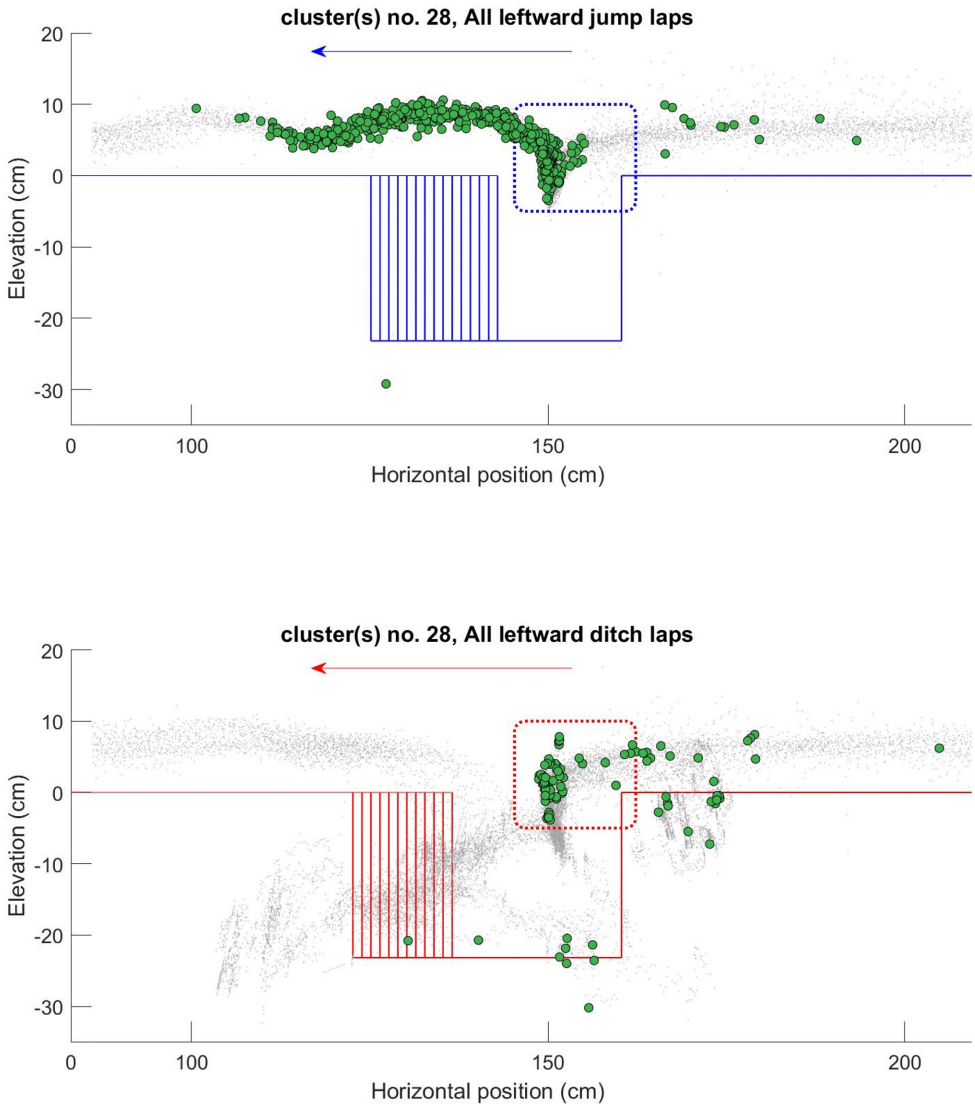

Figure 5.7: Side view pictures of the place field of a cell (no. 28) that is selective for jumping - active during jumping but silent during ditching. Green markers show the location of the head of the animal when the cell fires. Gray dots show the occupancy of the rat, and the blue and red vertical lines show the edges of the adjustable gap for each jumping and ditching trial, respectively. The direction of the arrows indicates the direction of the animal passage. The cell is active during jumping but is almost silent during ditching trials.

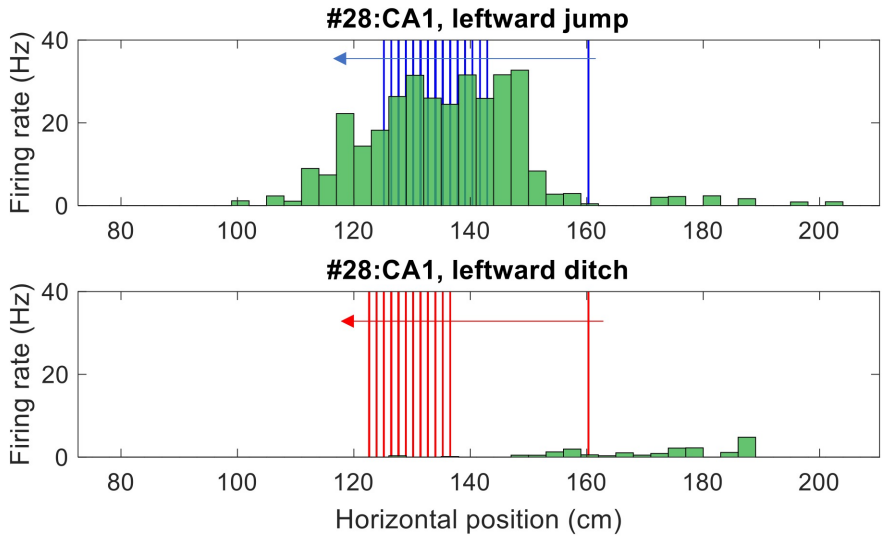

Figure 5.8: Firing rates comparison between jumping and ditching trials. for a place cell (no. 28) - the same cell as the one in Figure 5.7. This figure illustrates a cell that is selective for jumping. The direction of the arrows indicates the direction of the animal passage. The adjustable gap for each trial is denoted by vertical lines - blue for jumping trials and red for ditching trials.

This robust link signifies the capacity of place cells to differentiate and encode different locomotor actions and 3D trajectories in the same spatial context.

5.3.3 Special Cases

Several interesting special cases were observed in this study. For example, a place cell fired when the rat jumped out of the gap in one direction and again fired when the rat jumped out in the opposite direction. Figure 5.11 presents the place field of this cell. The cell fired regardless of the direction of the passage, which is indicated by the arrows in the figure. This interesting finding hints at the versatile encoding capabilities of place cells, indicating that the cell encoding is potentially action-dependent. However, this is just one anecdotal example and might have occurred by chance.

Additionally, some cells were observed to fire only at the perching location and had a

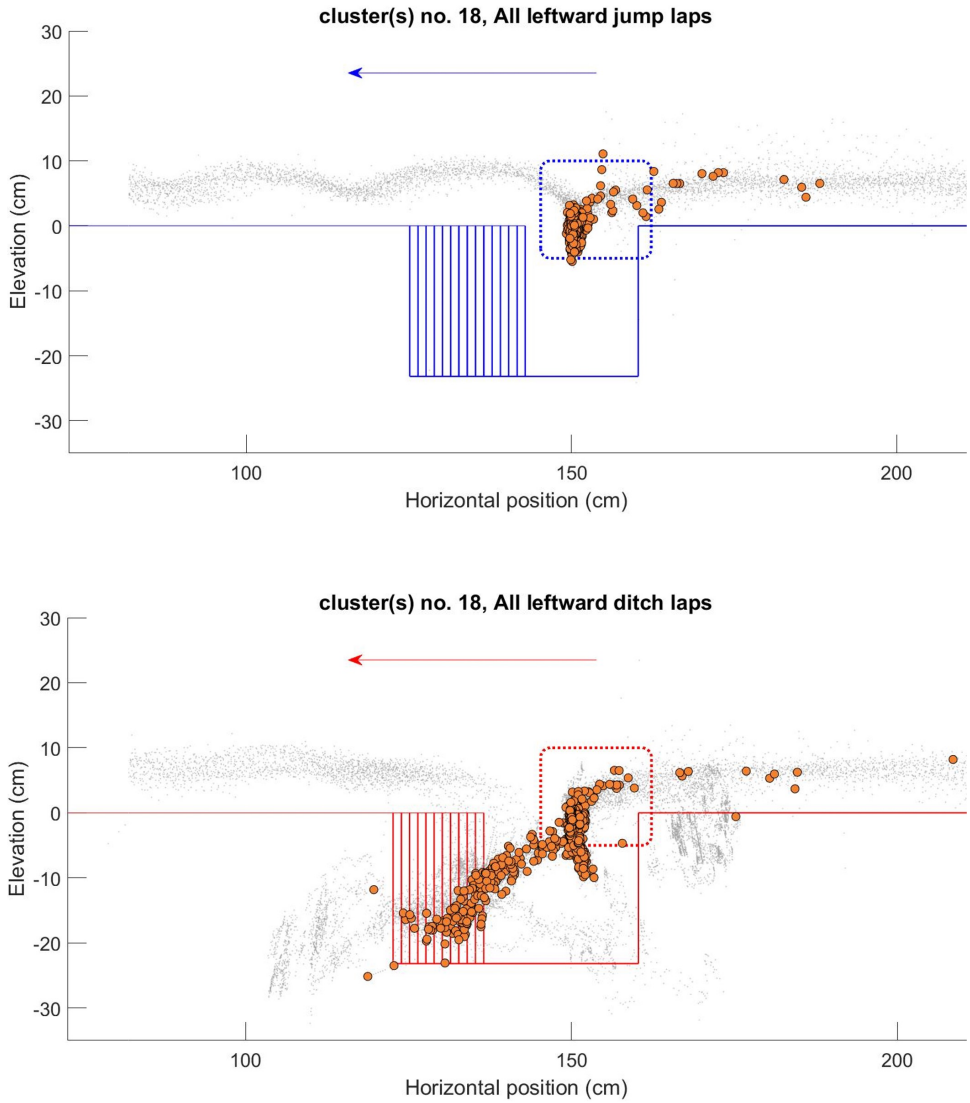

Figure 5.9: Side view pictures of the place field of a cell (no. 18) that is selective for ditching - active during ditching but silent during jumping. Orange markers show the location of the head of the animal when the cell fires. Gray dots show the occupancy of the rat, and the blue and red vertical lines show the edges of the adjustable gap for each jumping and ditching trial, respectively. The direction of the arrows indicates the direction of the animal passage. The cell is active during ditching but is almost silent during jumping trials.

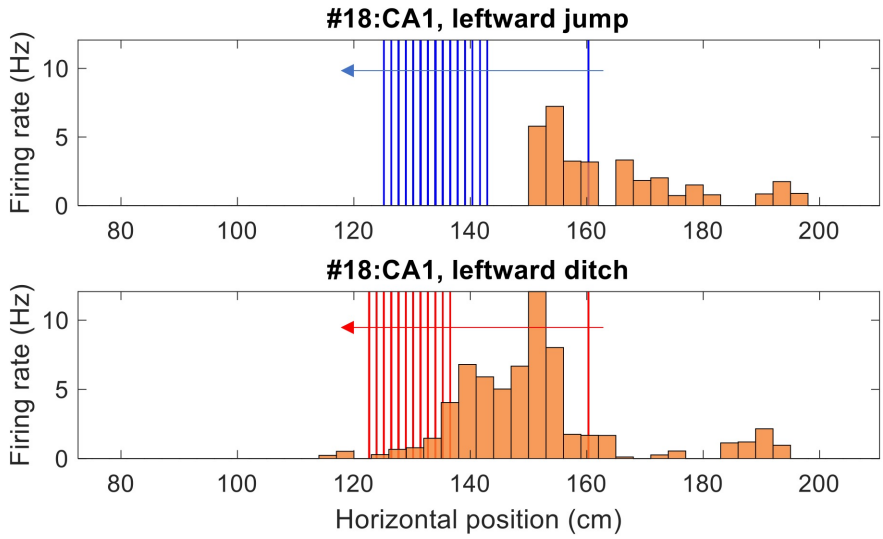

Figure 5.10: Firing rates comparison between jumping and ditching trials for a place cell (no. 18) - the same cell as the one in Figure 5.9. This figure illustrates a cell that is selective for ditching. The direction of the arrows indicates the direction of the animal passage. The adjustable gap for each trial is denoted by vertical lines - blue for jumping trials and red for ditching trials.

tiny place field, underscoring the diverse encoding capabilities of place cells. This category of cells, primarily predictive cells, is explained in detail in Section 6.1. Although these special cases underscore the rich dynamics of hippocampal place cells, some of them did not happen enough times to resemble a pattern. There should be more studies to understand their correlations.

5.4 Retrospective Encoding by Place Cells

Place cells not only encoded the current environment or the action of the animal but also exhibited encoding capabilities that spanned locations beyond the gap on the other side of the track. This emphasizes the ability of these cells to discriminate between different trajectories based on the animal's past actions.

Figure 5.12 illustrates two place cells with different firing rates at a location beyond the

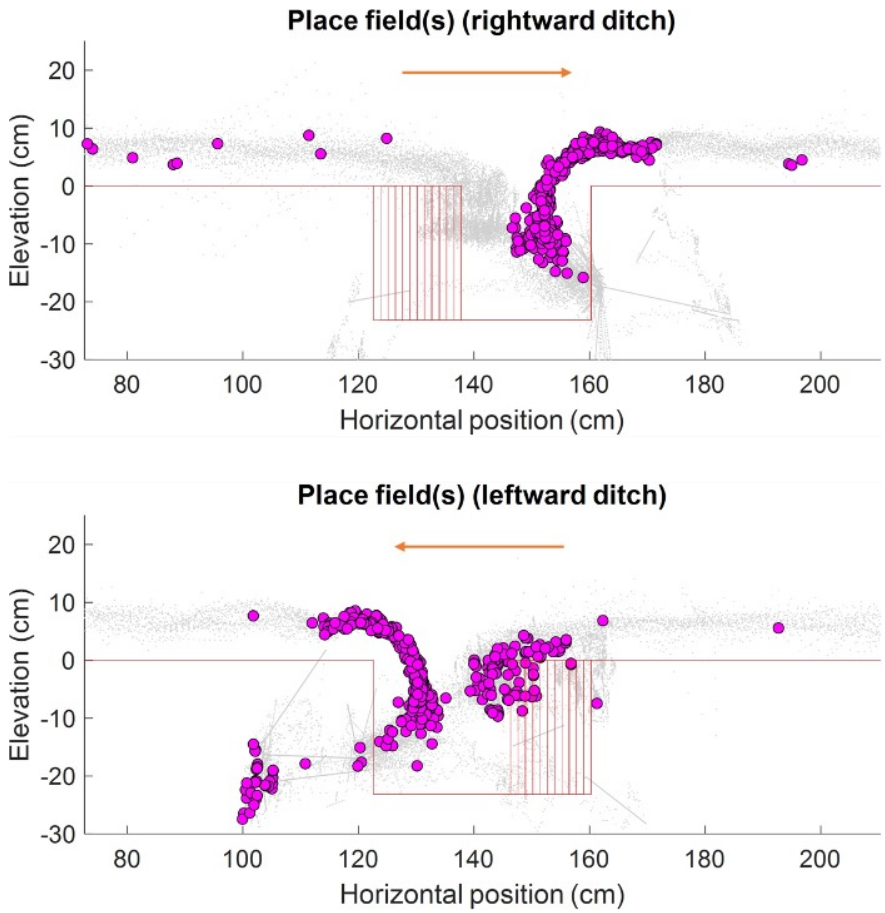

Figure 5.11: Side view images of the place fields of a single cell (no. 29) that fires when the animal jumps out of the gap in both directions. The cell is selective for ditching and is almost silent during jumping trials. Only ditching trials are displayed here. Magenta markers show the location of the head of the animal when the cell fires, and gray dots show the occupancy of the rat. The direction of the arrows indicates the direction of the animal passage. Vertical lines denote the adjustable gap for each trial.

gap depending on whether the rat had previously jumped or ditched at the gap location. The black dashed oval specifies the exact physical location but is encoded differently by these two cells. The cell marked orange fired in the dotted region only if the rat had traversed the gap by jumping, and similarly, the cell marked green fired in the area only after ditching. Since the firing of these cells at the current location (dashed oval) varies based on the previous trajectory or action of the animal, this phenomenon is referred to as retrospective coding.

5.5 Statistical Analysis

An objective statistical analysis was employed to determine if the place cells show selectivity towards specific jumping and ditching behaviors. The objective was to determine if there was a significant difference in the median firing rates of these cells during the two distinct trials. The Mann-Whitney U test was the preferred statistical method to achieve this goal. Section C.5 provides a detailed explanation of this test.

Figures 5.13 and 5.14 represent the distribution of firing rates of two different place cells within their field during jumping and ditching trials. By statistical comparison of these distributions, it can be determined whether the median of these two distributions is significantly different or not.

Some firing rate distributions like the one depicted in Figure 5.14 were normal, making Welch's T-test a potential candidate for assessing mean differences (see Section C.3.2.2). However, most observed distributions were zero-inflated (see Figure 5.13). Given the inherent characteristics of these distributions, the Mann-Whitney U test was considered more appropriate for comparing the populations, as it does not make any assumptions about the

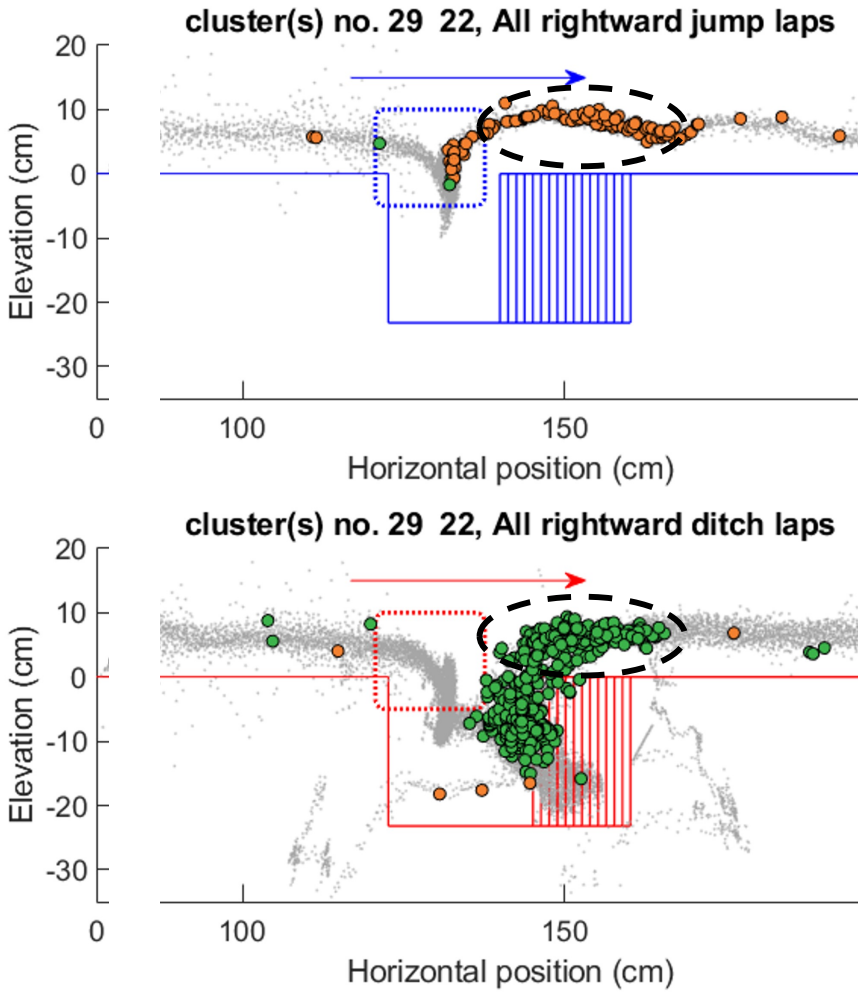

Figure 5.12: Side view images of the place fields of two cells (no. 22 and 29) that fire when the animal jumps over or out of the gap. Orange and green markers show the location of the head of the animal when the corresponding cell fires, and gray dots show the occupancy of the rat. Green place cells are almost silent during jumping trials. The direction of the animal passage is left to right, as indicated by the direction of the arrows. The adjustable gap for each trial is denoted by vertical lines - blue for jumping trials and green for ditching trials. Note that the black dashed oval specifies the same physical location but is encoded differently by these two cells. There is no firing of the green cell during any of the jumping trials.

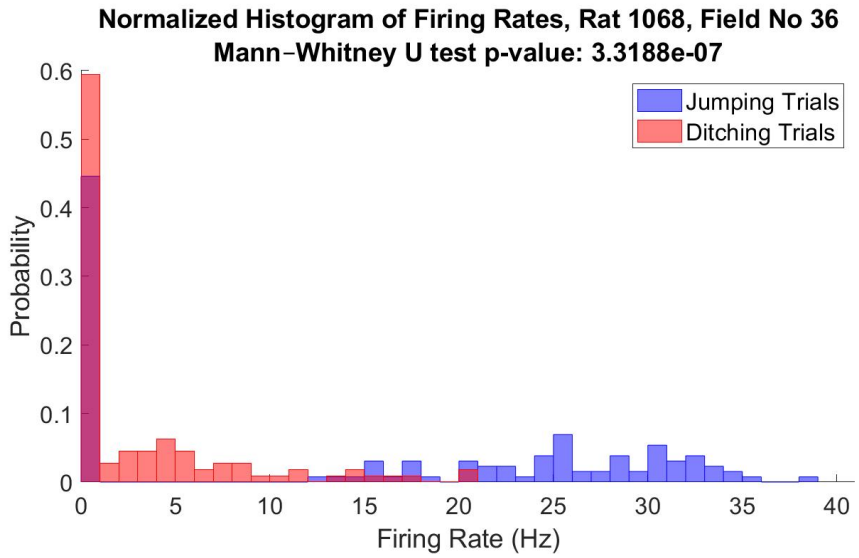

Figure 5.13: Firing rate distribution for a cell in its place field (no. 36) during an experimental session with one subject. The distribution for the jumping trials is plotted in blue, and the one for the ditching trials is plotted in red. This particular cell exhibited a significantly higher firing rate during jumping trials than ditching trials.

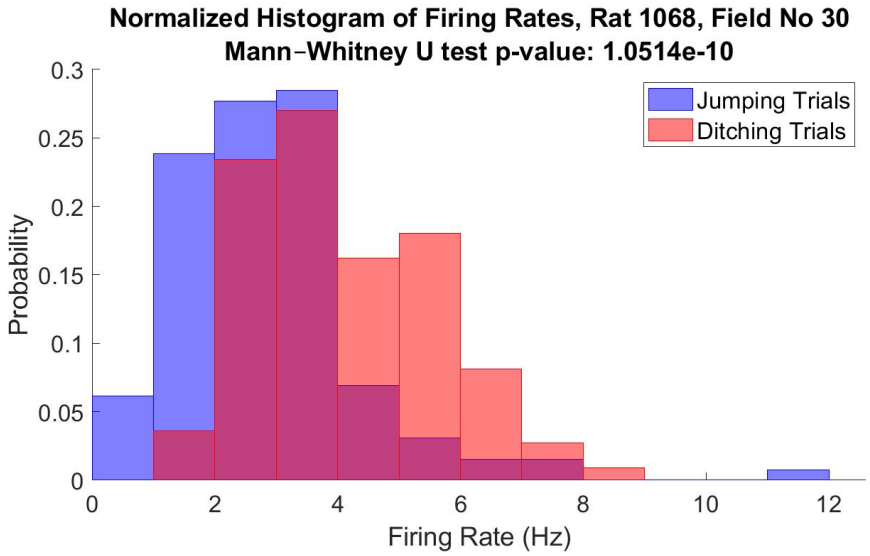

Figure 5.14: Firing rate distribution for a cell in its place field (no. 30) during an experimental session with one subject. The distribution for the jumping trials is plotted in blue, and the one for the ditching trials is plotted in red. For this cell, a significant increase in the firing rate was observed during ditching trials compared to jumping trials.

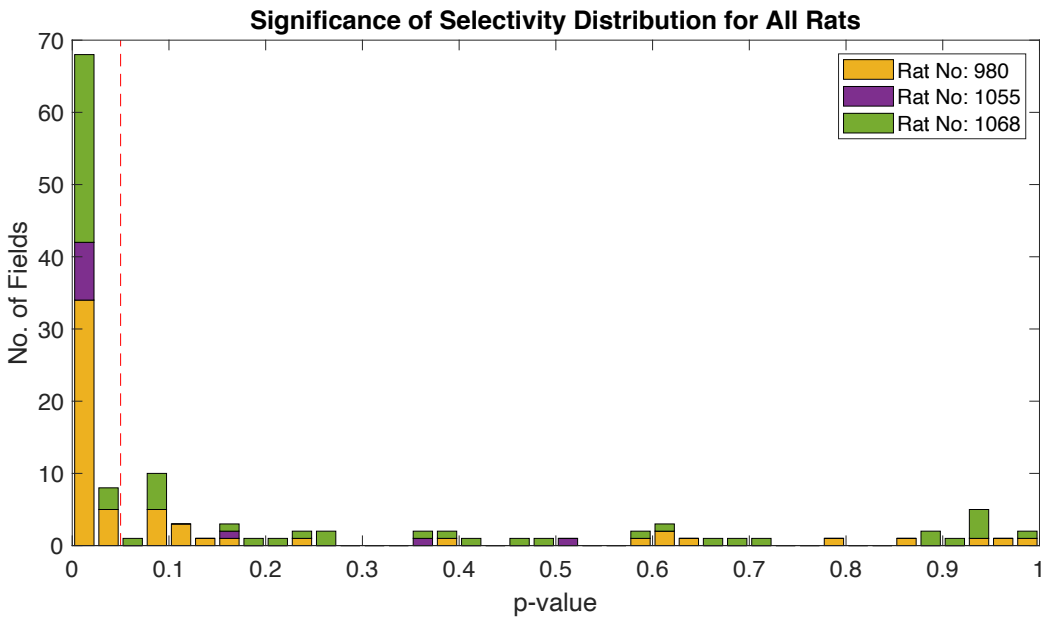

Figure 5.15: Histogram displaying the distribution of p-values obtained from the Mann-Whitney U test for numerous place cells across three different rats. Cells with p-values below 0.05 are considered to be significantly selective. The data indicates that a substantial number of place fields are indeed selective to either jumping or ditching trajectories.

underlying distribution of the data (see Section C.5).

The final statistical analysis focuses on the aggregate statistical significance across all the place cells studied. Figure 5.15 shows a histogram of the p-values from the Mann-Whitney U test for place cells recording from three rats during three sessions. A p-value threshold of 0.05 was set as the marker for statistical significance. Cells below this threshold indicate that many of these cells are significantly selective to either the jumping or ditching behaviors. This combined data provides a broader perspective, emphasizing the prevalence of selectivity among the analyzed place fields.

Figure 5.16 displays all the place fields from a single experimental session, represented as circle markers. The left and right plots show the leftward and rightward fields. The x-axis shows the location of the place field along the track, and the y-axis shows the selectivity

ratio. This ratio was calculated by first determining the firing rates for both jumping and ditching trials and then finding the ratio between the firing rate for jumping trials and the average rate across both trials. A ratio near zero points to higher selectivity for jumping, one close to one for ditching, and values in between suggest no selectivity. Place fields that are significantly selective ($p < 0.05$) for jumping are marked in blue, and the ones that are significantly selective for ditching are marked in red.

5.6 Discussion

As explained in this chapter, place cells in the hippocampus discriminated between jumping and ditching trials. These cells exhibited distinct firing patterns, with some cells displaying a selective response to jumping and others to ditching. Such distinctive encoding suggests that these cells actively encode different trajectories based on the behavioral choices made by the rats. Similar to the splitter cells discussed in Section 2.6, these findings provide evidence that place cells can adapt firing rates to reflect behavioral choices, demonstrating selectivity for different actions or trajectories and the capacity for coding them retrospectively.

The retrospective coding suggests that the firing properties of place cells are not solely determined by the current location of the animal but also reflect the animal's history of action or behavior. These findings are consistent with those reported by [92] and [90]. However, there is an essential difference in the experiment setup. In previous studies, the animals were navigating a flat, 2D maze, while in this work, they traversed distinctive 3D trajectories that had similar 2D projections onto the horizontal plane. In other words, the animals expanded the possible trajectories by jumping over the gap and connecting two

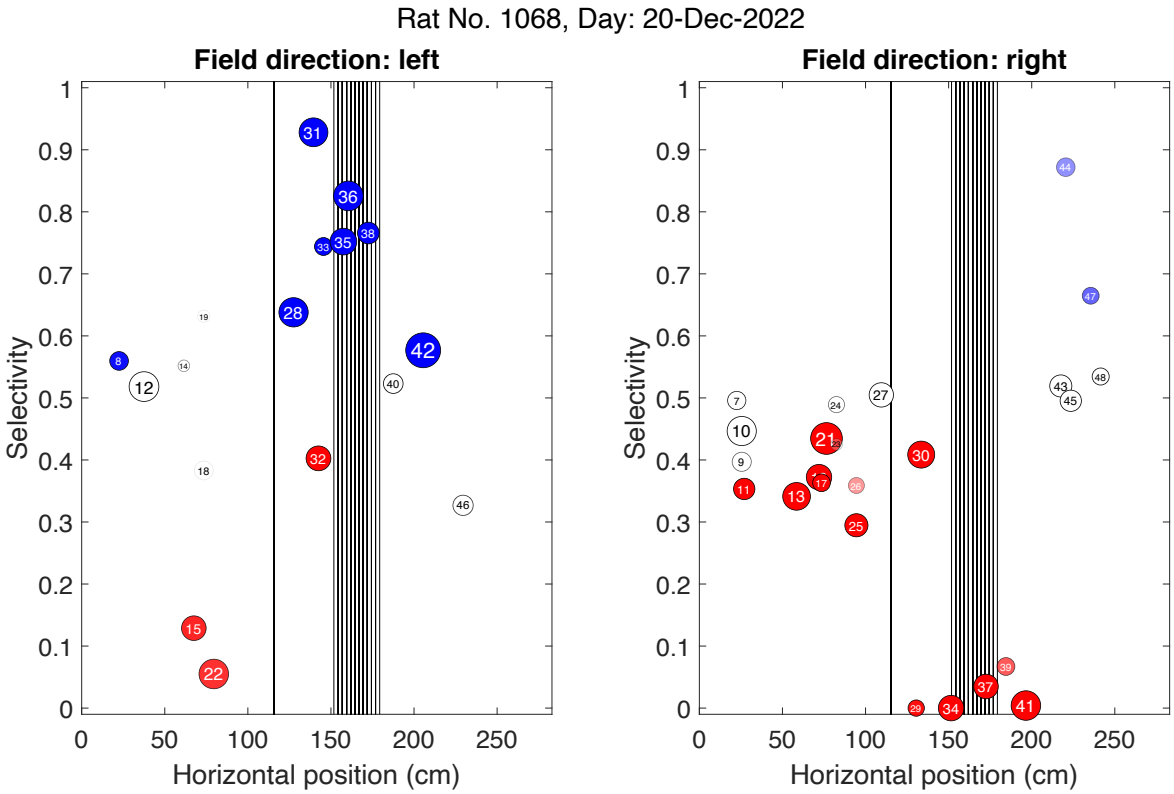

Figure 5.16: Selectivity of all the fields recorded during one experimental session that includes jumping and ditching. The left and right plots show the leftward and rightward fields. The x-axis shows the location of the center of the corresponding place fields, and the y-axis shows the selectivity of the fields for jumping or ditching. Selectivity is calculated by the ratio between the average firing rate of jumping trials divided by the sum of the average firing rates during both jumping and ditching trials. Ratios close to one indicate higher selectivity for jumping, ratios close to zero indicate higher selectivity for ditching, and ratios in the middle indicate no selectivity. Significantly selective fields ($p < 0.05$) are marked in blue for jumping and red for ditching. The size of the markers indicates the peak firing rate of the fields, while the opacity of the markers reflects the stability of the fields. Black vertical lines show the edges of the adjustable gap for each trial.

topologically disconnected locations.

These observations reveal a rich and complex role for place cells in spatial navigation, learning, and memory. The animal's retrospective encoding can be used to assign the outcome of a trial, such as food contingency, to the behavior of the animal. For instance, if the animal received different food rewards for different behaviors, the hippocampus would have the information required for associating different behaviors of jumping and ditching to different outcomes, helping the animal learn and choose the more efficient task. This can have implications for the broader understanding of how neural activity in the hippocampus contributes to complex locomotor behaviors.

The distinct encoding of 3D trajectories, especially the retrospective encoding, demonstrates the adaptability of hippocampal place cells to changes based on the complex locomotor behaviors of the animal. Since jumping and ditching trials are related to different behaviors and the animal navigates through different trajectories, it is impossible to distinguish if the hippocampal place cells are encoding different trajectories, actions, or a combination of the two. Through this differential encoding, place cells could provide a neural basis for the animal to remember and choose between different paths or strategies in the environment, thus playing a key role in decision-making processes. Differential encoding of jumping and ditching trajectories is illustrated in Figure 5.17. With distinct marker colors for different cells, the sequential firing of the place cells varies when the animal navigates in the jumping and ditching trajectories. This different sequential firing pattern indicates that the hippocampus encodes jumping and ditching experiences differently.

These findings provide a nuanced understanding of the role of hippocampal place cells in spatial navigation and memory. The distinctive encoding of jumping and ditching trials may

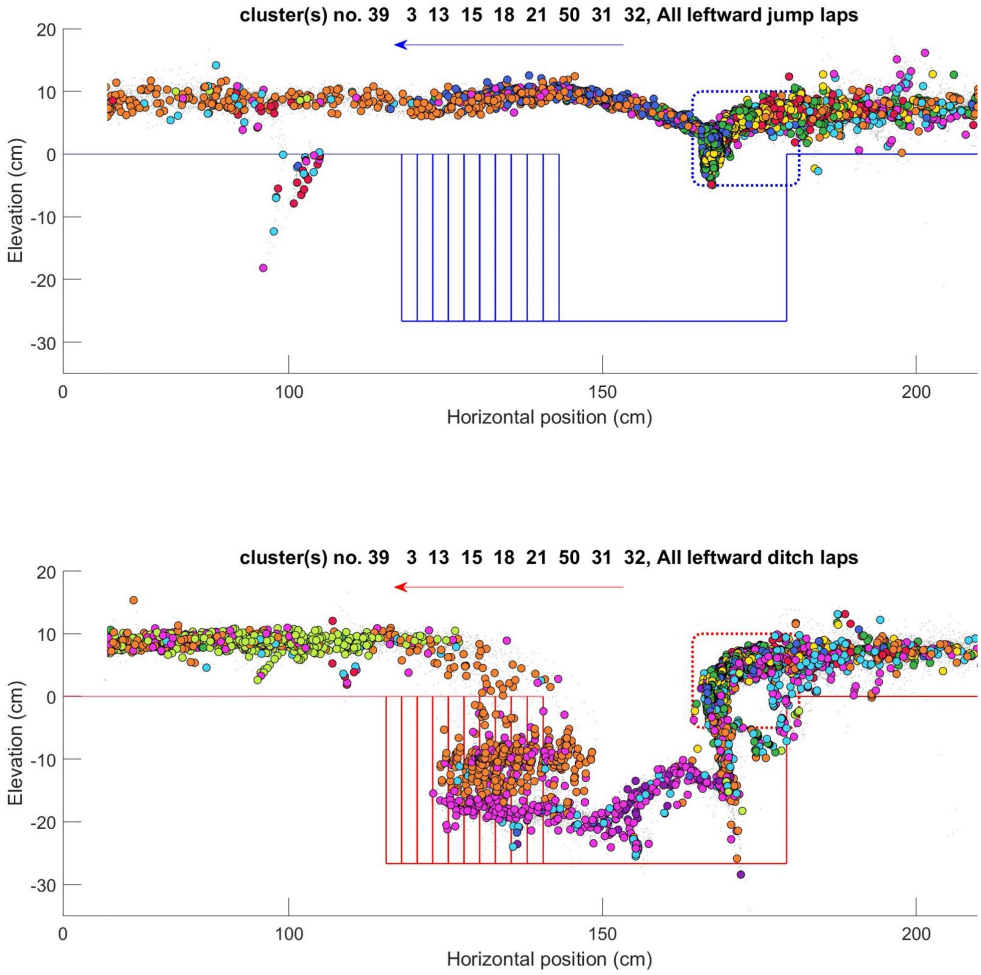

Figure 5.17: Encoding of splitter cells for jumping and ditching trajectories. The sequential firing of hippocampal place cells differs for these two trajectories, making them different experiences. The direction of the animal passage is right to left, as indicated by the arrows. The adjustable gap for each trial is denoted by vertical lines - blue for jumping trials and red for ditching trials.

serve as a form of memory that the animal can use to inform future behaviors or decisions. Furthermore, this retrospective coding might also underpin the ability of animals to navigate back to previously visited locations or to correct their trajectory based on past mistakes.

Chapter 6

Predictive Nature of Place Cell Activity

Building upon the findings established in Chapter 5 regarding immediate and retrospective coding in place cell activity, the question that presents itself is: Do place cells also exhibit prospective coding before performing complex locomotor behaviors? Can the neural activity of hippocampal place cells be utilized to predict an animal's navigation in 3D trajectories, specifically when choosing to jump or ditch when confronted with a gap?

This chapter explores the predictive nature of place cell activity before such complex locomotor behaviors. A key point of investigation is the differential firing rates of place cells before jumping and ditching. This characteristic plays an important role in creating a predictive model of the animal's behavior.

6.1 Prospective Encoding of Place Cells

Some place cells with a field on the launchpad region exhibited different firing rates when animals contemplated jumping or ditching, as mentioned in the previous chapter. This differential firing pattern was a key observation underpinning the development of the predictive decoder that will be discussed in this chapter. For example, Figure 6.1 illustrates a place cell with a place field at the decision point, precisely where the rat perches before making a behavioral choice. The cell becomes silent when the animal initiates the jumping or ditching action. Comparing the firing rate of this cell before jumping and ditching trials, as shown in Figure 6.2, shows that the peak firing rate of a cell was more than double before jumping trials compared to ditching trials. This higher firing rate during jump preparation suggests a prospective encoding by the cell.

6.2 Differential Encoding in Similar Physical Location

A crucial consideration in interpreting the differential firing rates of the place cells is the potential influence of the animal's position and orientation as it prepares for jumping versus ditching. A valid concern is that these spatial and orientation discrepancies might be driving the different firing rates instead of anticipating future behavior.

To address this concern, an extensive spatial analysis was conducted. The entire experimental space was meshed using 3D grids, and the occupancy of the rat was calculated in each cubic bin of a 3 cm edge. Bins corresponding to the decision-making region were focused on,

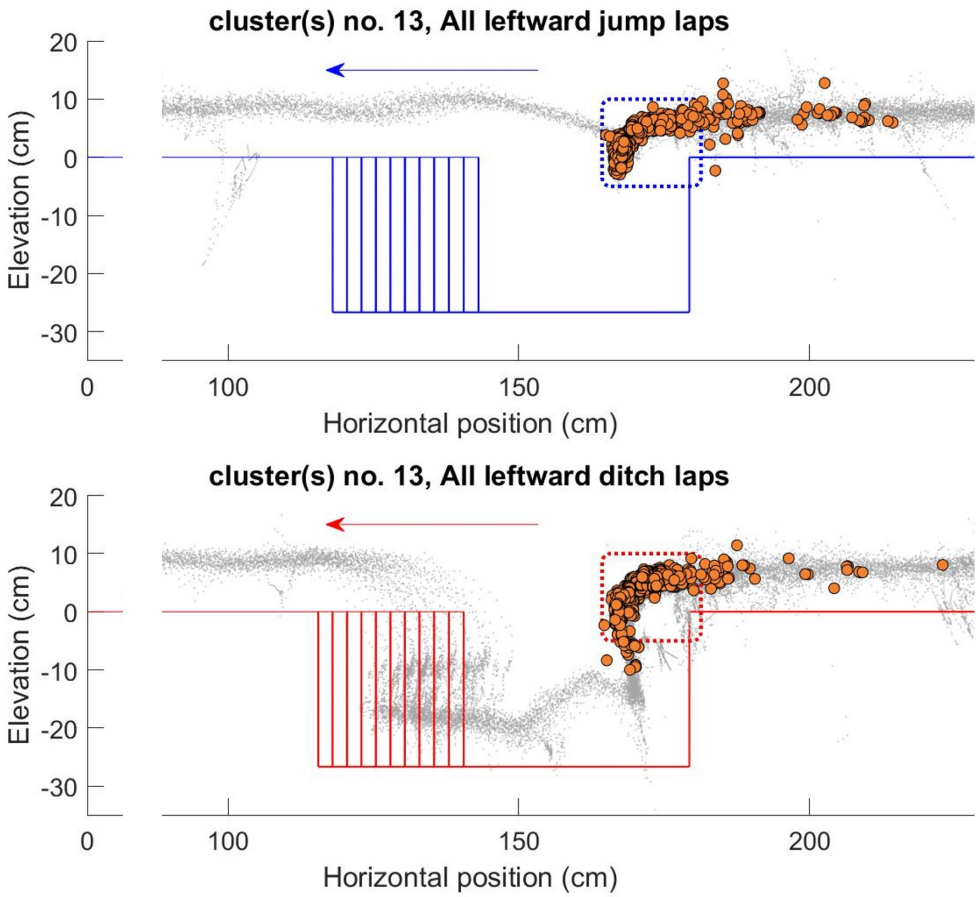

Figure 6.1: This figure displays an example of a cell exhibiting a place field exclusively at the rat's perching location when deciding to jump or ditch. The arrows indicate the direction of the animal's passage. Vertical lines denote the adjustable gap for each trial, and the dotted rectangle designates the perching location - blue for jumping and red for ditching trials.

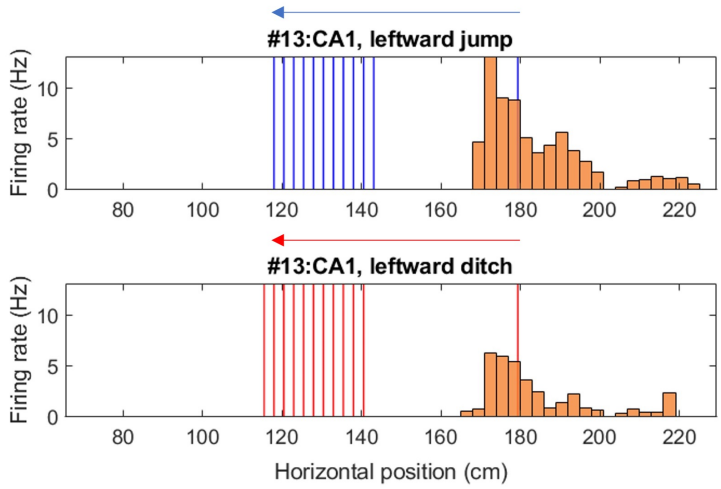

Figure 6.2: This figure displays an example of a cell exhibiting a place field exclusively at the rat's perching location when deciding to jump or ditch. On average, the cell's firing rate before jumping trials is more than double that of ditching trials. The direction of the arrows indicates the direction of the animal passage. The adjustable gap for each trial is denoted by vertical lines - blue for jumping trials and red for ditching trials.

with the criteria that the occupancy should be greater than 500 ms for both jumping and ditching trials. The last constraint was that the animal should be on the launchpad.

Figure 6.3 displays the position (markers) and orientation (arrows) of the rat's head after implementing the selection process described above. Blue and red are indicative of jumping and ditching trials, respectively. As seen in the figure, the position and orientation of the rat's head are quite comparable across both types of trials at the decision point. This similarity in spatial and orientation parameters strengthens the argument that the differential firing rates of the place cells represent an anticipation of the forthcoming behavior rather than merely a response to current spatial factors.

Figure 6.4 further illustrates the differential firing rates between jumping and ditching trials. In this representation, the radius of each purple 3D marker in the selected 3D bins indicates the cell's firing rate within that bin. Notably, the cell exhibits a higher firing rate prior to takeoff in jumping rather than ditching trials, even under similar spatial regions.

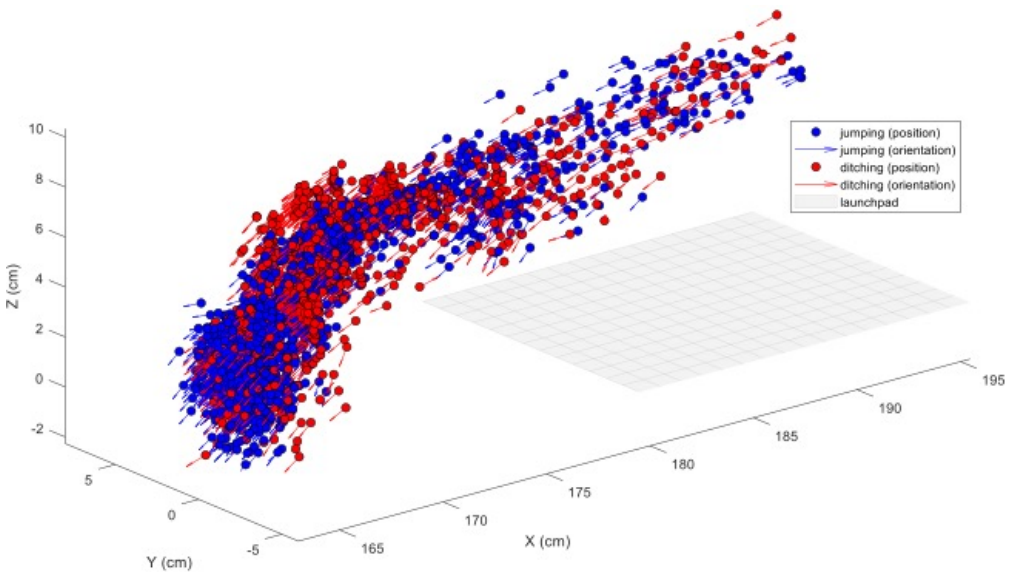

Figure 6.3: After selecting the data points within the 3D bins that had occupancy above a given threshold, the position and orientation of the rat's head appear similar for both jumping and ditching trials. The markers represent the position, while the arrows indicate the orientation of the rat's head - blue for jumping trials and red for ditching trials. The direction of the animal passage is from right to left. The data is downsampled at 10Hz for illustration.

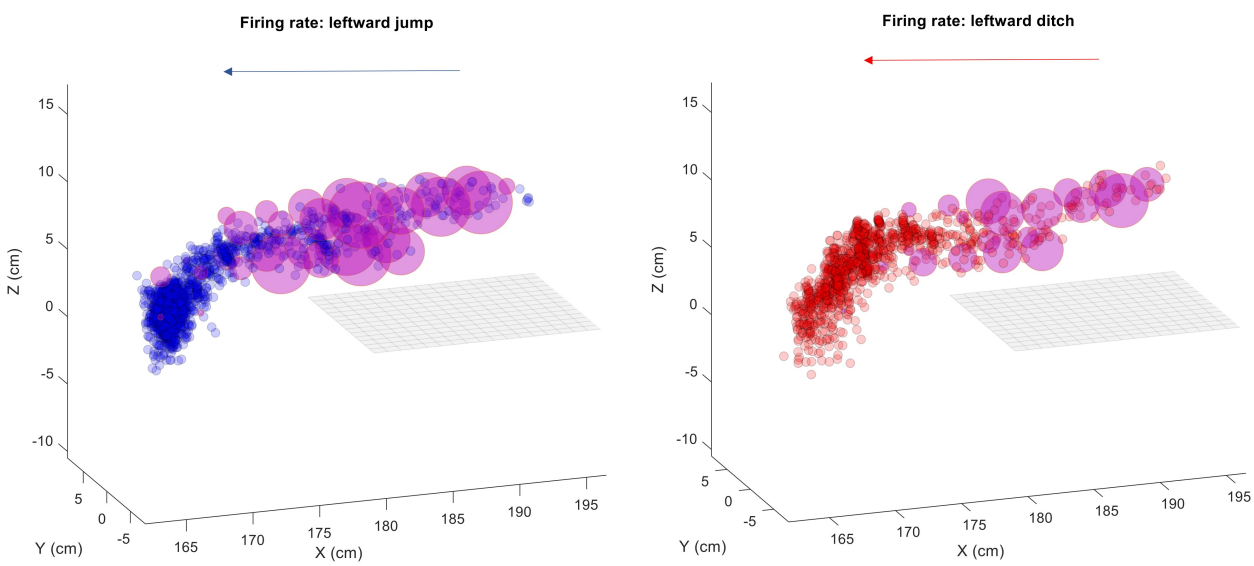

Figure 6.4: 3D spatial distribution of firing rates during the decision point in both jumping and ditching trials. The blue and red markers represent the position for jumping and ditching trials, respectively. The radius of the purple spheres in each selected 3D bin represents the firing rate of the cell. The direction of the animal passage is from right to left.

6.3 Bayesian Decoder

As shown with an example in the previous section, some place cells had a different firing rate before takeoff in jumping and ditching trials. In order to show the existence of predictive information in the cells, a neural Bayesian decoder was implemented to utilize the encoded information and predict the decision of the rats. This decoder used the average firing rates of the rats' place cells to forecast whether a rat would jump or ditch the gap at a given lap. Similar to the neural decoder, a behavioral decoder was developed by utilizing the average position and orientation of the animal's head at each lap to predict the decision of the animal.

For every lap, the decoder computed the rate of neural spikes (for the neural decoder) or the average head pose (for the behavioral decoder) within specific temporal and spatial constraints. The temporal constraint was 3 to 0.5 seconds before takeoff, and the spatial constraint was the area on the launchpad (up to 15 cm from the edge of the launchpad and height above 5 cm below the launchpad). The visual inspection confirmed similar occupancy for both jumping and ditching trials. Each lap was labeled as 'jump' or 'ditch' based on the decision of the animal. Information on the decoder's implementation can be found in Section 3.4.4, along with its corresponding pseudocode presented in Algorithm 1.

The Bayesian decoders established statistical models for the distribution of the firing rates by computing the mean vector and covariance matrix from multi-dimensional data. This model was then employed to estimate the likelihood and posterior probability of each behavioral category (jumping or ditching) based on the observed neural activity or the observed head pose. For each data point in the validation set, the behavior with the highest posterior probability was selected as the prediction.

To validate the performance of the Bayesian decoders, evaluation metrics such as accuracy were calculated and compared with the metrics from the random decoder. Accuracy shows the overall correctness of all predictions (see Section B.1). The random decoder predicts behaviors randomly based on the prior probabilities in the training dataset. For the statistical test of individual subjects, bootstrapping (sampling with replacement with 1000 repetitions) was utilized, and the significance of the accuracy of the Bayesian decoder was calculated. For more information about statistical analysis, see Section 6.4.

6.3.1 Neural Bayesian Decoder

The neural Bayesian decoder was developed and trained using the average firing rates of place cells before jumping and ditching behaviors. For every lap, the decoder computed the average firing rate of neural spikes within specific spatiotemporal constraints mentioned in the previous section (see Section 6.3 for more details).

To show the performance of the Bayesian decoder, total accuracy for both jumping and ditching predictions was calculated. These metrics were compared to a random decoder as a baseline. The comparison for one experiment session demonstrated in Figure 6.5 shows that the predictive capabilities of the Bayesian decoder are far better than random chance.

6.3.2 Behavioral Bayesian Decoder

As the findings in Section 4.1.3 showed, there is predictive information in the behavior of the animal when the animal is at the decision point. Specifically, the head bobbing frequency was higher before jumping trials than ditching trials. In order to extract predictive

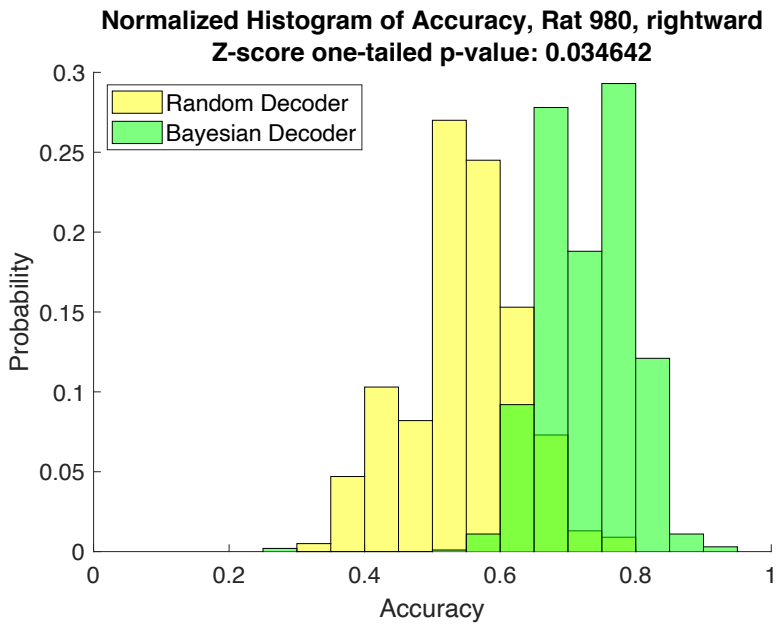

Figure 6.5: The histogram of the accuracy of the neural Bayesian decoder and the random decoder for rightward trials in an experiment session for rat 980. The histogram is calculated by bootstrapping the dataset selected for training and validation. Statistical analysis showed that the accuracy of the neural Bayesian is significantly higher than the accuracy of the random decoder.

information from animal behavior, a behavioral Bayesian decoder was developed and trained.

This decoder utilized the average of 6 degrees of freedom from the 3D position and orientation (roll, pitch, and yaw) of the rat's head within the aforementioned spatiotemporal constraints. Details about the 3D head pose tracker employed in this study can be found in Chapter 3.

Figure 6.6 illustrates the histogram of accuracies for the behavioral Bayesian decoder and the random decoder for both leftward trials in an experiment session. The predictive capabilities of the behavioral Bayesian decoder are far better than the random decoder.

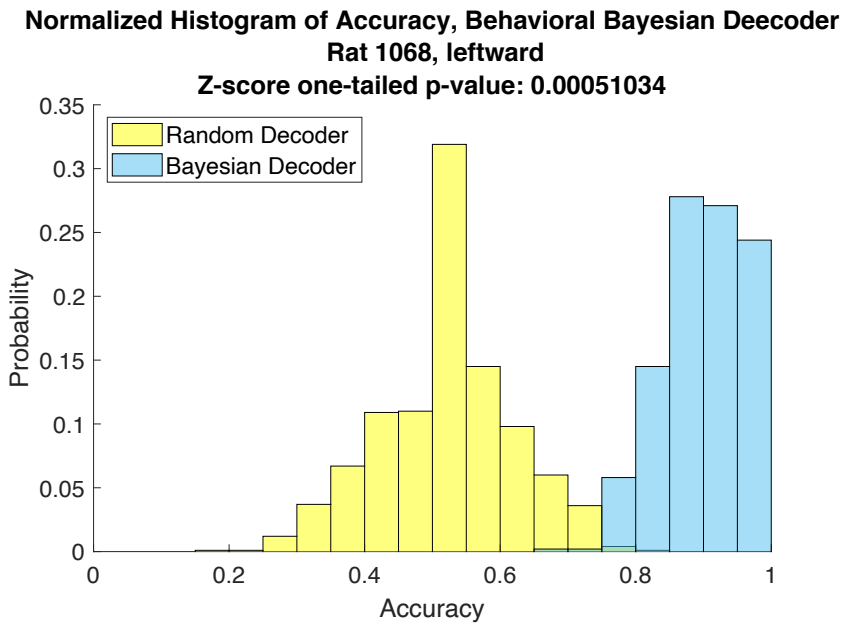

Figure 6.6: The histogram of the accuracy of the behavioral Bayesian decoder and the random decoder for leftward trials in an experiment session for rat 1068. The histogram is calculated by bootstrapping the dataset selected for training and validation. Statistical analysis showed that the accuracy of the behavioral Bayesian is significantly higher than the accuracy of the random decoder.

6.4 Statistical Analysis of Bayesian Decoders

In order to understand the Bayesian decoders' predictive capabilities, a statistical evaluation was conducted focusing on the accuracy of the decoders. Since the outcome of the Bayesian decoders is stochastic, bootstrapping (sampling with replacement with 1000 repetitions) was utilized to use different portions of the data for training and validation with each sampling to calculate accuracy. The results that are listed in 6.1 show the mean and standard deviation of the accuracy distributions for different sessions and decoders.

The neural decoder exhibited accuracies varying from 64% to 87%, which robustly substantiates the notion that place cell activity encodes predictive information for complex locomotor behaviors. Moreover, the behavioral decoder accuracies ranging from 73% to 95% also indicate that there is anticipatory behavior during the preparation time on the

Table 6.1: Comparison of the prediction accuracy of the neural and behavioral decoders against the random decoder. The random decoder only utilized prior probabilities for prediction. Both Bayesian decoders show significantly higher accuracy than that predicted by random chance ($p = 0.0156$, binomial test for 6 sessions and 3 rats). Furthermore, the behavioral decoder demonstrates statistically significantly higher ($p = 0.0156$, binomial test) accuracy than the neural decoder. The mean accuracy and standard deviation for each decoder are given in percentages.

Rat ID	Direction	Random Decoder	Neural Decoder	Behavioral Decoder
1068	Leftward	52% ± 7%	85% ± 5%	90% ± 6%
1068	Rightward	50% ± 7%	77% ± 6%	95% ± 4%
1055	Leftward	53% ± 7%	64% ± 8%	85% ± 7%
1055	Rightward	55% ± 7%	60% ± 14%	73% ± 9%
980	Leftward	52% ± 8%	75% ± 9%	93% ± 5%
980	Rightward	54% ± 8%	72% ± 6%	93% ± 6%

launchpad. These results also align with the anticipatory behavior of higher head-bobbing frequency before jumping.

The predictive accuracies of the Bayesian decoders were, on average higher than the corresponding random decoders. Given that the accuracy was above the chance in all 6 sessions, the binomial test shows that the Bayesian decoders were significantly higher than random chance given the binomial test ($p = 0.0156$). The random decoder served as a baseline model, with predictions solely based on the prior probabilities of the training dataset, providing a fundamental comparison metric. This comparative assessment significantly underscores the superior performance of the Bayesian decoder against the null hypothesis.

Table 6.2 shows the performance of the neural Bayesian decoder. It lists the number of cells utilized in the decoder, Cohen's d to measure the effect size (further discussed in Section C.6), and the p-values that signify the statistical significance of the results. To determine the p-values, the signed difference between the accuracies of the neural and random decoders was first computed for every bootstrapping sample. This led to the formation of a distribution of differential accuracies. From this distribution, a one-tailed z-score was

Table 6.2: Performance of the neural Bayesian decoder for different rats during a Titration session. Results are categorized by the direction of movement (leftward and rightward). Statistical significance is indicated by an asterisk(*) for p-values less than 0.05. 5 out of 6 Cohen's d values exceed 0.8, indicative of a large effect size. 4 out of 6 results are statistically significant.

Rat ID	Direction	Number of Cells	Cohen's d	P-value
1068	Leftward	9	5.45	6.51×10^{-5}*
1068	Rightward	5	4.11	0.00207*
1055	Leftward	2	1.48	0.148
1055	Rightward	1	0.41	0.385
980	Leftward	10	2.79	0.0192*
980	Rightward	5	2.50	0.0346*

calculated (as elaborated in Section C.2). The subsequent p-value was derived using this z-score. Notably, the table indicates that 4 out of the 6 sessions analyzed have achieved statistical significance.

The performance of the neural decoder depends on the availability of sufficient neural data to ensure meaningful accuracy. In certain sessions, there was a limited number of cells for input, for instances where only 1 or 2 cells were available for rat 1055. Such sessions predictably exhibited the lowest accuracy rates for the neural decoder.

The analysis of the behavioral Bayesian decoder is presented in Table 6.3. It shows that 5 out of the 6 sessions achieved statistical significance. The p-values were calculated using the same one-tailed z-score method used for the evaluation of neural decoders. Both the neural and behavioral decoders' results suggest that they can effectively predict the decision of the animal using either neural activity or anticipatory behavioral cues.

Table 6.3: Performance of the behavioral Bayesian decoder for different rats during a Titration session. Results are categorized by the direction of movement (leftward and rightward). Statistical significance is indicated by an asterisk(*) for p-values less than 0.05. All Cohen's d values exceed 0.8, indicative of a large effect size. 5 out of 6 results are statistically significant.

Rat ID	Direction	Cohen's d	P-value
1068	Leftward	4.6	0.00102*
1068	Rightward	5.8	4.01×10^{-5}*
1055	Leftward	3.6	0.0121*
1055	Rightward	1.9	0.192
980	Leftward	4.5	0.00117*
980	Rightward	4.2	0.00297*

6.5 Discussion

The findings presented in this chapter are important in understanding the prospective encoding abilities of place cells. The differential firing rates of these cells before a rat starts to jump or ditch constitute evidence for a prospective code. The distinction in the firing rates suggests that these cells predict the future behavior or trajectory of the animal.

A Bayesian decoder was utilized to demonstrate the predictive nature of place cells objectively. The decoder's significant accuracy compared to the random decoder showed that combined data from the population of the cells can be effectively utilized to predict behavior accurately. The neural decoder's ability to accurately predict the rats' choice to 'jump' or 'ditch' indicates that place cell activity contains anticipatory information.

The goal of the Bayesian decoder is not to predict the behavior of the animal in real time. It uses temporal information (between 3 to 0.5 seconds) relative to the time of takeoff in order to filter the data. However, the real-time decoder does not have access to this temporal information. The main objective of the Bayesian decoder was to prove the existence of predictive information in the place cells.

It is noteworthy that the general position and orientation of the animal head were visually comparable during preparation to jump or ditch. However, by using the minute differences between the position and orientation, the behavioral decoder was able to show that there are significant differences in the preparatory behavior that can be used to predict the decision of the rat. So, it is not yet clear if the neural information can predict decisions before the behavioral indicators or vice versa. As mentioned before, increasing the number of place cells enhances the accuracy of the neural decoder. Similarly, using other behavioral metrics, such as body posture, might also increase the accuracy of the behavioral decoder.

Lastly, this chapter's results provide a powerful argument for the predictivity of place cells. Studies have shown some neural mechanisms in the hippocampus of rats, such as replay and preplay, to use their cognitive map to predict future behaviors based on past experiences [84]. The prospective encoding of place cells presented in this chapter could also be a mechanism involved in decision-making processes, potentially contributing to the planning of 3D trajectories and predicting future actions.

Chapter 7

Conclusion and Future Directions

This dissertation presents a behavioral and neurophysiological study of rats performing complex locomotor behaviors, namely jumping and ditching. The research explored how previous choices of the animals influenced their current decision making and examined whether head posture or behaviors such as head bobbing could predict subsequent actions of the animals. It also examined the correlation between hippocampal theta rhythm frequency and speed during different kinematic phases of jumping. Furthermore, this work shed new light on the dynamic role of place cells in encoding trajectories associated with jumping and ditching. The hippocampus not only encoded these trajectories differently but also contained predictive information about the animal's decision, which could be decoded to predict its behavior. Overall, these findings deepen our understanding of the intricate role of the hippocampus during complex locomotor behaviors and lay the groundwork for future investigations in this domain.

7.1 Summary of Key Findings

Building upon existing literature [159, 160], this study reaffirmed the presence of a hysteresis effect during decision-making tasks in a novel context. Animals jumped longer distances when the gap length increased compared to when it decreased. The history of decisions influenced the current decision of the animal. This finding offers insight into the decision-making processes in animals based on their judgments. Perceptual judgments originate from both sensory experiences and the cognitive interpretation of those experiences [161]. The hysteresis effect for rats before jumping and ditching seems more of a cognitive effect, suggesting that prior experiences can influence subsequent actions and decisions, potentially as a safety mechanism or an adaptive strategy in assessing environmental challenges.

Furthermore, the behavior of the animals at the decision point was different before jumping versus ditching. Specifically, the frequency of head-bobbing was significantly higher before jumping than ditching. It is important to mention that the animals moved their bodies as well as their heads during head bobbing. Therefore, head and body movement was either a muscle preparation for the impending leap, a mechanism to estimate the distance of the gap (see Section 4.1.3), or a combination of both. In any event, the stakes were higher for jumping, so the higher head bobbing was in line with the expectation. Moreover, the nuanced differences in the head posture during the preparation time were enough such that the Bayesian decoder could predict the animal's decision significantly better than chance. It indicates that the animal showed a distinct head posture and probably corresponding body posture before jumping and ditching.

Another finding is the consistent relationship between theta frequency and speed, which

persisted even during the aerial phase of the jump. While such a correlation for running animals has been observed [142], it is the first time that this correlation is documented when the movement of its limbs does not control the speed of the animal during a voluntary movement. This suggests that the correlation between the frequency of the theta rhythm and speed is not due to the movements of limbs of the animals when running on the ground. This implies that the interplay between the theta rhythm frequency, an internal brain signal, and the animal's speed, an external kinematic variable, is not solely contingent on the animal's limb movements. So, even though the animals could not fully control their speed during the aerial phase, the frequency of their theta rhythms still correlated with their body speeds.

An intriguing observation emerged when examining theta frequency during various phases of jumping. While theta frequency displayed a correlation with speed in several kinematic phases of jumping, such as running, landing, and even the aerial phase, a unique pattern was observed during takeoff (specifically, within the 100-150 ms time window). During this phase, the theta frequency remained nearly constant, close to its maximum frequency. This behavior suggests that during the preparation phase, marked by noticeable head and body movements, the animal might increase its theta frequency in anticipation of achieving peak speed during the subsequent aerial phase. It is important to note that this discovery is unprecedented in existing literature.

Shifting the focus to place cells, they demonstrated the ability to change their firing rates to encode information during complex locomotor tasks, differentiating between jumping and ditching trajectories. This splitter-like phenomenon was similar to previous studies [92] but happened in a completely novel context. The distinct retrospective encoding of the same environment was not due to external cues or reward contingencies but because of the

decisions of the animal to choose different 3D trajectories based on the previous experiences and its assessment of the current gap.

Lastly, the place cell activity exhibited predictive information at the decision point before the initiation of jumping and ditching. This predictive aspect of place cells presents an interesting facet of their function and is in line with previous research on the prediction nature of the hippocampus in different time scales [162]. The experimenter did not enforce the decisions of the animals by external cues or reward contingencies. In titration experiments, adjustments to the gap length, based on the animal's last decision, enhanced decision making and reduced habitual behavior.

7.2 Implications of the Findings

The findings of this dissertation enrich our understanding of spatial navigation. By shedding light on the encoding of place cells during complex locomotor behaviors, this study offers a fresh perspective on neural mechanisms underpinning animal navigation. These implications can provide deeper insights into the field of neuroscience.

Theta rhythm is essential in encoding spatiotemporal information during navigational tasks [163]. This thesis contributes to the previous works by showing the correlation between theta frequency and speed during the aerial phase of the jump. This suggests a deeper linkage between the theta rhythm frequency and speed beyond just the locomotion mechanics. Furthermore, this research revealed that theta frequency was almost constant during a large range of speeds (from 10 m/s up to 400 m/s) during the takeoff time (for about 100-150 ms). This implies that theta rhythm increased in anticipation of peak speed

during a jump, indicative of an internal model that predicts animal speed based on planned tasks. Should future studies validate these findings, it would underscore the role of the theta rhythm as an independent mechanism that adjusts based on predictions of imminent actions.

Splitter cells have been studied in spatial tasks on planar mazes, differentiating between trajectories based on previous, current, or future behaviors [23]. This thesis expands on that and shows such splitter-like phenomena exist even when animals navigate through 3D trajectories using complex locomotor tasks. Previous works did not distinguish between the encoding of 3D space and the 2D projection of the animal onto the experiment rig. Animals in previous studies navigated on complex 3D surfaces, such as the surface of a 3D lattice [64] or the surface of inclined planes [139]. However, their navigation is restricted to the surface of the experiment rig. They are not navigating two distinct 3D paths that project the same trajectory onto the surface of the experiment rig. This dissertation shows such a novel phenomenon. This experiment paradigm, where animals traverse a gap by jumping or ditching, is distinctive because both trajectories have a similar projection onto the surface of the experiment apparatus. This implies that the place cells of rats encode 3D space and not 2D surfaces.

Robots inspired by biological systems utilize jumping mechanisms to address the problem of navigation through challenging terrains [32]. Moreover, algorithms inspired by the cognitive process in the brain of animals are used to control the navigation and decision making of mobile robots [164]. Two examples of such neuro-inspired algorithms include RatSLAM, which uses models of mapping by place cells [51], and EM-SOL, which uses models of episodic memory-based self-organizing learning [165]. Bioinspired algorithms get updated by getting more insight from animal studies. For instance, NeuroSLAM is the modified version of Rat-

SLAM for 3D environments [166] and was inspired by the models for 3D place cells and grid cells.

This dissertation provides new insight by demonstrating different hippocampal encodings during distinct behavioral choices of the animal. For example, a bioinspired SLAM algorithm can create multiple maps of the same environment based on the behavior of the robot, the state of the environment, or the task at hand and search for the optimal path within the state-based maps.

The results illuminate how spatial and event-related information is encoded in the brain. This expands our current understanding and opens up new possibilities for exploring cognitive processes in animals and, potentially, understanding the building blocks of cognition, such as memory and decision making in humans.

7.3 Potential Future Research Directions

Although many animals use their high-level cognition for navigation, most mobile robots do not have high-level cognitive control. By probing and modeling the biological algorithms, we can find new strategies for the control of robots, especially during navigational tasks. Based on retrospective or prospective information, there is an opportunity to develop the techniques that animals use, such as history-dependency and differential spatiotemporal encoding, for future robots.

One potential avenue for future research is investigating the biomechanical aspects of jumping and ditching. For example, the study of takeoff kinematics (e.g., angle, velocity, acceleration) and kinetics (ground reaction forces, energy) of takeoff and landing during long-

distance jumps[1] or the force analysis when animals pulling up from the bottom of deep gaps. Additionally, researchers can inspect the role of tails in stabilizing animal motion. Ongoing research studies the effect of tail usage in successful maneuvers, especially jumping out of the ditch [167]. Finally, energy calculations can help estimate the energetic costs associated with jumping and ditching at different lengths and depths. Energy can be used to find a mathematical model for decision making based on the cost function.

Exploring the neural dynamics underlying complex locomotor tasks would benefit from simultaneous recordings across multiple brain regions. For instance, understanding the relationship between the motor cortex and the hippocampus necessitates simultaneous recording of these areas. This is crucial as the communication and coordination of these regions are essential for both the planning and execution of these complex locomotor tasks. Furthermore, collecting data from other important regions, like the prefrontal cortex—responsible for decision-making and reward evaluation—and the posterior parietal cortex, integral to regulating head and body posture, demonstrates a comprehensive picture. It is worth mentioning that preliminary data has been collected during this research for the posterior parietal cortex.

As revealed by this research, the predictive capacity of place cell activity opens up exciting possibilities for future investigations. Future studies could probe deeper into how this predictive encoding interacts with other cognitive processes, such as decision making and memory, or how these predictive properties could vary under different behavioral tasks or trajectories. One example of a potential study could be investigating whether the predictive encoding remains consistent by introducing a middle platform as a third option for the ani-

[1] Jumps more than 60 cm.

mal. Another example is a sudden increase in the gap length when the animal has initiated a jump to see how the hippocampal firings respond when the animal forcibly changes its mind on the fly to land at the bottom of the ditch instead of the landing pad at the other side of the gap.

Another fascinating aspect is looking at the problem from the perspective of neuroeconomics. The multidisciplinary field of neuroeconomics studies the intersection of neuroscience, economics, and psychology to explore the neural mechanisms underlying decision-making processes [168]. It explores the neurobiological basis of value-based decision making in Pavlovian, habitual, and goal-directed categories [169]. By providing external cues before the decision point or by changing reward contingencies, one can study the behavior of the animal or the hippocampal activity during decision making or reward consumption.

As suggested in the previous section, a neuro-inspired algorithm for mobile robots can be developed to use multiple maps for an environment based on the state of the robot or the task at hand. During challenging times, the flexibility to switch between these maps could spark innovation. It can be seen as a bifurcation in the topological maps that happens at times of necessity at some cost. This is particularly evident when the regular strategy is ineffective, especially in situations where failure carries significant consequences.

Finally, the experiment paradigm in this dissertation demonstrated a correlation between trajectories and behavioral choices within the complex navigational tasks. As illustrated in Figure 1.1, when subjects opt to jump from point A to B or ditch via intermediary point C, they choose both the action and the trajectory. In other words, the action of jumping happens at trajectory A-B, and the action of ditching happens at trajectory A-C-B. Consequently, it remains ambiguous whether the splitter-like phenomena happen because

animals navigate between points (A) and (B) by different actions or 3D trajectories. Devising experimental paradigms that evaluate each factor independently could further illuminate the encoding capacities of place cells.

7.4 Final Remarks

This dissertation presents an exploration of the intricate dynamics of rat behavior during complex locomotor tasks alongside a deep analysis of the underlying neurophysiological mechanisms. The findings illustrate how prior experiences shape the decision-making processes in rats and how seemingly minor behaviors, such as head-bobbing or postural adjustments, carry significant predictive value for their impending actions.

The multifaceted relationship between hippocampal theta rhythm and kinematic aspects of movement, especially during aerial phases of jumping, adds depth to the existing knowledge on the interplay between hippocampal theta rhythm and behavior. Through this research, it becomes evident that the brain does not merely operate as a passive decoder of sensory experiences. Instead, it acts as an anticipatory, predictive entity that fine-tunes its theta rhythm in preparation for dynamic challenges.

One of the important takeaways from this study is the splitter-like encoding of place cells. The adaptability with which these cells adjust their firing rates, encoding distinct trajectories for different actions, demonstrates the flexibility of the neural systems guiding spatial navigation. Moreover, the predictive encoding of these cells at decision points further highlights the diverse functionalities of the hippocampus.

While this dissertation has shed light on numerous facets of rat behavior and its neu-

rophysiological mechanisms, many questions remain unanswered. For instance, how can robots, inspired by these cognitive strategies, better navigate challenging terrains? What biomechanical intricacies influence the rats' impressive jumps? How does predictive encoding integrate with other cognitive processes? These avenues, among others, present exciting opportunities for further exploration and research.

In conclusion, this dissertation emphasizes the significance of studying animal behavior in novel environments and the neurophysiological processes during complex but natural locomotor behaviors. Much like the rats' jumps, every leap in knowledge is built on preparation, anticipation, and the pursuit of the unknown. The insights obtained from this research not only contribute to the field of neuroscience but also open doors to new possibilities for bioinspired strategies in robotics.

Appendix A

Data Acquisition and Analysis

A.1 Comparison of Data Acquisition Devices

For an objective assessment of neural data acquisition devices, it is essential to evaluate specific attributes, performance metrics, and design elements. Table A.1 provides a specification comparison of several neurophysiological devices. It was utilized for the selection of an appropriate data acquisition device for this research.

Neuropixels 2.0 was characterized by its lightweight architecture. This was especially significant as it reduced the potential physical limitation for the subjects, thereby preserving the integrity of natural behaviors like head-bobbing for this study. Moreover, the real-time monitoring capability of the probe enhanced the ability to observe and listen to neural activity during the experiment, ensuring instantaneous data validation and adjustments where necessary. Its low-profile design minimized unintended head bumps during complex locomotor tasks in this study.

Table A.1: Device Specifications: Comparison of Data Acquisition Devices

Device	FreeLynx	RatLog-64	SpikeLog-64C	HH128	Neurologger 3	Neuropixels 2.0
Company	Neuralynx	Deuteron Technologies	Deuteron Technologies	SpikeGadgets	Evolocus	IMEC
Channels	256	64	64	128	64	384
Sample Rate (per channel)	30 kHz	32 kHz	32 kHz	30 kHz	10 kHz	30 kHz
Input Range	+/- 5mV	+/- 5 mV	+/- 5 mV	+/- 5 mV	+/- 5 mV	+/- 12.5 mV
Resolution	16 bits	16 bits	16 bits	16 bits	16 bits	14 bits
Noise RMS	$< 2.5\mu V$	$2.4\mu V$	$2.4\mu V$	$2.6\mu V$	$\sim 2\mu V$	$7.2\mu V$
Reference Channel Control	No	Yes	Yes	No	No	Yes
Height	35 mm	26 mm	20 mm	16.5 mm		14.3 mm
Battery	240 mAh	160 mAh	160 mAh	400 mAh	50 mAh	N/A
Recording Time with Battery	30 min	2 hours	2 hours	2 hours	2 hours	N/A
Battery Weight	6.8 g	3.2 g	3.3 g	8.4 g	1.58 g	N/A
Motion Sensor	9-axis	9-axis	9-axis	6-axis		N/A
Real-time Monitoring	Yes	Yes (preview)	Yes (preview)	No	No	Yes
Wireless Transmission	TCP/IP	Radio Link	Radio Link	N/A	N/A	Wired
Connector	QC	Omnetics	Omnetics	Hirose	Omnetics	
Linux Compatible	No	No	No	Yes	No	No
Total Weight (with Battery)	21.3 g	8 g	6.3 g	19 g	$\sim$ 5 g	$\sim$ 5 g
Price	$17.4k	$17.1k	N/A	$18.6k	$18.2k	$12k

A.2 Extracting Phase and Amplitude of a signal using Hilbert Transform

The Hilbert transform, denoted $H[x(t)]$ for a real-valued function $x(t)$, is defined as

$$H[x(t)] = \frac{1}{\pi} P.V. \int_{-\infty}^{\infty} \frac{x(u)}{t-u} du \tag{A.1}$$

where $P.V.$ is the Cauchy principal value. The analytic signal $x_a(t)$ is then given by

$$x_a(t) = x(t) + iH[x(t)] \tag{A.2}$$

where i is the imaginary number. After filtering raw signals, the Hilbert transform was applied to the theta signal to create the analytic signal using the following MATLAB code.

```
% Butterworth Filter
d = designfilt(‘bandpassiir’,‘FilterOrder’,2, ...
               ‘HalfPowerFrequency1’,6,‘HalfPowerFrequency2’,12, ...
               ‘SampleRate’,Fs);
filtered_signal = filtfilt(d, raw_signal);

% Hilbert Transform
analytic_signal = hilbert(filtered_signal);

% Compute the amplitude and phase
amplitude = abs(analytic_signal);
phase = angle(analytic_signal);
```

By applying the Hilbert transform to the theta signal and forming the analytic signal, it became possible to extract the instantaneous phase and amplitude of the theta rhythm.

Appendix B

Bayesian Decoder

B.1 Performance Metrics

This section explains 'accuracy' and 'precision' as statistical measures used to evaluate the performance of the Bayesian decoder. Accuracy shows the overall correctness of all predictions, while precision evaluates the quality of the most confident predictions. A balance between the two is crucial to ensure both a high rate of correct predictions and the reliability of confident predictions, leading to a more efficient and reliable Bayesian decoding process. In this dissertation, the primary objective is to demonstrate the presence of predictive information within hippocampal place cells. Therefore, the emphasis is on measuring accuracy, as it provides a sufficient assessment of the performance of the decoder for the specific research goal.

B.1.1 Accuracy

Accuracy is a general measure of the correctness of the decoder and can be expressed with the following equation:

$$\text{Accuracy} = \frac{TP + TN}{P + N} \tag{B.1}$$

where TP (true positives) is the number of correct predictions that are positive, TN (true negatives) is the number of correct predictions that are negative, P is the total number of actual positives, N is the total number of actual negatives. Accuracy, therefore, measures the proportion of total true predictions (both positive and negative) among all cases.

B.1.2 Precision

Precision is a measure of the exactness or quality of the decoder and can be expressed with the following equation:

$$\text{Precision} = \frac{TP}{TP + FP} \tag{B.2}$$

where TP (true positives) and FP (false positives) are defined as before. Precision, therefore, measures the proportion of true positive predictions among all positive predictions.

B.2 Pseudocode for the Bayesian Decoder

The Algorithm 1, Bayesian Decoder for Neural Analysis, is designed to process and analyze data from animal behavioral experiments. The decoder loads processed data, sets various parameters, and calculates the ratio of spike count to time count for each cluster and

lap. Subsequently, it performs multiple iterations where it splits the data into training and validation sets and calculates prior probabilities, mean, and covariance for each 'jump' and 'ditch' category. It further computes likelihood and posterior probabilities, makes predictions for the validation set, and calculates and plots accuracy and precision metrics. The process concludes with the performance of z-tests and the calculation of p-values and other metrics, providing a thorough statistical analysis of the animal behavioral responses.

Algorithm 1 Bayesian Decoder for Neural Analysis

```
Load processed data from processed_data.mat
Specify direction (left or right)
Assign field numbers for each case based on rat number and direction
Assign cluster numbers for each field
Set time range
Initialize empty labels array and lap numbers array
for each cluster do
    for each lap do
        Calculate index based on time, position, and direction of the cluster
        Count spikes
        Calculate index based on time, position, and direction of the lap
        Count time
    end for
    Store ratio of spike count to time count in data
end for
Initialize accuracy and precision arrays for both null and alternative hypothesis
for each iteration in num_iter do
    Split data into training and validation sets
    Calculate prior probabilities for 'jump' and 'ditch' categories
    Calculate mean and covariance of data for each category
    Define functions for calculating likelihood and posterior probability
    Make predictions for the validation set based on the highest posterior probability
    Calculate accuracy and precision metrics
end for
Plot and save histograms of accuracy and precision for both 'jump' and 'ditch' categories
Perform z-tests and calculate p-values and other metrics
```

Appendix C

Statistical Concepts

C.1 P-value

The p-value is a critical statistical measure used to determine the significance of outcomes in experimental studies. Essentially, the p-value quantifies the likelihood of obtaining the observed data in a study under the assumption that the null hypothesis is true [170]. It serves as a tool in hypothesis testing, involving two fundamental hypotheses: the null hypothesis (H_0) and the alternative hypothesis (H_1). The computation of the p-value is based on the test statistic and the statistical model that represents the data's likelihood.

The test statistic is derived from the sample data and forms the basis for deciding whether to reject or uphold the null hypothesis. Examples of test statistics include the z-score, the t-score, and the Rayleigh Z statistic. A statistical model, like the normal distribution or uniform distribution, is a mathematical representation used to describe the likelihood of different outcomes in a dataset based on the assumed underlying structure and relationships

among the variables. In hypothesis testing, a small p-value (typically ≤ 0.05) provides strong evidence against the null hypothesis, leading to its rejection. Conversely, a large p-value (> 0.05) provides weak evidence against the null hypothesis, and it suggests that the null hypothesis should not be rejected.

C.2 Z-test

The z-test is a statistical method for hypothesis testing that employs the standard normal distribution to assess whether the difference between the sample mean and the population mean is significant [171]. When we have a sample and know the population standard deviation (σ), a z-test is applicable.

Given a sample size of n, sample mean $\bar{x}$, population mean μ, and population standard deviation σ, the z-score is calculated using the formula:

$$z = \frac{\bar{x} - \mu}{\sigma/\sqrt{n}}. \tag{C.1}$$

Once we have the z-score, we can use the standard normal distribution to find the corresponding p-value. A smaller p-value indicates stronger evidence against the null hypothesis.

The z-test is suitable when data is approximately normally distributed, and the population standard deviation is known. For instance, it can be used to determine whether a given sample could plausibly come from a population with a specific mean.

The formula to calculate the p-value in a one-tailed z-test is:

$$P(Z \geq z) = 1 - \Phi(z), \tag{C.2}$$

where Z is a standard normal random variable, z is the observed test statistic, and Φ represents the cumulative distribution function of Z.

C.3 T-test

The t-test is used to ascertain whether there is a significant difference between the means of two groups [172]. Unlike the z-test, the t-test is applicable when the population standard deviation is unknown, and it estimates the standard deviation from the sample itself.

C.3.1 One-Sample T-test

A one-sample t-test is employed to compare a sample mean with a known population mean. Given a sample size of n, sample mean $\bar{x}$, population mean μ, and sample standard deviation s, the t-score is calculated using the formula:

$$t = \frac{\bar{x} - \mu}{s/\sqrt{n}}. \tag{C.3}$$

The degrees of freedom, in this case, are $n - 1$. After calculating the t-score, we refer to the t-distribution table to find the corresponding p-value.

C.3.2 Two-Sample T-test

Two-sample t-tests are employed when comparing the means of two independent groups to determine whether they are significantly different [173]. There are two types of two-sample t-tests: Student's t-test and Welch's t-test.

C.3.2.1 Student's T-test

Student's t-test assumes that the two groups have equal variances. Given two groups with sample sizes n_1 and n_2, sample means $\bar{x}_1$ and $\bar{x}_2$, and pooled sample standard deviation s_p, the t-score is computed as:

$$t = \frac{\bar{x}_1 - \bar{x}_2}{s_p \cdot \sqrt{1/n_1 + 1/n_2}}. \tag{C.4}$$

where s_p is the pooled standard deviation, calculated as:

$$s_p = \sqrt{\frac{(n_1 - 1)s_1^2 + (n_2 - 1)s_2^2}{n_1 + n_2 - 2}}. \tag{C.5}$$

C.3.2.2 Welch's T-test

Unlike Student's t-test, Welch's t-test doesn't assume equal variances, making it more reliable when this assumption is not met. Given two groups with sample sizes n_1 and n_2, sample means $\bar{x}_1$ and $\bar{x}_2$, and sample standard deviations s_1 and s_2, the t-score is computed as:

$$t = \frac{\bar{x}_1 - \bar{x}_2}{\sqrt{s_1^2/n_1 + s_2^2/n_2}}. \tag{C.6}$$

C.4 F-test for Equality of Variances

The F-test is a statistical analysis based on the F-distribution [174]. Fisher's F-test, known as the test for equality of variances, assesses whether the variances of two groups are equal. Like previous tests, this also requires the data to be normally distributed. For two groups with sample sizes n_1 and n_2, and sample variances s_1^2 and s_2^2, the F-statistic is calculated as:

$$F = \frac{s_1^2}{s_2^2}. \tag{C.7}$$

The subsequent p-value is determined using the cumulative distribution function of the F-distribution.

C.5 The Mann-Whitney U-test

The Mann-Whitney U-test (aka the Wilcoxon rank-sum test) is a non-parametric test designed to evaluate whether two independent samples come from identical distributions. The test ranks values from both samples together, aiming to determine if one group tends to have higher ranks than the other. The test statistic, U, is derived from the rank sums of the two samples. Specifically, for samples of sizes n_1 and n_2, with rank sums R_1 and R_2 respectively, the U-values are computed as

$$U_1 = n_1 n_2 + \frac{n_1(n_1+1)}{2} - R_1 \tag{C.8}$$

and

$$U_2 = n_1 n_2 + \frac{n_2(n_2+1)}{2} - R_2, \tag{C.9}$$

with the smaller value between U_1 and U_2 being used as the test statistic. A significantly small U value indicates a difference between the distributions of the two samples. This test is advantageous when the distribution of data is not normal.

C.6 Cohen's d

Cohen's d is an effect size measure that indicates the standardized difference between two means [175]. It's often used alongside a t-test to provide a comprehensive understanding of results.

Cohen's d is calculated as:

$$d = \frac{\bar{x}_1 - \bar{x}_2}{s_p}, \tag{C.10}$$

where $\bar{x}_1$ and $\bar{x}_2$ are the means of the two groups, and s_p is the pooled standard deviation (calculated as in Student's t-test).

A larger absolute value of Cohen's d indicates a greater difference between the two groups. Generally, a Cohen's d of 0.8 is considered a 'large' effect size. However, interpretations vary depending on context [176].

C.7 The Rayleigh Test

The Rayleigh test assesses circular data's uniformity, making it effective for identifying unimodal distributions around a specific angle [177]. Given a sample of n data points on a circle, with the jth data point represented as a complex number $z_j = e^{i\theta_j}$ (where θ_j is the angle of the point), the mean resultant length ($\bar{R}$) is calculated as:

$$\bar{R} = \left| \frac{1}{n} \sum_{j=1}^{n} e^{i\theta_j} \right|. \tag{C.11}$$

The Rayleigh statistic (Z) is then computed as:

$$Z = n\bar{R}^2. \tag{C.12}$$

Using the Rayleigh statistic, a p-value can be derived to test the null hypothesis of uniformity (data evenly distributed around the circle). The p-value can be found using the formula:

$$p = e^{-Z} \left(1 + \frac{2Z - Z^2}{4n} - \frac{24Z - 132Z^2 + 76Z^3 - 9Z^4}{288n^2} \right). \tag{C.13}$$

If the p-value is below a significance level (0.05), the null hypothesis is rejected, indicating that the data isn't uniformly distributed around the circle.

Bibliography

[1] S. G. Lashkari, B. M. Woronowicz, P. Ozel, B. Krishnan, J. J. Knierim, and N. J. Cowan, "Hippocampal place cell encoding during gap-crossing behaviors," in *The Society for Neuroscience Annual Meeting*, Nov. 2022.

[2] S. G. Lashkari, B. M. Woronowicz, P. Ozel, M. Hathiyari, V. Puliyadi, J. J. Knierim, and N. J. Cowan, "Predictive firing of place cells before gap-crossing behaviors," in *The Society for Neuroscience Annual Meeting*, To be presented at the Society for Neuroscience Annual Meeting, 2023, Nov. 2023.

[3] J. Lisman, G. Buzsáki, H. Eichenbaum, L. Nadel, C. Ranganath, and A. D. Redish, "Viewpoints: How the hippocampus contributes to memory, navigation and cognition," *Nature Neuroscience*, vol. 20, no. 11, pp. 1434–1447, 2017. DOI: 10.1038/nn.4661.

[4] A. Prochazka, F. Clarac, G. E. Loeb, J. C. Rothwell, and J. R. Wolpaw, "What do reflex and voluntary mean? modern views on an ancient debate," *Experimental Brain Research*, vol. 130, pp. 417–432, 2000. DOI: 10.1007/s002219900250.

[5] B. Brembs, "The brain as a dynamically active organ," *Biochemical and Biophysical Research Communications*, vol. 564, pp. 55–69, 2021. DOI: 10.1016/j.bbrc.2020.12.011.

[6] P. Holmes, R. J. Full, D. Koditschek, and J. Guckenheimer, "The dynamics of legged locomotion: Models, analyses, and challenges," *SIAM Review*, vol. 48, no. 2, pp. 207–304, 2006. DOI: 10.1137/S0036144504445133.

[7] W. Heiligenberg, "The neural basis of behavior: A neuroethological view," *Annual Review of Neuroscience*, vol. 14, no. 1, pp. 247–267, 1991. DOI: 10.1146/annurev.ne.14.030191.001335.

[8] C. J. Shatz, "The developing brain," *Scientific American*, vol. 267, no. 3, pp. 60–67, 1992.

[9] D. O. Hebb, *The organization of behavior; a neuropsychological theory.* Oxford, England: Wiley, 1949, vol. xix, 335.

[10] W. Schultz, P. Dayan, and P. R. Montague, "A neural substrate of prediction and reward," *Science*, vol. 275, no. 5306, pp. 1593–1599, 1997. DOI: 10.1126/science.275.5306.1593.

[11] G. Boulinguez-Ambroise, N. Dunham, T. Phelps, T. Mazonas, P. Nguyen, M. Bradley-Cronkwright, D. M. Boyer, G. S. Yapuncich, A. Zeininger, D. Schmitt, *et al.*, "Jumping performance in tree squirrels: Insights into primate evolution," *Journal of Human Evolution*, vol. 180, p. 103 386, 2023. DOI: 10.1016/j.jhevol.2023.103386.

[12] N. H. Hunt, J. Jinn, L. F. Jacobs, and R. J. Full, "Acrobatic squirrels learn to leap and land on tree branches without falling," *Science*, vol. 373, no. 6555, pp. 697–700, 2021. DOI: 10.1126/science.abe5753.

[13] E. H. Kay and H. E. Hoekstra, "Rodents," *Current Biology*, vol. 18, no. 10, R406–R410, 2008. DOI: 10.1016/j.cub.2008.03.019.

[14] C. D. Harvey, F. Collman, D. A. Dombeck, and D. W. Tank, "Intracellular dynamics of hippocampal place cells during virtual navigation," *Nature*, vol. 461, no. 7266, pp. 941–946, 2009. DOI: 10.1038/nature08499.

[15] M. S. Madhav, R. P. Jayakumar, S. G. Lashkari, F. Savelli, H. T. Blair, J. J. Knierim, and N. J. Cowan, "The dome: A virtual reality apparatus for freely locomoting rodents," *Journal of Neuroscience Methods*, vol. 368, p. 109 336, 2022. DOI: 10.1016/j.jneumeth.2021.109336.

[16] R. A. Wood, M. Bauza, J. Krupic, S. Burton, A. Delekate, D. Chan, and J. O'Keefe, "The honeycomb maze provides a novel test to study hippocampal-dependent spatial navigation," *Nature*, vol. 554, no. 7690, pp. 102–105, 2018. DOI: 10.1038/nature25433.

[17] J. J. Knierim, "From the gps to hm: Place cells, grid cells, and memory," *Hippocampus*, vol. 25, no. 6, pp. 719–725, 2015. DOI: https://doi.org/10.1002/hipo.22453.

[18] D. Schiller, H. Eichenbaum, E. A. Buffalo, L. Davachi, D. J. Foster, S. Leutgeb, and C. Ranganath, "Memory and space: Towards an understanding of the cognitive map," *Journal of Neuroscience*, vol. 35, no. 41, pp. 13 904–13 911, 2015, ISSN: 0270-6474. DOI: 10.1523/JNEUROSCI.2618-15.2015.

[19] K. M. Turner and T. H. Burne, "Comprehensive behavioural analysis of long evans and sprague-dawley rats reveals differential effects of housing conditions on tests relevant to neuropsychiatric disorders," *PLOS ONE*, vol. 9, no. 3, e93411, 2014. DOI: 10.1371/journal.pone.0093411.

[20] H. Mouritsen, D. Heyers, and O. Güntürkün, "The neural basis of long-distance navigation in birds," *Annual Review of Physiology*, vol. 78, pp. 133–154, 2016. DOI: 10.1146/annurev-physiol-021115-105054.

[21] T. Labhart and E. P. Meyer, "Neural mechanisms in insect navigation: Polarization compass and odometer," *Current Opinion in Neurobiology*, vol. 12, no. 6, pp. 707–714, 2002. DOI: 10.1016/s0959-4388(02)00384-7.

[22] B. Mimica, B. A. Dunn, T. Tombaz, V. P. T. N. C. S. Bojja, and J. R. Whitlock, "Efficient cortical coding of 3D posture in freely behaving rats," *Science*, vol. 362, no. 6414, pp. 584–589, 2018. DOI: 10.1126/science.aau2013.

[23] P. A. Dudchenko and E. R. Wood, "Splitter cells: Hippocampal place cells whose firing is modulated by where the animal is going or where it has been," in *Space, Time and Memory in the Hippocampal Formation*, D. Derdikman and J. J. Knierim, Eds. Springer Vienna, 2014, pp. 253–272, ISBN: 978-3-7091-1292-2. DOI: 10.1007/978-3-7091-1292-2_10.

[24] N. R. Kinsky, D. W. Mau Williamand Sullivan, S. J. Levy, E. A. Ruesch, and M. E. Hasselmo, "Trajectory-modulated hippocampal neurons persist throughout memory-guided navigation," *Nature Communications*, vol. 11, no. 1, p. 2443, 2020. DOI: 10.1038/s41467-020-16226-4.

[25] S. G. Lashkari, M. G. Wilkinson, B. Krishnan, J. J. Knierim, and N. J. Cowan, "Decision-making and path planning for jumping rats," in *Dynamic Walking*, Poconos, PA, USA, May 2020.

[26] R. Pfeifer, M. Lungarella, and F. Iida, "Self-organization, embodiment, and biologically inspired robotics," *Science*, vol. 318, no. 5853, pp. 1088–1093, 2007. DOI: 10.1126/science.1145803.

[27] R. Full, "Biological inspiration: Lessons from many-legged locomotors," in *Robotics Research: The Ninth International Symposium*, Springer, 2000, pp. 337–341. DOI: 10.1007/978-1-4471-0765-1_41.

[28] A. J. Ijspeert, "Biorobotics: Using robots to emulate and investigate agile locomotion," *Science*, vol. 346, no. 6206, pp. 196–203, 2014. DOI: 10.1126/science.1254486.

[29] D. E. Koditschek, "What is robotics? why do we need it and how can we get it?" *Annual Review of Control, Robotics, and Autonomous Systems*, vol. 4, pp. 1–33, 2021. DOI: 10.1146/annurev-control-080320-011601.

[30] B. Chang, J. Myeong, E. Virot, C. Clanet, H.-Y. Kim, and S. Jung, "Jumping dynamics of aquatic animals," *Journal of the Royal Society Interface*, vol. 16, no. 152, p. 20 190 014, 2019. DOI: 10.1098/rsif.2019.0014.

[31] X. Mo, W. Ge, M. Miraglia, F. Inglese, D. Zhao, C. Stefanini, and D. Romano, "Jumping locomotion strategies: From animals to bioinspired robots," *Applied Sciences*, vol. 10, no. 23, p. 8607, 2020. DOI: 10.3390/app10238607.

[32] R. Armour, K. Paskins, A. Bowyer, J. Vincent, and W. Megill, "Jumping robots: A biomimetic solution to locomotion across rough terrain," *Bioinspiration & Biomimetics*, vol. 2, no. 3, S65, 2007. DOI: 10.1109/ROBIO.2009.4913124.

[33] R. Siddall, G. Byrnes, R. J. Full, and A. Jusufi, "Tails stabilize landing of gliding geckos crashing head-first into tree trunks," *Communications Biology*, vol. 4, no. 1, p. 1020, 2021. DOI: 10.1038/s42003-021-02378-6.

[34] P. Manoonpong, L. Patanè, X. Xiong, I. Brodoline, J. Dupeyroux, S. Viollet, P. Arena, and J. R. Serres, "Insect-inspired robots: Bridging biological and artificial systems," *Sensors*, vol. 21, no. 22, p. 7609, 2021. DOI: 10.3390/s21227609.

[35] U. Saranli, M. Buehler, and D. E. Koditschek, "RHex: A simple and highly mobile hexapod robot," *The International Journal of Robotics Research*, vol. 20, no. 7, pp. 616–631, 2001. DOI: 10.1177/02783640122067570.

[36] M. J. Spenko, G. C. Haynes, J. Saunders, M. R. Cutkosky, A. A. Rizzi, R. J. Full, and D. E. Koditschek, "Biologically inspired climbing with a hexapedal robot," *Journal of Field Robotics*, vol. 25, no. 4-5, pp. 223–242, 2008. DOI: 10.1002/rob.20238.

[37] S. Kim, C. Laschi, and B. Trimmer, "Soft robotics: A bioinspired evolution in robotics," *Trends in Biotechnology*, vol. 31, no. 5, pp. 287–294, 2013. DOI: 10.1016/j.tibtech.2013.03.002.

[38] C. Menon, M. Murphy, and M. Sitti, "Gecko inspired surface climbing robots," in *2004 IEEE International Conference on Robotics and Biomimetics*, IEEE, 2004, pp. 431–436. DOI: 10.1109/ROBIO.2004.1521817.

[39] M. R. Cutkosky, "Climbing with adhesion: From bioinspiration to biounderstanding," *Interface Focus*, vol. 5, no. 4, p. 20 150 015, 2015. DOI: 10.1098/rsfs.2015.0015.

[40] A. J. Ijspeert, "Central pattern generators for locomotion control in animals and robots: A review," *Neural Networks*, vol. 21, no. 4, pp. 642–653, 2008. DOI: 10.1016/j.neunet.2008.03.014.

[41] P. Ramdya and A. J. Ijspeert, "The neuromechanics of animal locomotion: From biology to robotics and back," *Science Robotics*, vol. 8, no. 78, eadg0279, 2023. DOI: 10.1126/scirobotics.adg0279.

[42] R. S. Sutton and A. G. Barto, *Reinforcement learning: An introduction*. MIT Press, 2018.

[43] A. Darwish, "Bio-inspired computing: Algorithms review, deep analysis, and the scope of applications," *Future Computing and Informatics Journal*, vol. 3, no. 2, pp. 231–246, 2018. DOI: 10.1016/j.fcij.2018.06.001.

[44] X.-S. Yang, *Nature-inspired optimization algorithms*. Academic Press, 2020, ISBN: 9780128219867.

[45] W. S. McCulloch and W. Pitts, "A logical calculus of the ideas immanent in nervous activity," *The Bulletin of Mathematical Biophysics*, vol. 5, pp. 115–133, 1943. DOI: 10.1007/BF02478259.

[46] J. H. Holland, *Adaptation in natural and artificial systems: an introductory analysis with applications to biology, control, and artificial intelligence*. MIT press, 1992.

[47] J. Kennedy and R. Eberhart, "Particle swarm optimization," in *Proceedings of ICNN'95-International Conference on Neural Networks*, IEEE, vol. 4, 1995, pp. 1942–1948. DOI: 10.1109/ICNN.1995.488968.

[48] X.-S. Yang and S. Deb, "Cuckoo search via lévy flights," in *2009 World Congress on Nature & Biologically Inspired Computing (NaBIC)*, IEEE, 2009, pp. 210–214. DOI: 10.1109/NABIC.2009.5393690.

[49] M. J. Matarić, "Navigating with a rat brain: A neurobiologically-inspired model for robot spatial representation," in *From Animals to Animats: Proceedings of the First International Conference on Simulation of Adaptive Behavior*, J.-A. Meyer and S. W. Wilson, Eds., The MIT Press, 1991, pp. 169–175, ISBN: 9780262256674. DOI: 10.7551/mitpress/3115.003.0023.

[50] D. Sheynikhovich, R. Chavarriaga, T. Strösslin, and W. Gerstner, "Spatial representation and navigation in a bio-inspired robot," in *Biomimetic Neural Learning for Intelligent Robots: Intelligent Systems, Cognitive Robotics, and Neuroscience*, Berlin, Heidelberg: Springer, 2005, pp. 245–264. DOI: 10.1007/11521082_15.

[51] M. J. Milford, G. F. Wyeth, and D. Prasser, "RatSLAM: A hippocampal model for simultaneous localization and mapping," in *IEEE International Conference on Robotics and Automation, 2004. Proceedings. ICRA'04. 2004*, IEEE, vol. 1, 2004, pp. 403–408. DOI: 10.1109/ROBOT.2004.1307183.

[52] E. C. Tolman, "Cognitive maps in rats and men.," *Psychological Review*, vol. 55, no. 4, p. 189, 1948. DOI: 10.1037/h0061626.

[53] J. O'Keefe and J. Dostrovsky, "The hippocampus as a spatial map: Preliminary evidence from unit activity in the freely-moving rat.," *Brain Research*, 1971. DOI: 10.1016/0006-8993(71)90358-1.

[54] J. O'Keefe, "Place units in the hippocampus of the freely moving rat," *Experimental Neurology*, vol. 51, no. 1, pp. 78–109, 1976. DOI: 10.1016/0014-4886(76)90055-8.

[55] J. O'Keefe and L. Nadel, *The Hippocampus as a Cognitive Map*. Clarendon Press, 1978, ISBN: 9780198572060. [Online]. Available: https://discovery.ucl.ac.uk/id/eprint/10103569/1/HCMComplete.pdf.

[56] R. G. Morris, "Spatial localization does not require the presence of local cues," *Learning and Motivation*, vol. 12, no. 2, pp. 239–260, 1981. DOI: 10.1016/0023-9690(81)90020-5.

[57] B. L. McNaughton, C. A. Barnes, and J. O'Keefe, "The contributions of position, direction, and velocity to single unit activity in the hippocampus of freely-moving rats," *Experimental Brain Research*, vol. 52, pp. 41–49, 1983. DOI: 10.1007/BF00237147.

[58] J. O'Keefe and N. Burgess, "Geometric determinants of the place fields of hippocampal neurons," *Nature*, vol. 381, no. 6581, pp. 425–428, 1996. DOI: 10.1038/381425a0.

[59] R. P. Jayakumar, M. S. Madhav, F. Savelli, H. T. Blair, N. J. Cowan, and J. J. Knierim, "Recalibration of path integration in hippocampal place cells," *Nature*, vol. 566, no. 45, pp. 533–537, 2019. DOI: 10.1038/s41586-019-0939-3.

[60] F. Savelli and J. J. Knierim, "Coming up: In search of the vertical dimension in the brain," *Nature Neuroscience*, vol. 14, no. 9, pp. 1102–1103, 2011. DOI: 10.1038/nn.2913.

[61] B. S. Porter, R. Schmidt, and D. K. Bilkey, "Hippocampal place cell encoding of sloping terrain," *Hippocampus*, vol. 28, no. 11, pp. 767–782, 2018. DOI: 10.1002/hipo.22966.

[62] R. Hayman, M. A. Verriotis, A. Jovalekic, A. A. Fenton, and K. J. Jeffery, "Anisotropic encoding of three-dimensional space by place cells and grid cells," *Nature Neuroscience*, vol. 14, no. 9, pp. 1182–1188, 2011. DOI: 10.1038/nn.2892.

[63] M. M. Yartsev and N. Ulanovsky, "Representation of three-dimensional space in the hippocampus of flying bats," *Science*, vol. 340, no. 6130, pp. 367–372, 2013. DOI: 10.1126/science.1235338.

[64] R. M. Grieves, S. Jedidi-Ayoub, K. Mishchanchuk, A. Liu, S. Renaudineau, and K. J. Jeffery, "The place-cell representation of volumetric space in rats," *Nature Communications*, vol. 11, no. 1, p. 789, 2020. DOI: 10.1038/s41467-020-14611-7.

[65] D. Aronov, R. Nevers, and D. W. Tank, "Mapping of a non-spatial dimension by the hippocampal–entorhinal circuit," *Nature*, vol. 543, no. 7647, pp. 719–722, 2017. DOI: 10.1038/nature21692.

[66] H. Eichenbaum, "Time cells in the hippocampus: A new dimension for mapping memories," *Nature Reviews Neuroscience*, vol. 15, no. 11, pp. 732–744, 2014. DOI: 10.1038/nrn3827.

[67] Y. Sakurai, "Coding of auditory temporal and pitch information by hippocampal individual cells and cell assemblies in the rat," *Neuroscience*, vol. 115, no. 4, pp. 1153–1163, 2002. DOI: 10.1016/S0306-4522(02)00509-2.

[68] H. Eichenbaum, M. Kuperstein, A. Fagan, and J. Nagode, "Cue-sampling and goal-approach correlates of hippocampal unit activity in rats performing an odor-discrimination task," *Journal of Neuroscience*, vol. 7, no. 3, pp. 716–732, 1987. DOI: 10.1523/JNEUROSCI.07-03-00716.1987.

[69] J. Ferbinteanu and M. L. Shapiro, "Prospective and retrospective memory coding in the hippocampus," *Neuron*, vol. 40, no. 6, pp. 1227–1239, 2003. DOI: 10.1016/S0896-6273(03)00752-9.

[70] W. B. Scoville and B. Milner, "Loss of recent memory after bilateral hippocampal lesions," *Journal of Neurology, Neurosurgery, and Psychiatry*, vol. 20, no. 1, p. 11, 1957. DOI: 10.1136/jnnp.20.1.11.

[71] B. Kaada, E. W. Rasmussen, and O. Kveim, "Effects of hippocampal lesions on maze learning and retention in rats," *Experimental Neurology*, vol. 3, no. 4, pp. 333–355, 1961. DOI: 10.1016/0014-4886(61)90009-7.

[72] C. Pavlides and J. Winson, "Influences of hippocampal place cell firing in the awake state on the activity of these cells during subsequent sleep episodes," *Journal of Neuroscience*, vol. 9, no. 8, pp. 2907–2918, 1989. DOI: 10.1523/JNEUROSCI.09-08-02907.1989.

[73] M. A. Wilson and B. L. McNaughton, "Reactivation of hippocampal ensemble memories during sleep," *Science*, vol. 265, no. 5172, pp. 676–679, 1994. DOI: 10.1126/science.8036517.

[74] W. E. Skaggs and B. L. McNaughton, "Replay of neuronal firing sequences in rat hippocampus during sleep following spatial experience," *Science*, vol. 271, no. 5257, pp. 1870–1873, 1996. DOI: 10.1126/science.271.5257.1870.

[75] D. J. Foster and M. A. Wilson, "Reverse replay of behavioural sequences in hippocampal place cells during the awake state," *Nature*, vol. 440, no. 7084, pp. 680–683, 2006. DOI: 10.1038/nature04587.

[76] S. P. Jadhav, C. Kemere, P. W. German, and L. M. Frank, "Awake hippocampal sharp-wave ripples support spatial memory," *Science*, vol. 336, no. 6087, pp. 1454–1458, 2012. DOI: 10.1126/science.121723.

[77] N. S. Clayton and A. Dickinson, "Episodic-like memory during cache recovery by scrub jays," *Nature*, vol. 395, no. 6699, pp. 272–274, 1998. DOI: 10.1038/26216.

[78] H. Eichenbaum, "Hippocampus: Cognitive processes and neural representations that underlie declarative memory," *Neuron*, vol. 44, no. 1, pp. 109–120, 2004. DOI: 10.1016/j.neuron.2004.08.028.

[79] J. D. Crystal, "Episodic-like memory in animals," *Behavioural Brain Research*, vol. 215, no. 2, pp. 235–243, 2010. DOI: 10.1016/j.bbr.2010.03.005.

[80] C. Ergorul and H. Eichenbaum, "The hippocampus and memory for "what," "where," and "when"," *Learning & Memory*, vol. 11, no. 4, pp. 397–405, 2004. DOI: 10.1101/lm.73304.

[81] K. Diba and G. Buzsáki, "Forward and reverse hippocampal place-cell sequences during ripples," *Nature Neuroscience*, vol. 10, no. 10, pp. 1241–1242, 2007. DOI: 10.1038/nn1961.

[82] K. J. Miller, M. M. Botvinick, and C. D. Brody, "Dorsal hippocampus contributes to model-based planning," *Nature Neuroscience*, vol. 20, no. 9, pp. 1269–1276, 2017. DOI: 10.1038/nn.4613.

[83] B. E. Pfeiffer and D. J. Foster, "Hippocampal place-cell sequences depict future paths to remembered goals," *Nature*, vol. 497, no. 7447, pp. 74–79, 2013. DOI: 10.1038/nature12112.

[84] R. L. Buckner, "The role of the hippocampus in prediction and imagination," *Annual Review of Psychology*, vol. 61, pp. 27–48, 2010. DOI: 10.1146/annurev.psych.60.110707.163508.

[85] A. C. Singer, M. F. Carr, M. P. Karlsson, and L. M. Frank, "Hippocampal swr activity predicts correct decisions during the initial learning of an alternation task," *Neuron*, vol. 77, no. 6, pp. 1163–1173, 2013. DOI: 10.1016/j.neuron.2013.01.027.

[86] K. Kay, J. E. Chung, M. Sosa, J. S. Schor, M. P. Karlsson, M. C. Larkin, D. F. Liu, and L. M. Frank, "Constant sub-second cycling between representations of possible futures in the hippocampus," *Cell*, vol. 180, no. 3, pp. 552–567, 2020. DOI: 10.1016/j.cell.2020.01.014.

[87] A. D. Redish, "Vicarious trial and error," *Nature Reviews Neuroscience*, vol. 17, no. 3, pp. 147–159, 2016. DOI: 10.1038/nrn.2015.30.

[88] K. L. Stachenfeld, M. M. Botvinick, and S. J. Gershman, "The hippocampus as a predictive map," *Nature Neuroscience*, vol. 20, no. 11, pp. 1643–1653, 2017. DOI: 10.1038/nn.4650.

[89] H. F. Ólafsdóttir, D. Bush, and C. Barry, "The role of hippocampal replay in memory and planning," *Current Biology*, vol. 28, no. 1, R37–R50, 2018. DOI: 10.1016/j.cub.2017.10.073.

[90] L. M. Frank, E. N. Brown, and M. Wilson, "Trajectory encoding in the hippocampus and entorhinal cortex," *Neuron*, vol. 27, no. 1, pp. 169–178, 2000. DOI: 10.1016/S0896-6273(00)00018-0.

[91] J. A. Ainge, M. Tamosiunaite, F. Wörgötter, and P. A. Dudchenko, "Hippocampal place cells encode intended destination, and not a discriminative stimulus, in a conditional t-maze task," *Hippocampus*, vol. 22, no. 3, pp. 534–543, 2012. DOI: 10.1002/hipo.20919.

[92] E. R. Wood, P. A. Dudchenko, R. J. Robitsek, and H. Eichenbaum, "Hippocampal neurons encode information about different types of memory episodes occurring in the same location," *Neuron*, vol. 27, no. 3, pp. 623–633, 2000. DOI: 10.1016/S0896-6273(00)00071-4.

[93] É. Duvelle, R. M. Grieves, and M. A. Van der Meer, "Temporal context and latent state inference in the hippocampal splitter signal," *eLife*, vol. 12, e82357, 2023. DOI: 10.7554/eLife.82357.

[94] A. E. Goss and G. J. Wischner, "Vicarious trial and error and related behavior.," *Psychological Bulletin*, vol. 53, no. 1, p. 35, 1956. DOI: 10.1037/h0045108.

[95] K. F. Muenzinger and F. M. Fletcher, "Motivation in learning. vi. escape from electric shock compared with hunger-food tension in the visual discrimination habit.," *Journal of Comparative Psychology*, vol. 22, no. 1, p. 79, 1936. DOI: 10.1037/h0057664.

[96] K. F. Muenzinger, "Vicarious trial and error at a point of choice: I. a general survey of its relation to learning efficiency," *The Pedagogical Seminary and Journal of Genetic Psychology*, vol. 53, no. 1, pp. 75–86, 1938. DOI: 10.1080/08856559.1938.10533799.

[97] K. F. Muenzinger, "On the origin and early use of the term vicarious trial and error (vte).," *Psychological Bulletin*, vol. 53, no. 6, p. 493, 1956. DOI: 10.1037/h0044135.

[98] A. Amsel, "Hippocampal function in the rat: Cognitive mapping or vicarious trial and error?" *Hippocampus*, vol. 3, no. 3, pp. 251–256, 1993. DOI: 10.1073/pnas.92.12.5506.

[99] A. Johnson and A. D. Redish, "Neural ensembles in CA3 transiently encode paths forward of the animal at a decision point," *Journal of Neuroscience*, vol. 27, no. 45, pp. 12 176–12 189, 2007. DOI: 10.1523/JNEUROSCI.3761-07.2007.

[100] J. O'Keefe, "Hippocampal neurophysiology in the behaving animal," in *The Hippocampus Book*, P. Andersen, R. Morris, D. Amaral, T. Bliss, and J. O'Keefe, Eds. Oxford University Press, Dec. 2006, pp. 475–548, ISBN: 9780195100273. DOI: 10.1093/acprof:oso/9780195100273.001.0001.

[101] J. J. Knierim, "The hippocampus," *Current Biology*, vol. 25, no. 23, R1116–R1121, 2015. DOI: 10.1016/j.cub.2015.10.049.

[102] G. Buzsáki, *Rhythms of the Brain*. Oxford University Press, Oct. 2006. DOI: 10.1093/acprof:oso/9780195301069.001.0001.

[103] I. Whishaw and C. H. Vanderwolf, "Hippocampal EEG and behavior: Change in amplitude and frequency of RSA (theta rhythm) associated with spontaneous and

learned movement patterns in rats and cats," *Behavioral Biology*, vol. 8, no. 4, pp. 461–484, 1973. DOI: 10.1016/S0091-6773(73)80041-0.

[104] T. Myhrer, "Normal jump avoidance performance in rats with the hippocampal theta rhythm selectively disrupted," *Behavioral Biology*, vol. 14, no. 4, pp. 489–498, 1975. DOI: 10.1016/S0091-6773(75)90660-4.

[105] S. Grillner and P. Wallen, "Central pattern generators for locomotion, with special reference to vertebrates," *Annual Review of Neuroscience*, vol. 8, no. 1, pp. 233–261, 1985. DOI: 10.1146/annurev.ne.08.030185.001313.

[106] K. Takakusaki, "Functional neuroanatomy for posture and gait control," *Journal of Movement Disorders*, vol. 10, no. 1, p. 1, 2017. DOI: 10.14802/jmd.16062.

[107] A. Ledberg and D. Robbe, "Locomotion-related oscillatory body movements at 6–12 hz modulate the hippocampal theta rhythm," *PLOS ONE*, vol. 6, no. 11, e27575, 2011. DOI: 10.1371/journal.pone.0027575.

[108] A. Joshi, E. L. Denovellis, A. Mankili, Y. Meneksedag, T. J. Davidson, A. K. Gillespie, J. A. Guidera, D. Roumis, and L. M. Frank, "Dynamic synchronization between hippocampal representations and stepping," *Nature*, pp. 1–7, 2023. DOI: 10.1038/s41586-023-05928-6.

[109] J. O'Keefe and M. L. Recce, "Phase relationship between hippocampal place units and the EEG theta rhythm," *Hippocampus*, vol. 3, no. 3, pp. 317–330, 1993. DOI: 10.1002/hipo.450030307.

[110] J. Huxter, N. Burgess, and J. O'Keefe, "Independent rate and temporal coding in hippocampal pyramidal cells," *Nature*, vol. 425, no. 6960, pp. 828–832, 2003. DOI: 10.1038/nature02058.

[111] W. E. Skaggs, B. L. McNaughton, M. A. Wilson, and C. A. Barnes, "Theta phase precession in hippocampal neuronal populations and the compression of temporal sequences," *Hippocampus*, vol. 6, no. 2, pp. 149–172, 1996. DOI: 10.1002/(SICI)1098-1063(1996)6:2<149::AID-HIPO6>3.0.CO;2-K.

[112] M. Langer, *Lecture 13: Psychophysics*, COMP 546 - Computational Perception - Winter 2018, pp. 1-2, 2018. [Online]. Available: https://www.cim.mcgill.ca/~langer/546.html.

[113] F. A. Wichmann and N. J. Hill, "The psychometric function: I. fitting, sampling, and goodness of fit," *Perception & Psychophysics*, vol. 63, no. 8, pp. 1293–1313, 2001. DOI: 10.3758/BF03194544.

[114] L. Zhong, Y. Zhang, C. A. Duan, J. Deng, J. Pan, and N.-l. Xu, "Causal contributions of parietal cortex to perceptual decision-making during stimulus categorization," *Nature Neuroscience*, vol. 22, no. 6, pp. 963–973, 2019. DOI: 10.1038/s41593-019-0383-6.

[115] G. Dutilh and J. Rieskamp, "Comparing perceptual and preferential decision making," *Psychonomic Bulletin & Review*, vol. 23, pp. 723–737, 2016. DOI: 10.3758/s13423-015-0941-1.

[116] C. G. Ellard, M. A. Goodale, and B. Timney, "Distance estimation in the mongolian gerbil: The role of dynamic depth cues," *Behavioural Brain Research*, vol. 14, no. 1, pp. 29–39, 1984. DOI: 10.1016/0166-4328(84)90017-2.

[117] A. Bergeron, S. Matsuo, and D. Guitton, "Superior colliculus encodes distance to target, not saccade amplitude, in multi-step gaze shifts," *Nature Neuroscience*, vol. 6, no. 4, pp. 404–413, 2003. DOI: 10.1038/nn1027.

[118] C. G. Ellard, "Visually guided locomotion in the gerbil: A comparison of open-and closed-loop control," *Behavioural Brain Research*, vol. 149, no. 1, pp. 41–48, 2004. DOI: 10.1016/S0166-4328(03)00210-9.

[119] P. R. Parker, E. T. Abe, N. T. Beatie, E. S. Leonard, D. M. Martins, S. L. Sharp, D. G. Wyrick, L. Mazzucato, and C. M. Niell, "Distance estimation from monocular cues in an ethological visuomotor task," *eLife*, vol. 11, e74708, 2022. DOI: 10.7554/eLife.74708.sa0.

[120] B. Renshaw, A. Forbes, and B. Morison, "Activity of isocortex and hippocampus: Electrical studies with micro-electrodes," *Journal of Neurophysiology*, vol. 3, no. 1, pp. 74–105, 1940. DOI: 10.1152/jn.1940.3.1.74.

[121] A. Ylinen, A. Bragin, Z. Nádasdy, G. Jandó, I. Szabo, A. Sik, and G. Buzsáki, "Sharp wave-associated high-frequency oscillation (200 hz) in the intact hippocampus: Network and intracellular mechanisms," *Journal of Neuroscience*, vol. 15, no. 1, pp. 30–46, 1995. DOI: 10.1523/JNEUROSCI.15-01-00030.1995.

[122] C. M. Gray, P. E. Maldonado, M. Wilson, and B. McNaughton, "Tetrodes markedly improve the reliability and yield of multiple single-unit isolation from multi-unit

recordings in cat striate cortex," *Journal of Neuroscience Methods*, vol. 63, no. 1-2, pp. 43–54, 1995. DOI: https://doi.org/10.1016/0165-0270(95)00085-2.

[123] G. Buzsáki, "Large-scale recording of neuronal ensembles," *Nature Neuroscience*, vol. 7, no. 5, pp. 446–451, 2004. DOI: 10.1038/nn1233.

[124] J. J. Jun, N. A. Steinmetz, J. H. Siegle, D. J. Denman, M. Bauza, B. Barbarits, A. K. Lee, C. A. Anastassiou, A. Andrei, Ç. Aydın, *et al.*, "Fully integrated silicon probes for high-density recording of neural activity," *Nature*, vol. 551, no. 7679, pp. 232–236, 2017. DOI: 10.1038/nature24636.

[125] N. A. Steinmetz, C. Aydin, A. Lebedeva, M. Okun, M. Pachitariu, M. Bauza, M. Beau, J. Bhagat, C. Böhm, M. Broux, *et al.*, "Neuropixels 2.0: A miniaturized high-density probe for stable, long-term brain recordings," *Science*, vol. 372, no. 6539, eabf4588, 2021. DOI: 10.1126/science.abf4588.

[126] T. Z. Luo, A. G. Bondy, D. Gupta, V. A. Elliott, C. D. Kopec, and C. D. Brody, "An approach for long-term, multi-probe neuropixels recordings in unrestrained rats," *eLife*, vol. 9, e59716, 2020. DOI: 10.7554/eLife.59716.

[127] K. Zhang, I. Ginzburg, B. L. McNaughton, and T. J. Sejnowski, "Interpreting neuronal population activity by reconstruction: Unified framework with application to hippocampal place cells," *Journal of Neurophysiology*, vol. 79, no. 2, pp. 1017–1044, 1998. DOI: 10.1152/jn.1998.79.2.1017.

[128] K. Doya, *Bayesian Brain: Probabilistic Approaches to Neural Coding* (Computational neuroscience). MIT Press, 2007, ISBN: 9780262042383. DOI: 10.7551/mitpress/9780262042383.001.0001.

[129] M. W. Oram, P. Földiák, D. I. Perrett, and F. Sengpiel, "Theideal homunculus': Decoding neural population signals," *Trends in Neurosciences*, vol. 21, no. 6, pp. 259–265, 1998. DOI: 10.1016/S0166-2236(97)01216-2.

[130] D. C. Knill and A. Pouget, "The Bayesian brain: The role of uncertainty in neural coding and computation," *Trends in Neurosciences*, vol. 27, no. 12, pp. 712–719, 2004. DOI: 10.1016/j.tins.2004.10.007.

[131] J. M. McNamara, R. F. Green, and O. Olsson, "Bayes' theorem and its applications in animal behaviour," *Oikos*, vol. 112, no. 2, pp. 243–251, 2006. DOI: 10.1111/j.0030-1299.2006.14228.x.

[132] J. A. Rice, *Mathematical statistics and data analysis*. Cengage Learning, 2006.

[133] Z. Chen, "An overview of Bayesian methods for neural spike train analysis," *Computational Intelligence and Neuroscience*, vol. 2013, pp. 1–1, 2013. DOI: 10.1155/2013/251905.

[134] E. N. Brown, L. M. Frank, D. Tang, M. C. Quirk, and M. A. Wilson, "A statistical paradigm for neural spike train decoding applied to position prediction from ensemble firing patterns of rat hippocampal place cells," *Journal of Neuroscience*, vol. 18, no. 18, pp. 7411–7425, 1998. DOI: 10.1523/JNEUROSCI.18-18-07411.1998.

[135] F. Kloosterman, S. P. Layton, Z. Chen, and M. A. Wilson, "Bayesian decoding using unsorted spikes in the rat hippocampus," *Journal of Neurophysiology*, vol. 111, no. 1, pp. 217–227, 2014. DOI: 10.1152/jn.01046.2012.

[136] X. Deng, D. F. Liu, K. Kay, L. M. Frank, and U. T. Eden, "Clusterless decoding of position from multiunit activity using a marked point process filter," *Neural Computation*, vol. 27, no. 7, pp. 1438–1460, 2015. DOI: 10.1162/NECO_a_00744.

[137] S. Todorova, P. Sadtler, A. Batista, S. Chase, and V. Ventura, "To sort or not to sort: The impact of spike-sorting on neural decoding performance," *Journal of Neural Engineering*, vol. 11, no. 5, p. 056 005, 2014. DOI: 10.1088/1741-2560/11/5/056005.

[138] L. Green, D. Tingley, J. Rinzel, and G. Buzsáki, "Action-driven remapping of hippocampal neuronal populations in jumping rats," *Proceedings of the National Academy of Sciences*, vol. 119, no. 26, e2122141119, 2022. DOI: 10.1073/pnas.2122141119.

[139] J. J. Knierim and B. L. McNaughton, "Hippocampal place-cell firing during movement in three-dimensional space," *Journal of Neurophysiology*, vol. 85, no. 1, pp. 105–116, 2001. DOI: 10.1152/jn.2001.85.1.105.

[140] Y. Dabaghian, V. L. Brandt, and L. M. Frank, "Reconceiving the hippocampal map as a topological template," *eLife*, vol. 3, e03476, 2014. DOI: 10.7554/eLife.03476.

[141] B. R. Komisaruk, "Synchrony between limbic system theta activity and rhythmical behavior in rats.," *Journal of Comparative and Physiological Psychology*, vol. 70, no. 3p1, p. 482, 1970. DOI: 10.1037/h0028709.

[142] W. L. McFarland, H. Teitelbaum, and E. K. Hedges, "Relationship between hippocampal theta activity and running speed in the rat.," *Journal of Comparative and Physiological Psychology*, vol. 88, no. 1, p. 324, 1975. DOI: 10.1037/h0076177.

[143] P.-P. Lenck-Santini, A. A. Fenton, and R. U. Muller, "Discharge properties of hippocampal neurons during performance of a jump avoidance task," *Journal of Neuroscience*, vol. 28, no. 27, pp. 6773–6786, 2008. DOI: 10.1523/JNEUROSCI.5329-07.2008.

[144] B. H. Bland, J. Jackson, D. Derrie-Gillespie, T. Azad, A. Rickhi, and J. Abriam, "Amplitude, frequency, and phase analysis of hippocampal theta during sensorimotor processing in a jump avoidance task," *Hippocampus*, vol. 16, no. 8, pp. 673–681, 2006. DOI: 10.1002/hipo.20210.

[145] L. Van Pelt, "Ketamine and xylazine for surgical anesthesia in rats.," *Journal of the American Veterinary Medical Association*, vol. 171, no. 9, pp. 842–844, 1977, PMID: 924855.

[146] G. Paxinos and C. Watson, *The Rat Brain in Stereotaxic Coordinates*. Elsevier Science, 2013, ISBN: 9780123919496.

[147] I. Lee, D. Yoganarasimha, G. Rao, and J. J. Knierim, "Comparison of population coherence of place cells in hippocampal subfields CA1 and CA3," *Nature*, vol. 430, no. 6998, pp. 456–459, 2004. DOI: 10.1038/nature02739.

[148] B. P. Vagvolgyi, R. P. Jayakumar, M. S. Madhav, J. J. Knierim, and N. J. Cowan, "Wide-angle, monocular head tracking using passive markers," *Journal of Neuroscience Methods*, vol. 368, p. 109 453, 2022. DOI: 10.1016/j.jneumeth.2021.109453.

[149] M. Vöröslakos, P. C. Petersen, B. Vöröslakos, and G. Buzsáki, "Metal microdrive and head cap system for silicon probe recovery in freely moving rodent," *eLife*, vol. 10, e65859, 2021. DOI: 10.7554/eLife.65859.

[150] B. Karsh, *Spikeglx*, https://github.com/billkarsh/SpikeGLX/releases/tag/Release_v20220101-phase30, Version 20220101, Imec phase30 v3.51, 2022.

[151] G. Bradski, "The OpenCV Library," *Dr. Dobb's Journal of Software Tools*, 2000.

[152] G. Buzsáki, "Theta oscillations in the hippocampus," *Neuron*, vol. 33, no. 3, pp. 325–340, 2002. DOI: 10.1016/S0896-6273(02)00586-X.

[153] R. Kempter, C. Leibold, G. Buzsáki, K. Diba, and R. Schmidt, "Quantifying circular–linear associations: Hippocampal phase precession," *Journal of Neuroscience Methods*, vol. 207, no. 1, pp. 113–124, 2012. DOI: 10.1016/j.jneumeth.2012.03.007.

[154] P. Berens, "Circstat: A matlab toolbox for circular statistics," *Journal of Statistical Software*, vol. 31, pp. 1–21, 2009. DOI: 10.18637/jss.v031.i10.

[155] G. G. Kui, M. Krysiak, K. Banda, and H. R. Rodman, "Context dependence of head bobs in gerbils and potential neural contributions," *Behavioural Brain Research*, vol. 418, p. 113 622, 2022. DOI: 10.1016/j.bbr.2021.113622.

[156] M. L. Shapiro, H. Tanila, and H. Eichenbaum, "Cues that hippocampal place cells encode: Dynamic and hierarchical representation of local and distal stimuli," *Hippocampus*, vol. 7, no. 6, pp. 624–642, 1997. DOI: 10.1002/(SICI)1098-1063(1997)7:6<624::AID-HIPO5>3.0.CO;2-E.

[157] K. M. Gothard, W. E. Skaggs, and B. L. McNaughton, "Dynamics of mismatch correction in the hippocampal ensemble code for space: Interaction between path integration and environmental cues," *Journal of Neuroscience*, vol. 16, no. 24, pp. 8027–8040, 1996. DOI: 10.1523/JNEUROSCI.16-24-08027.1996.

[158] J. J. Knierim and D. A. Hamilton, "Framing spatial cognition: Neural representations of proximal and distal frames of reference and their roles in navigation," *Physiological Reviews*, vol. 91, no. 4, pp. 1245–1279, 2011. DOI: 10.1152/physrev.00021.2010.

[159] E. Liaci, A. Fischer, H. Atmanspacher, M. Heinrichs, L. Tebartz van Elst, and J. Kornmeier, "Positive and negative hysteresis effects for the perception of geometric and emotional ambiguities," *PLOS ONE*, vol. 13, no. 9, e0202398, 2018. DOI: 10.1371/journal.pone.0202398.

[160] I. Hachen, S. Reinartz, R. Brasselet, A. Stroligo, and M. Diamond, "Dynamics of history-dependent perceptual judgment," *Nature Communications*, vol. 12, no. 1, p. 6036, 2021. DOI: 10.1038/s41467-021-26104-2.

[161] R. M. Gallagher, T. Suddendorf, and D. H. Arnold, "Confidence as a diagnostic tool for perceptual aftereffects," *Scientific Reports*, vol. 9, no. 1, p. 7124, 2019. DOI: 10.1038/s41598-019-43170-1.

[162] W. Tang, J. D. Shin, and S. P. Jadhav, "Multiple time-scales of decision-making in the hippocampus and prefrontal cortex," *eLife*, vol. 10, e66227, 2021. DOI: 10.7554/eLife.66227.

[163] M. E. Hasselmo and C. E. Stern, "Theta rhythm and the encoding and retrieval of space and time," *Neuroimage*, vol. 85, pp. 656–666, 2014. DOI: 10.1016/j.neuroimage.2013.06.022.

[164] V. A. Shim, B. Tian, M. Yuan, H. Tang, and H. Li, "Direction-driven navigation using cognitive map for mobile robots," in *2014 IEEE/RSJ International Conference*

on Intelligent Robots and Systems, IEEE, 2014, pp. 2639–2646. DOI: 10.1109/IROS.2014.6942923.

[165] Q. Zou, M. Cong, D. Liu, and Y. Du, "A neurobiologically inspired mapping and navigating framework for mobile robots," *Neurocomputing*, vol. 460, pp. 181–194, 2021. DOI: 10.1016/j.neucom.2021.07.025.

[166] F. Yu, J. Shang, Y. Hu, and M. Milford, "NeuroSLAM: A brain-inspired SLAM system for 3D environments," *Biological Cybernetics*, vol. 113, pp. 515–545, 2019. DOI: 10.1007/s00422-019-00806-9.

[167] B. Woronowicz, M. Hathiyari, S. G. Lashkari, and N. J. Cowan, "Tail-assisted climbing in rats," in *The Society for Integrative and Comparative Biology Annual Meeting*, To be presented at the Society for Integrative and Comparative Biology Annual Meeting, 2024, Jan. 2024.

[168] P. Glimcher and E. Fehr, *Neuroeconomics: Decision Making and the Brain*. Elsevier Science, 2013, ISBN: 9780123914699. DOI: 10.1016/C2011-0-05512-6. [Online]. Available: https://www.sciencedirect.com/book/9780124160088/neuroeconomics.

[169] A. Rangel, C. Camerer, and P. R. Montague, "A framework for studying the neurobiology of value-based decision making," *Nature Reviews Neuroscience*, vol. 9, no. 7, pp. 545–556, 2008, ISSN: 1471003X. DOI: 10.1038/nrn2357.

[170] R. L. Wasserstein and N. A. Lazar, "The ASA statement on p-values: Context, process, and purpose," *The American Statistician*, vol. 70, no. 2, pp. 129–133, 2016. DOI: 10.1080/00031305.2016.1154108.

[171] M. Crawley, *Statistics: An Introduction Using R*. Wiley, 2014, ISBN: 9781118941119. [Online]. Available: https://books.google.com/books?id=KR-FBAAAQBAJ.

[172] Student, "The probable error of a mean," *Biometrika*, vol. 6, no. 1, pp. 1–25, 1908. DOI: 10.2307/2331554.

[173] B. L. Welch, "The generalization of 'Student's' problem when several different population varlances are involved," *Biometrika*, vol. 34, no. 1-2, pp. 28–35, 1947. DOI: 10.2307/2332510.

[174] S. C. Pearce, "Introduction to Fisher (1925) statistical methods for research workers," in *Breakthroughs in Statistics: Methodology and Distribution*, S. Kotz and N. L. Johnson, Eds. New York, NY: Springer New York, 1992, ch. 5, pp. 59–65. DOI: 10.1007/978-1-4612-4380-9_5.

[175] J. Cohen, *Statistical power analysis for the behavioral sciences*, Second. Academic press, 1988. DOI: 10.4324/9780203771587.

[176] D. Lakens, "Calculating and reporting effect sizes to facilitate cumulative science: A practical primer for t-tests and ANOVAs," *Frontiers in Psychology*, vol. 4, p. 863, 2013. DOI: 10.3389/fpsyg.2013.00863.

[177] K. Mardia and P. Jupp, *Directional Statistics* (Wiley Series in Probability and Statistics). Wiley, 2009, ISBN: 9780470317815.

Shahin G. Lashkari

Summary of Qualifications

• 6+ years of experience in programming languages such as C++, Python, MATLAB, and Simulink for data processing, signal processing, and modeling.
• Collaboration with interdisciplinary teams of graduate students in neuroscience and engineering to record and analyze neurophysiological data inside an immersive virtual reality environment.
• Strong background in mathematical analysis, modeling, and control, with a focus on developing innovative and bio-inspired approaches for autonomous systems.

Education

- Ph.D. in Mechanical Engineering, **Johns Hopkins University** 2023
- M.S. in Electrical Engineering, **Clemson University** 2017
- M.S. in Mechanical Engineering, **Sharif University of Technology** 2011
- B.S. in Mechanical Engineering, **Amirkabir University of Technology** 2008

Skills

- Programming: **C/C++** (C++14, STL, OpenCV), Bash, Git, HTML.
- Data Science: **Python** (NumPy, Pandas, Matplotlib, SciPy, scikit-learn), MATLAB, Jupyter.
- CAD, Prototyping, and HW Control: SolidWorks, AutoCAD, LabVIEW, Simulink, LTspice.
- Robotics: ROS, Computer Vision, Optimization, Sensor Fusion, Embedded Systems, APIs.
- Control Systems: PID, Optimal, Adaptive, and Model Predictive Control, State Estimation.

Experiences

▷ **Robotics and Control Internship**, **Johnson and Johnson** 2022

• Developed an object-oriented Python library using nonlinear optimization to achieve kinematic calibration of surgical robots. The library, now incorporated into the production line, has successfully reduced calibration error by 50%.

• Developed modules for extracting DH parameters from URDF files and performed frame calibration for base and end-effector fixtures using least squares optimization.

▷ **Research Assistant**, **Laboratory for Computational Sensing and Robotics (LCSR)**, Johns Hopkins University 2018-2023

• Collaborated with a team of engineers and neuroscientists to design and implement a low-latency virtual reality (VR) dome to study hippocampal and cortical neural recordings of animals during immersive VR experiences.

• Led a multidisciplinary team to design and construct an embedded experimental system for studying animal biomechanics and neurophysiology during gap crossing. Behavioral correlates of the neural data were analyzed using the force and 3D pose data.

• Developed a robust and accurate real-time tracking system using the OpenCV library in C++, complemented by a Kalman filter for the fusion of tracking data and IMU data for enhanced precision and reliability.

• Conducted comprehensive data analysis using MATLAB and Python, employing Bayesian and SVM classifiers, to model and decode neural and behavioral information and predict animals' decisions with accuracy of 75% ± 10%.

• Utilized a combination of C++ and Python for the development of ROS nodes, and incorporated APIs for communication with machine vision cameras, DAQ, and motor drivers.

▷ **Teaching Assistant**, **Mechanical Engineering Department**, Johns Hopkins University 2018-2019

• Assisted in teaching graduate courses of "Robot Devices, Kinematics, Dynamics, and Control" and "Adaptive Control", which included hands-on projects for controlling UR5 robot arms.

▷ **Research Assistant**, **Biosystems Research Complex**, Clemson University 2014-2017

• Implemented a sensor-based and model predictive controller for a bioreactor, utilizing finite state machines and an adaptive state estimator for estimating oxygen uptake rate, to enhance robust and efficient production of recombinant proteins.

• Employed Hardware-in-the-Loop (HIL) to control the hardware using Simulink Real-Time.

▷ **Teaching Assistant**, **Electrical Engineering Department**, Clemson University 2014-2016

• Assisted the professors in teaching a variety of courses ranging from theoretical classes such as "Continuous and Discrete Systems Design" and "Modeling and Analysis of Dynamic Systems" to hands-on labs like "Electrical Engineering Laboratory IV."

• Supervised and guided teams of undergraduate students in "Senior Design" projects.

Honors and Awards

◇ Creel Family Teaching Assistant Award 2020
◇ Johns Hopkins University Mechanical Engineering Departmental Fellowship 2017-2018
◇ Phi Kappa Phi Honor Society 2016

Publications

• **S. G. Lashkari**, B. M. Woronowicz, P. Ozel, B. Krishnan, J. J. Knierim, N. J. Cowan, *Hippocampal place cell encoding during gap-crossing behaviors,* Society for Neuroscience, San Diego, California, USA, 2022.

• B. Krishnan, G. Secer, F. Savelli, **S. G. Lashkari**, R. P. Jayakumar, K. L. Wright, N. J. Cowan, J. J. Knierim, *Population Responses in Medial Entorhinal Cortex During Recalibration of Path Integration Gain,* Society for Neuroscience, San Diego, California, USA, 2022.

• M. S. Madhav, R. P. Jayakumar, **S. G. Lashkari**, F. Savelli, H. T. Blair, J. J. Knierim and N. J. Cowan, *The Dome: A virtual reality apparatus for freely locomoting rodents,* J. Neurosci. Methods, 109336, 2022.

• **S. G. Lashkari**, M. G. Wilkinson, B. Krishnan, J. J. Knierim, and N. J. Cowan, *Decision-making and path planning for jumping rats,* Dynamic Walking, Hawley, Pennsylvania, USA, 2020.

• M. S. Madhav, R. P. Jayakumar, **S. G. Lashkari**, F. Savelli, N. J. Cowan, and J. J. Knierim, *Using augmented reality and a control theoretic approach to characterize computation of path integration in rodents,* Society for Neuroscience, Chicago, Illinois, USA, 2019.

• R. Groff, S. Harcum, M. Pepper, **S. G. Lashkari**, M. Mayyan, *Controlling E. coli cultures to the Boundary of Oxidative and Overflow Metabolism (BOOM) using a low-latency OUR estimator,* IFPAC, North Bethesda, Maryland, USA, 2017.

• M. Hadipour, M. T. Ahmadian, **S. G. Lashkari** , A. Barari, *Natural Frequency Improvement of a Suspended FGM Bridge,* in Proceedings of IMECE2011-63411, Denver, Colorado, USA, 2011.

Selected Coursework

Robot Operating System (ROS)
Matrix Analysis
Modern Control Engineering
Kinematics and Dynamics of Robots
Advanced Kinematics in Robotics
Optimal Control
Optimal Estimation
Analysis of Linear Systems
Algorithms for Sensor-Based Robotics
Intelligent Systems Modeling and Control
Digital Image Processing
Advanced Dynamics
Advanced Analytical Dynamics
Adaptive Systems and Control